IFAC

INTERNATIONAL FEDERATION
OF AUTOMATIC CONTROL

WARSZAWA 1969

Nonlinear Systems

Fourth Congress of the International
Federation of Automatic Control
Warszawa 16–21 June 1969

TECHNICAL
SESSION
41

Organized by
Naczelna Organizacja Techniczna w Polsce

INTERNATIONAL FEDERATION OF AUTOMATIC CONTROL

Nonlinear Systems

TECHNICAL SESSION No 41

FOURTH CONGRESS OF THE INTERNATIONAL
FEDERATION OF AUTOMATIC CONTROL
WARSZAWA 16 – 21 JUNE 1969

Organized by
Naczelna Organizacja Techniczna w Polsce

Contents

Wydawn NOT - Polska

Zakład Poligraficzny WCT NOT. Zam. 68 69.

INPUT - OUTPUT STABILITY - A GENERAL VIEWPOINT

by

P. L. Falb

Division of Applied Mathematics, Brown University
Providence, Rhode Island
NASA Electronics Research Center
Cambridge, Massachusetts

M. I. Freedman

NASA Electronics Research Center
Cambridge, Massachusetts

G. Zames

NASA Electronics Research Center
Cambridge, Massachusetts

1. Introduction

This paper is devoted to the study of the stability of the system of Fig. 1, which consists of two elements in a feedback loop. This simple configuration is a model for many controllers, amplifiers and modulators; its range of application is extended to include multi-element, sampled data, and distributed systems in this paper and in[2]. Here, the relation between input-output behavior and stability is studied from a general functional viewpoint which leads to a generalized circle criterion for stability applicable to a wide class of systems. The theory, which is developed in detail in[2], represents a natural and useful extension of the results of Zames[3], Kudrewicz[6], and Sandberg.[7,8]

A transform theory for causal operator - valued functions defined over a locally compact abelian group G was developed in[1]. This transform theory relied heavily on the classic work of the Russian mathematician Gelfand on commutative Banach algebras[5]. The results in[1] were used to obtain frequency domain stability criteria of Popov type for a wide class of nonlinear systems in[2].

Two particularly important groups to which the theory applies are the reals, R, and the integers, J, under addition. These groups correspond to continuous and discrete time systems, respectively. The relevant

This work has been supported in part by the National Science Foundation under Grant No. GK 967 and in part by the United States Air Force under Grant No. AFOSR 693-67.

commutative Banach algebras (under appropriate notions of convolution) are
(a) $L_1[0,\infty) = \{f(t)\colon f(t)$ Lebesgue measurable and $\int_0^\infty |f(t)|\,dt < \infty\}$
and
(b) $L_1(J^+) = \{\{a_n\}\colon n \geq 0,\ a_n$ real and $\sum_{n=0}^{\infty} |a_n| < \infty\}$
(where $J^+ = \{n\colon n \geq 0\}$). Both of these algebras have well-studied maximal ideal spaces and, in fact, the Gelfand representations of (a) and (b) correspond to the familiar Laplace and z-transforms, respectively. Because of this correspondence, we shall be able to give versions of the main result of[2] for R and J here, without requiring the reader to draw on any knowledge of the general Gelfand theory. However, we note that the full power of our results only comes to the fore in the very general setting provided in[2].

The results presented here can be viewed as a generalization of the circle criterion[3]. We consider a system consisting of a linear part and a nonlinear part which is, in a certain sense, restricted to lie in a sector. Corresponding to this sector, we consider an appropriate circle in the complex plane and we show that stability is assured if the eigenvalues (more accurately, the spectrum) of certain operators avoid this circle.

2. Preliminaries

Let H be a real Hilbert space and let $L_2(R^+,H)$ denote the space of square integrable maps $f(\cdot)$ of R into H satisfying $f(t) = 0$ for $t < 0$. We let $|\cdot|$ denote the norm on H so that $\|f\| = (\int_0^\infty |f(t)|^2 dt)^{1/2}$ is the norm on $L_2(R^+,H)$. Similarly, we let $L_2(J^+,H)$ be the space of square summable sequences $\{a_n\}_{-\infty}^{\infty}$ with $a_n \in H$ satisfying $a_n = 0$ for $n < 0$. The norm on $L_2(J^+,H)$ is given by $\|\{a_n\}\| = (\sum_0^\infty |a_n|^2)^{1/2}$. With stability considerations in mind, we introduce several extended spaces $L_{2p}(R^+,H)$ and $L_{2p}(J^+,H)$. These spaces are defined as follows:

$$L_{2p}(R^+,H) = \{f\colon f\mathfrak{X}_t \in L_2(R^+,H) \quad \text{for} \quad t \geq 0\} \tag{1}$$

where $\mathfrak{X}_t(s) = 1$ if $s < t$ and $\mathfrak{X}_t(s) = 0$ if $s \geq t$;

$$L_{2p}(J^+,H) = \{\{a_n\}\colon \{a_n\mathfrak{X}_k(n)\} \in L_2(J^+,H) \quad \text{for} \quad k \geq 0\} \tag{2}$$

where $\mathfrak{X}_k(n) = 1$ if $n < k$ and $\mathfrak{X}_k(n) = 0$ if $n \geq k$. We often denote elements of $L_{2p}(J^+,H)$ by $\{a(n)\}$.

We are now ready to define stability.

DEFINITION 1 Let Φ,Ψ be maps of $L_{2p}(R^+,H)$ into $L_{2p}(R^+,H)$ (or of $L_{2p}(J^+,H)$ into $L_{2p}(J^+,H)$). Then the operator equation

$$e(\cdot) + \Phi[(\Psi e)(\cdot) + x_1(\cdot)] = x_2(\cdot) \tag{3}$$

is called L_2-stable if, for any $A > 0$, there is a $K(A) \geq 0$ such that if $\|x_1(\cdot)\| \leq A$ and $\|x_2(\cdot)\| \leq A$, then $\|e(\cdot)\| \leq K(A)$ for every solution $e(\cdot)$ of (3) with $e(\cdot) \in L_{2p}(R^+,H)$ (or $L_{2p}(J^+,H)$).

We shall deal with the case of each group, R and J, separately. Each case is subsumed under the general theory developed in[2] and consequently, the two cases will follow parallel paths.

3. The Case of the Group R: Continuous Time

Let $\mathcal{L}(H,H)$ denote the space of bounded linear maps of H into itself. Suppose that $\varphi(\cdot)$ is a measurable map of R into $\mathcal{L}(H,H)$ with the following properties: (i) $\varphi(\cdot)$ is integrable (i.e. $\int_{-\infty}^{\infty}\|\varphi(t)\|dt < \infty$), and (ii) $\operatorname{supp}\varphi \subset [0,\infty)$ where $\operatorname{supp}\varphi$ is the support of φ (i.e. $\varphi(t) = 0$ for $t < 0$). Then we can easily see that φ induces a map Φ of $L_{2p}(R^+,H)$ into $L_{2p}(R^+,H)$ which is given by

$$(\Phi x)(t) = (\varphi * x)(t) = \int_{-\infty}^{\infty}\varphi(t-\tau)x(\tau)d\tau = \int_{-\infty}^{t}\varphi(t-\tau)x(\tau)d\tau \tag{4}$$

(cf.[1]). We denote the set of all such maps Φ by $B_{[0,\infty)}$.

If Φ is an element of $B_{[0,\infty)}$, then we can introduce a notion of Laplace transform for Φ. More precisely, we let $\hat{\Phi}(s)$, for $\operatorname{Re}\{s\} \geq 0$, be the element of $\mathcal{L}(H^c,H^c)$ given by

$$\hat{\Phi}(s) = \int_0^{\infty}e^{-st}\varphi(t)dt \tag{5}$$

where H^c is the complexification of H and we call $\hat{\Phi}(s)$ the Laplace transform of Φ. The integral in (5) converges as a Banach space valued integral (see [1,4]). Finally, we let $\operatorname{spec}\{\hat{\Phi}(s)\}$ denote the spectrum of $\hat{\Phi}(s)$ so that

$$\operatorname{spec}\{\hat{\Phi}(s)\} = \{\lambda \in C: \hat{\Phi}(s) - \lambda I \text{ is not invertible in } \mathcal{L}(H^c,H^c)\}. \tag{6}$$

We now have

DEFINITION 2 Let Φ be an element of $B_{[0,\infty)}$. Then Φ is called

approximable if $\hat{\Phi}(s)$ is completely continuous for all s with $\mathrm{Re}\{s\} \geq 0$.

DEFINITION 3 Let N be a map of H into H. Then N is called a bounded nonlinearity if $N(0) = 0$ and $|N(h)| \leq c|h|$ for all h in H, where c is a constant.

THEOREM 1 Let Φ be an element of $B_{[0,\infty)}$, let N be a bounded nonlinearity, and let a and b be positive numbers with $a < b$. Suppose that the following conditions are satisfied:

(i) Φ is approximable;

(ii) $\hat{\Phi}(i\omega)$ is normal for all $i\omega$ with $-\infty < \omega < \infty$;

(iii) $< bh-N(h), N(h)-ah > \geq 0$ for all h in H;

(iv) $-b^{-1} \notin \bigcup_{\mathrm{Re}\{s\} \geq 0} \mathrm{spec}\,\{\hat{\Phi}(s)\}$; and

(v) the set $\bigcup_{-\infty < \omega < \infty} \mathrm{spec}\,\{\hat{\Phi}(i\omega)\}$ in the complex plane remains outside of and does not intersect the circle with center $-1/2(1/a+1/b)$ and radius $1/2(1/a-1/b)$.

Then the operator equations

$$e(\cdot) + \Phi[(\underset{\sim}{N}e)(\cdot) + x_1(\cdot)] = x_2(\cdot) \tag{7}$$

$$e(\cdot) + \underset{\sim}{N}[(\Phi e)(\cdot) + x_1(\cdot)] = x_2(\cdot) \tag{8}$$

where $(\underset{\sim}{N}y)(t) = N(y(t))$, are both L_2-stable.

We note that a proof of this theorem is given in[2] and that (7) and (8) may be written out in full as

$$e(t) + \int_0^t \varphi(t-\tau)[N(e(\tau)) + x_1(\tau)]d\tau = x_2(t) \tag{9}$$

$$e(t) + N(\int_0^t \varphi(t-\tau)e(\tau)d\tau + x_1(t)) = x_2(t). \tag{10}$$

We also observe that if $\bigcup_{-\infty < \omega < \infty} \mathrm{spec}\,\{\hat{\Phi}(i\omega)\}$ lies in a simply connected domain excluding the point $-b^{-1}$, then condition (iv) of the theorem is satisfied by virtue of the principle of the argument. Thus, (iv) and (v) can be replaced by the following condition:

(iv)' $\bigcup_{-\infty < \omega < \infty} \mathrm{spec}\,\{\hat{\Phi}(i\omega)\}$ is contained in a simply connected domain with the property that the circle with center $-1/2(1/a+1/b)$ and radius $1/2(1/a-1/b)$ lies entirely in its exterior. We now turn our attention to some examples.

EXAMPLE 1 Let $H = R_2$ be two dimensional Euclidean space and consider the system of nonlinear differential equations

$$\ddot{y}_1 + 6\dot{y}_1 + 5y_1 + 2\dot{y}_2 + 2y_2 + y_1(d + \cos y_2) = 0 \qquad (11)$$
$$2\dot{y}_1 + 2y_1 + \ddot{y}_2 + 3y_2 + cy_2 = 0$$

for $t \geq 0$ where c and d are positive constants. We suppose that the initial conditions for (11) are given by

$$y_1(0) = \alpha, \quad \dot{y}_1(0) = \alpha' \qquad (12)$$
$$y_2(0) = \beta, \quad \dot{y}_2(0) = \beta'$$

where $\alpha,\alpha',\beta,\beta'$ are appropriate constants. Letting $\underset{\sim}{y}(t) = \begin{bmatrix} y_1(t) \\ y_2(t) \end{bmatrix}$ and letting N be the map of R_2 into itself given by

$$N\left(\begin{bmatrix} r_1 \\ r_2 \end{bmatrix}\right) = \begin{bmatrix} r_1(d + \cos r_2) \\ cr_2 \end{bmatrix} \qquad (13)$$

we may rewrite (11) as a nonlinear integral equation of the form

$$\underset{\sim}{y}(t) = \underset{\sim}{y}_0(t) - \int_0^t \varphi(t-\tau)N(\underset{\sim}{y}(\tau))d\tau, \quad t \geq 0 \qquad (14)$$

where $\underset{\sim}{y}_0(t)$ depends only on the initial data (12) and where $\varphi(t)$ is the appropriate Green's function for (11). The system is illustrated in Fig. 2. We note that $\int_0^\infty < \underset{\sim}{y}_0(t), \underset{\sim}{y}_0(t) > dt < \infty$ and that the map Φ which corresponds to φ has the Laplace transform

$$\hat{\Phi}(s) = \frac{1}{(s+1)^2(s+6)} \begin{bmatrix} s+2 & -2 \\ -2 & s+5 \end{bmatrix}.$$

It is clear that $\hat{\Phi}(s)$ is a normal matrix for all s with $\mathrm{Re}\,[s] \geq 0$. Moreover, Φ is automatically approximable since the Hilbert space $H(= R_2)$ is finite dimensional. Thus, conditions (i) and (ii) are satisfied.

We can easily see that condition (iii) will be satisfied if a and b are any positive numbers for which $a \leq c \leq b$, $d \geq 1 + a$, and $b \geq 1 + d$.

Now the spectrum of $\hat{\Phi}(s)$ consists of the eigenvalues

$$\lambda_1(s) = \frac{1}{(s+6)(s+1)}, \quad \lambda_2(s) = \frac{1}{(s+1)^2} \tag{16}$$

for $\mathrm{Re}\{s\} \geq 0$. It is clear that the equations $\lambda_1(s) = -b^{-1}$, $\lambda_2(s) = -b^{-1}$ have no solutions for $b > 0$ and so, (iv) is satisfied. Finally, (v) will be satisfied provided that $\lambda_1(i\omega)$ and $\lambda_2(i\omega)$ do not intersect and remain outside of the circle with center $-1/2(1/a+1/b)$ and radius $1/2(1/a-1/b)$. See Fig. 3. It follows that under these conditions (11) will be L_2-stable in that given $A > 0$, there is a $K(A) > 0$ such that $\|y_0(\cdot)\| \leq A$ implies that $y(\cdot) \in L_2[0,\infty)$ and $\|y(\cdot)\| \leq K(A)$.

EXAMPLE 2 Let $H = L_2[0,1]$ so that H is a separable infinite dimensional Hilbert space. Consider the nonlinear integral equation

$$u(x,t) = u_0(x,t) - \int_0^t\int_0^1 \varphi(x,y,t-\tau)N(u(y,\tau))dyd\tau, \quad t \geq 0 \tag{17}$$

where it is assumed that N is any bounded map of $L_2[0,1]$ into itself with $N(0) = 0$ and that

$$\int_{-\infty}^{\infty}\int_0^1\int_0^1 |\varphi(x,y,t)|\,dxdydt < \infty \tag{18}$$

$$\varphi(x,y,t) = \varphi(y,x,t) \tag{19}$$

$$\varphi(x,y,t) = 0 \quad \text{for} \quad t < 0. \tag{20}$$

We shall determine conditions for the L_2-stability of (17) in the sense that given $A > 0$, there is a $K(A) > 0$ such that if $\int_0^\infty\int_0^1 |u_0(x,t)|^2 dxdt \leq A$, then every solution $u(x,t)$ of (17) satisfies $\int_0^\infty\int_0^1 |u(x,t)|^2 dxdt \leq K(A)$.

With the objective of proving stability in mind, we define a map Φ (in $B_{[0,\infty)}$) by setting

$$(\Phi v)(x,t) = \int_0^t\int_0^1 \varphi(x,y,t-\tau)v(t,\tau)dyd\tau \tag{21}$$

for v in $L_{2p}(R^+, L_2[0,1])$. The Laplace transform $\hat{\Phi}(s)$ of Φ is then given by

$$\hat{\Phi}(s)w(x) = \int_0^1 \hat{\varphi}(x,y,s)w(y)dy \tag{22}$$

where $\hat{\varphi}(x,y,s) = \int_0^\infty e^{-st}\varphi(x,y,t)dt$. Now $\hat{\Phi}(i\omega)$ is normal by virtue of

(19) and $\hat{\Phi}(s)$ is completely continuous for each s with $\mathrm{Re}\,[s] \geq 0$ by virtue of (18) (see[4]). It follows that (17) will be L_2-stable if (iii), (iv) and (v) are satisfied.

Let us look at a particular example. We consider the nonlinear partial differential equation

$$\frac{\partial^4 u}{\partial t^2 \partial x^2} + 3\frac{\partial^3 u}{\partial t \partial x^2} + 2\frac{\partial^2 u}{\partial x^2} = N(u) \tag{23}$$

with the auxiliary data

$$\begin{aligned} u(0,t) &= u(1,t) = 0 \\ u(x,0) &= f_1(x) \\ \frac{\partial u}{\partial t}(x,0) &= f_2(x) \end{aligned} \tag{24}$$

where f_1 and f_2 are elements of $L_2[0,1]$ and N is a bounded nonlinearity on $L_2[0,1]$. We may reformulate (23) as an integral equation of the form (17). To do this, we let $\Gamma(x,y)$ be the Green's function for the Sturm-Liouville problem on $[0,1]$ given by

$$-\frac{d^2 q(x)}{dx^2} = f(x), \quad q(0) = q(1) = 0 \tag{25}$$

so that

$$\Gamma(x,y) = \begin{cases} x(1-y) & x < y \\ (1-x)y & x > y \end{cases} \tag{26}$$

for x,y in $[0,1]$. We also let $\psi(t)$ be the impulse response for the operator $D_t^2 + 3D_t + 2$ so that

$$\psi(t) = \begin{cases} e^{-t} - e^{-2t} & t \geq 0 \\ 0 & t < 0 \end{cases} \tag{27}$$

Then (23) has the equivalent integral form

$$u(x,t) = u_0(x,t) - \int_0^t\int_0^1 \Gamma(x,y)\psi(t-\tau)N(u(y,\tau))dyd\tau \tag{28}$$

where $u_0(x,t)$ is the solution of the equation $(D_t^2+3D_t+2)u_0(x,t) = 0$ satisfying the initial conditions $u_0(x,0) = f_1(x)$, $\frac{du_0}{dt}(x,0) = f_2(x)$. We note that $\int_0^\infty\int_0^1 |u_0(x,t)|^2 dxdt < \infty$. Now (28) has the required form with $\varphi(x,y,t) = \Gamma(x,y)\psi(t)$. Moreover, $\Gamma(x,y)\psi(t)$ satisfies (18), (19) and (20).

In order to apply the theorem 1, we must compute spec $\{\hat{\Phi}(s)\}$. Here, $\hat{\varphi}(x,y,s) = \Gamma(x,y)/(s+1)(s+2)$ and so,

$$\hat{\Phi}(s)w(x) = \frac{1}{(s+1)(s+2)} \int_0^1 \Gamma(x,y)w(y)dy \tag{29}$$

for $w(\cdot)$ in $L_2[0,1]$. Now, the operator T given by $(Tw)(x) = \int_0^1 \Gamma(x,y)w(y)dy$ is well-known to have the spectrum $\{0, 1/n^2\pi^2: n = 1,2,\ldots\}$ since $\Gamma(x,y) = -2\sum_1^\infty \frac{\sin n\pi x}{n^2\pi^2}\sin n\pi y$. It follows that spec $\{\hat{\Phi}(s)\} = \{0, 1/(s+2)(s+1)n^2\pi^2\}$.

Let a and b be positive numbers with $a < b$. Then $-b^{-1} \notin$ spec $\{\hat{\Phi}(s)\}$ for any s with Re $\{s\} \geq 0$ and so, (iv) is satisfied. If, in addition, we assume that $\{0, 1/(i\omega+2)(i\omega+1)n^2\pi^2: -\infty < \omega < \infty, n = 1,2,\ldots\}$ does not intersect and remains outside the proper circle, then (v) will be satisfied. Thus, the system (28) will be L_2-stable provided that the nonlinearity N satisfies the condition

$$\int_0^1 (bw(x) - N(w(x)))(N(w(x)) - aw(x))dx \geq 0 \tag{30}$$

for all $w(\cdot)$ in $L_2[0,1]$.

4. The Case of the Group J: Discrete Time

Again we let $\mathcal{L}(H,H)$ denote the space of bounded linear maps of H into itself. Suppose that $\varphi(\cdot)$ is a map of J into $\mathcal{L}(H,H)$ with the following properties: (i) $\varphi(\cdot)$ is summable (i.e. $\sum_{n=-\infty}^{\infty}\|\varphi(n)\| < \infty$), and (ii) $\varphi(n) = 0$ if $n < 0$. Then we can easily see that $\varphi(\cdot)$ induces a map Φ of $L_{2p}(J^+,H)$ into $L_{2p}(J^+,H)$ which is given by

$$(\Phi x)(n) = (\varphi * x)(n) = \sum_{j=-\infty}^{\infty}\varphi(n-j)x(j) = \sum_{j=-\infty}^{n}\varphi(n-j)x(j) \tag{31}$$

for x in $L_{2P}(J^+,H)$. We denote the set of all such map by B_{J^+}.

If Φ is an element of B_{J^+}, then we can introduce a notion of z-transform for Φ. More precisely, we let $\hat{\Phi}(z)$, for $z \in C$ with $|z| \leq 1$, be the element of $\mathcal{L}(H^c,H^c)$ given by

$$\hat{\Phi}(z) = \sum_{n=0}^{\infty} \varphi(n) z^n \tag{32}$$

where H^c is the complexification of H and we call $\hat{\Phi}(z)$ the z-transform of Φ. Finally, we let spec $\{\hat{\Phi}(z)\}$ denote the spectrum of $\hat{\Phi}(z)$ so that

$$\text{spec } \{\hat{\Phi}(z)\} = \{\lambda \in C: \hat{\Phi}(z) - \lambda I \text{ is not invertible in } \mathcal{L}(H^c,H^c)\}. \tag{33}$$

We now have (just as in section 3)

DEFINITION 4 Let Φ be an element of B_{J^+}. Then Φ is called approximable if $\hat{\Phi}(z)$ is completely continuous for all z with $|z| \leq 1$.

THEOREM 2 Let Φ be an element of B_{J^+}, let N be a bounded nonlinearity, and let a and b be positive numbers with $a < b$. Suppose that the following conditions are satisfied:

(i) Φ is approximable;

(ii) $\hat{\Phi}(e^{i\theta})$ is normal for all $i\theta$ with $0 \leq \theta < 2\pi$;

(iii) $< bh - N(h), N(h) - ah > \geq 0$ for all h in H;

(iv) $-b^{-1} \notin \bigcup_{|z| \leq 1}$ spec $\{\hat{\Phi}(z)\}$; and

(v) the set $\bigcup_{0 \leq \theta < 2\pi}$ spec $\{\hat{\Phi}(e^{i\theta})\}$ in the complex plane remains outside of and does not intersect the circle with center $-1/2(1/a+1/b)$ and radius $1/2(1/a-1/b)$.

Then the operator equations

$$e(\cdot) + \Phi[(\underset{\sim}{N}e)(\cdot) + x_1(\cdot)] = x_2(\cdot) \tag{34}$$

$$e(\cdot) + \underset{\sim}{N}[(\Phi e)(\cdot) + x_1(\cdot)] = x_2(\cdot) \tag{35}$$

where $(\underset{\sim}{N}y)(n) = N(y(n))$, are both L_2-stable.

We note that a proof of this theorem is given in[2] and that (34) and (35) may be written out in full as

$$e(n) + \sum_{0}^{n} \varphi(n-j)[N(e(j)) + x_1(j)] = x_2(n) \tag{36}$$

$$e(n) + N(\sum_{0}^{n} \varphi(n-j)e(j) + x_1(n)) = x_2(n). \tag{37}$$

Let us now examine an example.

EXAMPLE 3 Let $H = L_2[0,1]$ and consider the nonlinear differential-difference equation

$$\frac{d^2u_{n+2}(x)}{dx^2} - \frac{1}{4}\frac{d^2u_n(x)}{dx^2} = N(u_n(x))$$

with the auxiliary data

$$u_n(0) = u_n'(1) = 0$$
$$u_0(x) = f_0(x)$$
$$u_1(x) = f_1(x)$$

where f_0 and f_1 are elements of $L_2[0,1]$ and N is a bounded nonlinearity on $L_2[0,1]$. We seek to determine conditions which insure that $\sum_{n=0}^{\infty}\int_0^1 |u_n(x)|^2 dx < \infty$ for all f_0 and f_1.

To simplify matters, let us write $u(x,n)$ in place of $u_n(x)$, etc. With this convention in mind, we let $\gamma(x,n)$ be the solution of the homogeneous version of (38) with the auxiliary data (39) [i.e. $\gamma(0,n) = \gamma'(1,n) = 0$ and $\gamma(x,0) = f_0(x)$, $\gamma(x,1) = f_1(x)$]. It is easy to check that $\sum_{n=0}^{\infty}\int_0^1 |\gamma(x,n)|^2 dx < \infty$. Now we can reformulate (38) as an operator equation. To do this, we let $\Gamma(x,y)$ be the Green's function for the Sturm-Liouville problem on $[0,1]$ given by

$$-\frac{d^2}{dx^2}q(x) = f(x), \quad q(0) = q'(1) = 0 \tag{40}$$

so that

$$\Gamma(x,y) = \begin{cases} x & x < y \\ y & x > y \end{cases} \tag{41}$$

for x,y in $[0,1]$. We also let $\{\psi(n)\}$ be the "impulse response" for

the operator $(E^2-(1/4)I)$ on ℓ_2 (square summable sequences) where E is given by $E[\{a_n\}] = \{a_{n+1}\}$ (i.e. is a shift). Then,

$$\psi(n) = \begin{cases} 0 & n \text{ odd, zero or negative} \\ 1/2^{n-2} & n \text{ even} \end{cases} \tag{42}$$

It follows that (38), (39) has the equivalent representation

$$u(x,n) = \gamma(x,n) + \sum_{k=0}^{n}\int_0^1 \psi(n-k)\Gamma(x,y)N(u(y,k))dy. \tag{43}$$

Now (43) has the required form and we shall use theorem 2 to establish L_2-stability.

We let Φ be the element of B_{J^+} given by

$$(\Phi v)(x,n) = \sum_{k=0}^{n}\psi(n-k)\int_0^1\Gamma(x,y)v(y,k)dy \tag{44}$$

and we note that the z-transform of Φ, $\hat{\Phi}(z)$, is defined by

$$(\hat{\Phi}(z)w)(x) = \frac{z^2}{1-z^2/4}\int_0^1\Gamma(x,y)w(y)dy \tag{45}$$

for $w(\cdot)$ in $L_2[0,1]$ and $z \in C$ with $|z| \leq 1$. Since $\Gamma(x,y) = \Gamma(y,x)$, $\hat{\Phi}(z)$ is normal. Moreover, $\hat{\Phi}(z)$ is completely continuous on $|z| \leq 1$ as $\int_0^1\int_0^1|\Gamma(x,y)|dxdy < \infty$ and so, Φ is approximable. Now, to determine the spectrum of $\hat{\Phi}(z)$, it will be sufficient to determine the spectrum of the operator T given by

$$(Tw)(x) = \int_0^1\Gamma(x,y)w(y)dy \tag{46}$$

and then multiply by $z^2/(1-z^2/4)$. But it is well-known that the spectrum of T is the set $\{0, 1/(n+1/2)^2\pi^2 : n = 1,2,\ldots\}$ and so, spec $\{\hat{\Phi}(z)\} = \{0, z^2/(1-z^2/4)(n+1/2)^2\pi^2\}$. Thus, if we suppose that $-b^{-1} \neq (n+1/2)^{-2}\pi^{-2}(z^2/(1-z^2/4))$ for $|z| \leq 1$ and that the set $\{0, (1/(n+1/2)^2\pi^2)(e^{2i\theta}/(1-e^{2i\theta}/4)) : n = 1,2,\ldots, 0 \leq \theta < 2\pi\}$ remains outside of and does not intersect the proper circle, then the system (38) will be L_2-stable for any bounded nonlinearity N satisfying the inequality

$$\int_0^1[bw(x) - N(w(x))][N(w(x)) - aw(x)]dx \geq 0 \tag{47}$$

for all $w(x)$ in $L_2[0,1]$.

5. Conclusions

We have indicated in theorems 1 and 2 and in the examples, the rudiments of a very general theory of stability for systems defined over locally compact abelian groups. Detailed aspects of the general theory appear in[1] and[2].

Our results in this paper involve a generalization of the circle criterion (see, for example, [3]) in which the eigenvalues of certain operators being restricted to lie outside of an appropriate circle is a sufficient condition for stability. The results thus represent readily usable frequency domain criteria. We also note here that the general theory is applicable to a very wide class of systems. In particular, nonlinear problems involving systems described by ordinary differential equations, partial differential equations, differential-difference equations, and integral equations can be treated via the general theory.

References

[1] P.L. Falb and M.I. Freedman, A generalized transform theory for causal operators, to appear in SIAM J. on Control.

[2] M.I. Freedman, P.L. Falb and G. Zames, A Hilbert space stability theory over locally compact abelian groups, to appear.

[3] G. Zames, On the input - output stability of time-varying nonlinear feedback systems, Parts I, II. IEEE Trans. Automatic Control, AC-11(1966), 228-238, 465-476.

[4] N. Dunford and J. Schwartz, "Linear Operators, Part I: General Theory", Interscience, New York, 1958.

[5] M. Naimark, "Normed Rings", P. Noordhoff, Groningen, 1959.

[6] J. Kudrewicz, Stability of nonlinear feedback systems, Automatika i Telemechanika, vol. 25, 1964.

[7] I. W. Sandberg, On the properties of some systems that distort signals, Bell Sys. Tech. J., 43(1964), 91-112.

[8] I. W. Sandberg, On the L_2-boundedness of solutions of nonlinear functional equations, Bell Sys. Tech. J., 43(1964), 1581-1599.

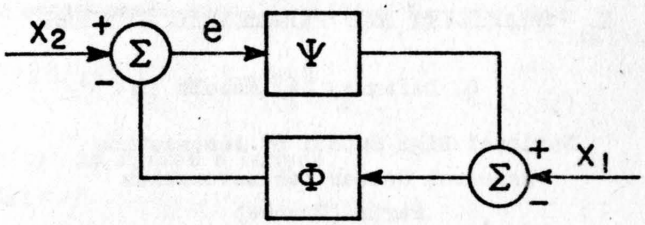

FIGURE 1: A feedback loop with two elements.

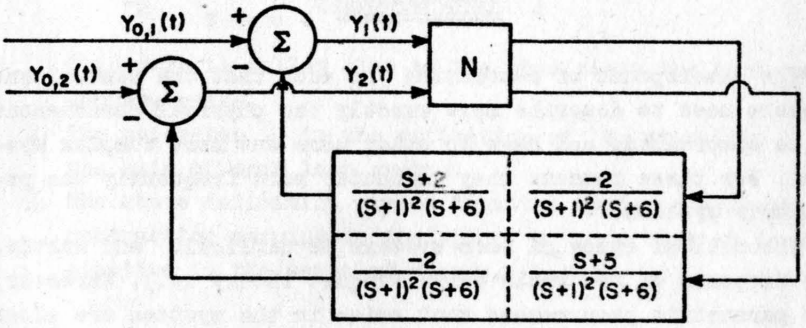

FIGURE 2: The system of Example 1.

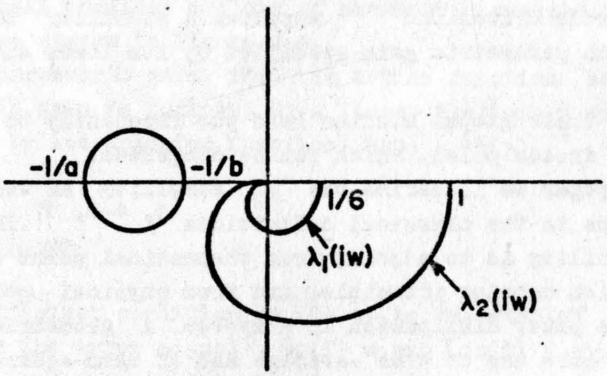

FIGURE 3: The "Nyquist" plots for Example 1.

M_2 STABILITY AND PARAMETRIC SYSTEMS

C. Lefevre, A. Raoult

National High School of Aeronautics
Research Center for Automation
Paris (France)

INTRODUCTION

The development of automation is such that the control engineers need to describe more exactly the physical phenomenons to be controlled, and have to study more and more complex systems. For these reasons they encounter more frequently the parametric systems.

Theoretical study of such systems is difficult and subtle, and disposes of few tools only (Floquet theory ...). Moreover, the parametric phenomenons that arise in the systems are often not well defined. Hence, it is necessary to possess the methods adapted to the acquired knowledge on a system. In such a way, the circle criterion [1, 3] supplies a stability test for a system with parametric gain specified by its lower and upper bound.

However, these global studies lead too frequently to the hypothesis of frozen poles, which can be dangerous.

In this paper we'll define the M_2 stability as well as its relations to the classical definitions [1, 4-6, 17]. This notion of stability is to adjoin, from theoretical point of view, to contraction mapping principle, and from physical point of view, to the power dissipation in a system. A geometric criterion that make use of time -average and of mean-square value of the varying parameter, will be established.

I. NOTATION AND DEFINITIONS

1-1. Definition: M_2 stability.
A control system is called "M_2-stable" if $\exists \lambda \in]0,1[$ such

that for every error signal $\varepsilon(t) \in M_2$ one has:

$$\lambda \| \varepsilon(t) \|_{M_2} = \| s(t) \|_{M_2} \qquad (1\text{-}1)$$

where $s(t)$ is system's output.

Remarks:

1. The space M_2 is composed of functions $f(t)$ such that

$$\|f(t)\|_{M_2} = \left[\lim_{T \to \infty} \frac{1}{T} \int_0^T |f(t)|^2 \, dt \right]^{1/2}$$

   This norm is called also by the physicists the root-mean-square value.
2. The parameter λ in the definition of M_2 stability is the gain of open loop system.
3. The above definition states that the system represents a contraction mapping in the space M_2, or that it is dissipative in the sense of energy.

1-2. System under study

We shall consider a class of parametric systems represented by the system in Figure 1-1.

The parametric gain $f(t)$ is a time function belonging to M_2. This gain is followed by a linear stationary operator described by its transfer function $G(p) = [H(p)]^{-1}$, strictly stable.

1-3. Lemma

A sufficient condition on (S) to be "M_2-stable" is that whatever the error signal $\varepsilon_\nu(t) = \exp[j\nu t]$ ($\forall \nu \in R$) is, the corresponding output signal satisfies:

$$\lambda_\nu \| \exp(j\nu t) \|_{M_2} = \| s_\nu(t) \|_{M_2} \qquad (1\text{-}2)$$

with $\lambda_\nu \in]0,1[$

or: $$\varepsilon'_\nu(j\omega) = \varepsilon(j\omega) \cdot \delta(\omega - \nu)$$

corresponding to a sinusoidal error signal with pulsation γ . Hence we have:

$$\mathcal{E}(j\omega) = \int_{-\infty}^{+\infty} \mathcal{E}'_{\gamma}(j\omega)\, d\omega$$

If $S'_{\gamma}(j\omega)$ is a Fourier transform of an output signal corresponding to $\mathcal{E}'_{\gamma}(t)$, $S(j\omega)$ that is relative to $\mathcal{E}(t)$ can be written as:

$$S(j\omega) = \int_{-\infty}^{+\infty} S'_{\gamma}(j\omega)\, d\gamma$$

Following the proof given in the Appendix, we write:

$$\|s(t)\|^2_{M_2} = \int_{-\infty}^{+\infty} \left|S(j\omega)\right|^2 d\omega \qquad (1\text{-}3)$$

$$= \int_{-\infty}^{+\infty} \left| \int_{-\infty}^{+\infty} S'_{\gamma}(j\omega)\, d\gamma \right|^2 d\omega \leq \int_{-\infty}^{+\infty} d\gamma \int_{-\infty}^{+\infty} \left|S'_{\gamma}(j\omega)\right|^2 d\omega$$

Assuming that the condition (1-2) is verified, we write:

$$\|s(t)\|^2_{M_2} \leqslant \int_{-\infty}^{+\infty} \lambda_{\gamma}^2 \left|\mathcal{E}(j\omega)\right|^2 d\omega$$

with

$$\lambda_{\gamma} \in \,]0,1[$$

Taking $\lambda = \operatorname{Sup}_{\gamma} \lambda_{\gamma}$ we have

$$\|s(t)\|_{M_2} \leq \lambda \|\mathcal{E}(t)\|_{M_2}$$

with

$$\lambda \in \,]0,1[$$

1-4. Relation "M_2-stability" - "L_2-stability"

A formal study of systems stability leads to search a func-

tion space the output $s(t)$ belongs to, given the space of the input $e(t)$. The spaces L_2 and L_∞ have been used[1,5, 16] to study an equi-asymptotic stability and bounded input-bounded output stability, respectively. The study of stability in M_2-space uses the signal power as principal variable. It has been shown recently that the sufficient condition of M_2-stability is that the system is contractiv for signals $\mathcal{E}(t) = \exp(j\nu t)$ $(\forall \nu \in R)$. This condition is close to the describing function method, nevertheless it is more global, since it takes into account the power only and doesn't take the amplitude and the phase.

On the other hand, it is interesting to show that the "M_2--stability" includes the "L_2-stability". Let us have a system (S), "M_2-stable":

$$\|s(t)\|_{M_2} = \lambda \|e(t) - s(t)\|_{M_2}$$

and

$$\|s(t)\|_{M_2} \leqslant \lambda \|e(t)\|_{M_2} + \lambda \|s(t)\|_{M_2}$$

then

$$\|s(t)\|_{M_2} \leqslant \frac{\lambda}{1-\lambda} \|e(t)\|_{M_2} \qquad (1\text{-}4)$$

which implies $s(t) \in M_2$ if $e(t) \in M_2$.

Note that if $e(t) \in L_2$, then $\|e(t)\|_{M_2} = 0$, and according to (1-4), $\|s(t)\|_{M_2} = 0$, which proves that $s(t)$ belongs to L_2. Hence, a system (S) which is "M_2-stable", is "L_2--stable" also.

Remark:

$$\|e(t)\|_{L_2} = \left[\int_0^{+\infty} |e(t)|^2 \, dt\right]^{1/2}$$

1-5. "λ M_2-stability"

Definition. A system (S) is said to be "λM_2-stable" if its output is stable as $\exp(-\lambda t)$.

For $s(t)$ to converge as $\exp(-\lambda t)$ it is sufficient that: $\tilde{s}(t) = s(t) \exp(\lambda t)$ is the output of a "M_2-stable" system.

Let us consider the system $(\tilde{S})$ with a structure equivalent to that of (S), described by the following equations:

$$\begin{aligned} \tilde{u}(t) &= -g(t)\ \tilde{s}(t) \\ \tilde{U}(p) &= \tilde{H}(p)\ \tilde{S}(p) \end{aligned} \qquad (1\text{-}5)$$

We seek a relation between H and $\tilde{H}$.

Starting from the equations defining (S):

$$u(t) = -g(t)\ s(t)$$

$$U(p) = H(p)\ S(p)$$

multiplying first equation by $\exp(\lambda t)$ and replacing p by $p-\lambda$ in the second, we get:

$$u(t)\exp(\lambda t) = -g(t)\ s(t)\exp(\lambda t)$$

$$U(p-\lambda) = H(p-\lambda)\ S(p-\lambda)$$

which can be written as:

$$\begin{aligned} \tilde{u}(t) &= u(t)\exp(\lambda t) = -g(t)\ \tilde{s}(t) \\ \tilde{U}(p) &= U(p-\lambda) = H(p-\lambda)\ \tilde{S}(p) \end{aligned} \qquad (1\text{-}6)$$

The system defined by (1-6) is represented in Fig. 1-2, where the operator $\tilde{H}(p) = H(p-\lambda)$.

The study of "λM_2-stability" of a system (S) is therefore equivalent to that of "M_2-stability" of the system (S) obtained by replacing p by $p-\lambda$.

A criterion that we'll prove later will allow to define a margin of absolute stability having greater practical significance than the stability limit.

II. CRITERION OF "M_2-STABILITY"

2-1. Criterion (C1)

A sufficient condition for a system (S) to be "M_2-stable" is that:

$$\|f(t)\|_{M_2} < \inf_{\omega} |H(j\omega)| \qquad (C1)$$

If $\xi(t) = \exp(j\nu t)$, the system (S) is defined by

$$u(t) = f(t)\exp(j\nu t) \tag{2-1}$$

$$U(p) = H(p)\,S_\nu(p) \tag{2-2}$$

Starting from (2-2) we'll write (see Appendix):

$$\|u(t)\|_{M_2}^2 = \int_{-\infty}^{+\infty} |H(j\omega)\,S_\nu(j\omega)|^2\,d\omega$$

$$\|u(t)\|_{M_2}^2 \geq \inf_\omega |H(j\omega)|^2 \int_{-\infty}^{+\infty} |S_\nu(j\omega)|^2\,d\omega$$

$$\|u(t)\|_{M_2}^2 \geq \inf_\omega |H(j\omega)|^2 \|s_\nu(t)\|_{M_2}^2$$

Consequently

$$\|s_\nu(t)\|_{M_2} \leq \frac{\|u(t)\|_{M_2}}{\inf_\omega |H(j\omega)|}$$

We apply "M_2-stability" condition (lemma 1-3). It will be satisfied if

$$\frac{\|u(t)\|_{M_2}}{\inf_\omega |H(j\omega)|} = \lambda_\nu \tag{2-3}$$

On the other hand, equation (2-1) yields:

$$\|u(t)\|_{M_2} = \|f(t)\exp(j\nu t)\|_{M_2} = \|f(t)\|_{M_2}$$

and equation (2-3) can be written as:

$$\|f(t)\|_{M_2} = \lambda_\nu \inf_\omega |H(j\omega)| \quad \text{with} \quad \lambda_\nu \in\,]0,1[\quad \forall \nu \in \mathbb{R}$$

the above formula yields the criterion (C1):

$$\|f(t)\|_{M_2} < \inf_\omega |H(j\omega)| \tag{C1}$$

Remarks:

1. If a linear system with transfer function $G(p) = \frac{1}{H(p)}$ is at the stability limit, $\inf_{\omega} H(j\omega) = 0$, the parametric system is there also, $\|f(t)\|_{M_2} = 0$.

2. If the nature of function $f(t)$ is better defined, it is possible to improve this criterion. In particular, it $f(t)$ can be represented by $f(t) = \sum_n f_n \exp(j\omega_n t)$, a more efficient criterion is valid [13, 17] :

$$1 > \text{Sup} \sum_n |f_n|^2 |G(\omega + \omega_n)|^2 \qquad (C'1)$$

2-2. Criterion (C2)

Consider now a modified system (Sm) (see Fig. 2-1). This system is equivalent to the system (S). A study of the stability of (Sm) supplies the one of (S).

Let us denote:

$$f(t) = g(t) + M$$

where

$$M = \lim_{T \to \infty} \frac{1}{T} \int_0^T f(t)\, dt$$

By application of criterion (C1) to the system (Sm) we get:

$$\lambda_\nu \inf_{\omega} |H(j\omega) + M - L(j\omega)| = \|(g(t) + L(j\nu)) \exp(j\nu t)\|_{M_2}$$

or, alternately:

$$\lambda_\nu^2 \inf_{\omega} |H(j\omega) + M - L(j\omega)|^2 = \|g(t)\|_{M_2}^2 + |L(j\nu)|^2$$

The stability condition given previously has to be verified for all ν, which implies:

$$\inf_{\omega} \left| H(j\omega) + M - L(j\omega) \right|^2 - \max_{\nu} \left| L(j\nu) \right| > \| g(t) \|_{M_2}^2 \qquad (2\text{-}4)$$

Transfer function $L(p)$ has to be determined in such a manner that inequality (2-4) is optimised, that is:

$$\| g(t) \|_{M_2}^2 < \max_{L} \left(\inf_{\omega} \left| H(j\omega) + M - L(j\omega) \right|^2 + - \max_{\nu} \left| L(j\nu) \right|^2 \right) \qquad (C2)$$

Remarks:

1. The linear part of the system (Sm) is always stable in the domain of application of criterion (C2). Indeed, the stability limit of (Sm) involves
$$\inf_{\omega} \left| H(j\omega) + M - L(j\omega) \right| = 0$$
which corresponds to $\| g(t) \|_{M_2} < 0$, an impossible condition.
2. The problem of determining an optimal operator $L(p)$ remains to the solved. One may expect that this would enable to close together the necessary and the sufficient stability condition.

2-3. Geometric criterion

Let $L(p) \equiv \mu$, a real constant. Criterion (C2) becomes therefore in the limit:

$$\| g(t) \|_{M_2}^2 = \max_{\mu} \left(\inf_{\omega} \left| H(j\omega) + M - \mu \right|^2 - \mu^2 \right) \qquad (2\text{-}5)$$

Consider a locus of $H(j\omega) + M$ in the complex plane (Fig. 2-2). For fixed value of μ a locus of $H(j\omega) + M - \mu$ can be obtained from the previous one by translation μ of the imaginary axis, or I'm this new axis. We'll seek next the smallest circle inscribed into $H(j\omega) + M$, centered into O'. A radius R of this circle is such that: $R = \inf_{\omega} \left| H(j\omega) + M - \mu \right|$

Let us consider the triangle O'OA :

$$\overline{O'A}^2 = \overline{OO'}^2 + \overline{OA}^2$$

or

$$R^2 - \mu^2 = \overline{OA}^2 \tag{2-6}$$

Equations (2-6) and (2-5) involve: $g(t)_{M_2} = OA$ for fixed value of μ . μ is an arbitrary parameter that may be choosed such that $\|g(t)\|_{M_2}$ is maximum. This is realized for a value of μ such that the intersection (point A in Figure 2-2) of the imaginary axis with the inscribed circle centered on the real axis, is the closest possible to the point B .

We consider now a case when the inscribed circle is tangent at B (Fig. 2-3). We have then:

$$\text{Im } (H(j\omega) + M) = \|g(t)\|_{M_2}$$

$$\text{Re } (H(j\omega) + M) = 0$$

$$\mu = \text{Im } (H(j\omega) + M) \frac{d \text{ Im } (H(j\omega) + M)}{d \text{ Re } (H(j\omega) + M)}$$

eliminating the limit (see equation(2-5)) we get:

$$\boxed{\begin{array}{c} \|g(t)\|_{M_2} < \text{Im } H(j\omega) \\ M = -\text{Re } H(j\omega) \end{array}} \tag{C3}$$

with

$$\mu = \text{Im } H(j\omega) \frac{d \text{ Im } H(j\omega)}{d \text{ Re } H(j\omega)}$$

Geometric interpretation of (C3) is given in Fig. 2-4.

2-4. Examples

Criterion (C3) allowed us to determine the stability as well as the "$\exp(-\lambda t)$- stability" of a third order system.The results are given in Fig. 2-4.

Criteria (C'1) and (C3) have been applied to a system representing Hill equation. A comparison of classical stability criteria have been performed on this example, and the results are shown in Fig. 2-5.

2-5. Application of the geometric criterion

We define three types of systems that corresponds to different applications of the criterion (C3).

Type 1 systems

These are the systems for which the best result is obtained with $\mu = 0$. Criterion (C3) yields the same result as criterion (C1).

In inverse locus, the inscribed circle centered at the origin is tangent to $H(j\omega) + M$ on the imaginary axis. Common tangent line is horizontal (Fig. 2-7-a).

In direct locus, the circumscribed circle centered at the origin is tangent to a locus $G'(j\omega) = [H(j\omega) + M]^{-1}$ on the imaginary axis. Common tangent line is horizontal (Fig. 2-7-b).

Type 2 systems

These are the systems for which the criterion (C3) is directly applicable and yields better results that the criterion (C1).

The circumscribed circle of type 2 systems as well as the inscribed one are not centered at the origin (Fig. 2-8-a, b).

Type 3 systems

These are the systems that do not belong to the type 1 nor 2. The criterion (C3) is not applicable.

There is no circle tangent to $H(j\omega) + M$ on the imaginary axis, and $\|g(t)\|_{M_2} = OA \neq OB$ (see section 2-3 and Fig. 2-9b). Likewise, there is no circle circumscribered on $G'(j\omega)$, tangent on the imaginary axis (Fig. 2-9-a). One has:

$$\overline{OA'} = -\left[\|g(t)\|_{M_2}\right]^{-1} .$$

This classification shows that the criterion (C3) obtained for $L(p) = \mu$ is not fully satisfying (see section 2-2, remark 2), and that there exists perhaps a better operator $L(p)$. This problem remains entirely unsolved.

CONCLUSION

Introduction of the "M_2-stability" into the theory of parametric systems has allowed to establish new stability criteria. These criteria are easy to apply, and the geometric form of one of them is particularly simple and synthetic. The simplicity of application by no means alters the quality of results, which are better than those obtained by the classical criteria.

The "M_2-stability" is a tool that is sufficiently elaborated to detect stable parametric system with possibly instable instantaneous poles (frozen poles). This mathematical tool, that uses functional analysis, is akin to the frequency analysis, being more global however.

The "M_2-stability" is particularly well adapted to system's theory, and it is expected that a synthesis of the methods used for parametric and nonlinear systems will be therefore possible.

APPENDIX

If $s(t) \in M_2$, according to Bohr theorem [*], $s(t)$ can be represented by $s(t) = \sum_n S_n \exp(j\omega_n t)$, where the set $\{\omega_n\}$ is finite or denumerable.

A Fourier transform of $s(t)$ may be written as:

$$S(j\omega) = \sum_n S_n \cdot \delta(\omega - \omega_n)$$

Hence

$$\int_{+\infty}^{-\infty} |S(j\omega)|^2 \, d\omega = \int_{-\infty}^{+\infty} \sum_n \sum_m S_n S_m^{*} \, \delta(\omega - \omega_n)\, \delta(\omega - \omega_m) d\omega$$

and according to an elementary property of distributions:

---

[*] F. Riesz, B. Nagy, Budapest 1953.

$$\int_{-\infty}^{+\infty} \delta(\omega - \omega_n)\,\delta(\omega - \omega_m)\,d\omega = \delta(\omega_n - \omega_m)$$

it becomes

$$\int_{-\infty}^{+\infty} |S(j\omega)|^2\,d\omega = \sum_n \sum_m S_n S_m^{*}\,\delta(\omega_n - \omega_m) =$$

$$= \sum_n |S_n|^2 = \lim_{T \to \infty} \frac{1}{2T} \int_{-T}^{+T} |s(t)|^2\,dt$$

or

$$\int_{-\infty}^{+\infty} |S(j\omega)|^2\,d\omega = \|s(t)\|_{M_2}$$

Remark

If $\|s(t)\|_{M_2} = 0$, $s(t)$ belongs then to L_2 and the above reasoning is not valid.

REFERENCES

1. J.W. Sandberg, A frequency domain condition for the stability of systems containing a single time varying non-linear element. Bell Syst. Techn. J. July 1964.
2. J.J. Bongiorno, Real frequency stability criteria for linear time varying systems. Proc. IEEE vol. 52.
3. B.N. Naumov, Frequency method for investigation of absolute process stability in non-linear automatic control systems. IFAC Congr. London June 1966.
4. R.W. Brockett, The status of stability theory for deterministic systems. IEEE Winter-Convention, March 1966.
5. G. Zames, On the input-output stability of time varying non-linear feedback systems. Pt. 1. IEEE Trans. on Automatic Control vol. AC - 11, Avril 1966.

6. G. Zames, On the input-output stability of time varying non-linear feedback systems.Pt. 2.IEEE Trans. on Automatic Control July 1966.
7. A. Rault, Stability of time varying feedback systems. P.H. D. Thesis University of California Berkeley 1966.
8. M. Cotsaftis, Conditions nécessaires et suffisantes de stabilité globale d'une classe de mouvements non-linéaires , non dissipatifs. C.R. Acad. Sci. Paris Octobre 1967.
9. C. Lefevre, M. Houdebine, J. Richalet, Systèmes linéaires paramétriques et commande structurelle. IFAC Congr. London 1966.
10. J. Richalet, C. Fefevre, Système d'ordre quelconque à coefficients périodiques. C.R. Acad. Sci. Paris Mars 1966.
11. C. Lefevre, Systèmes linéaires à structure variable. C.R. Acad. Sci. Paris Décembre 1966.
12. C. Lefevre, M. Cotsaftis, Un critère de stabilité globale des systèmes paramétriques. C.R. Acad. Sci. Paris Novembre 1967.
13. C. Lefevre, M. Cotsaftis, Un critère de stabilité pour des systèmes à structure périodique ou presque périodique. C R. Acad. Sci. Paris Décembre 1967.
14. M. Cotsaftis, C. Lefevre, Une condition de stabilité globale des systèmes non-linéaires. C.R. Acad. Sci. Paris t. 266 Série A, 15 Janvier 1968.
15. J. Richalet, C. Lefevre, Critères énergétiques de stabilité. Onde Electrique Janvier 1968.
16. J. Kudrewicz, Stability of non linear feedback systems.Automatykha i Telemekhanyka vol. XXV 1964 No. 8.
17. J. Kudrewicz, Stabilność układów zawierających element zmienny w czasie prawie okresowo. Prace IV Krajowej Konferencji Automatyki 1967 (in Polish).

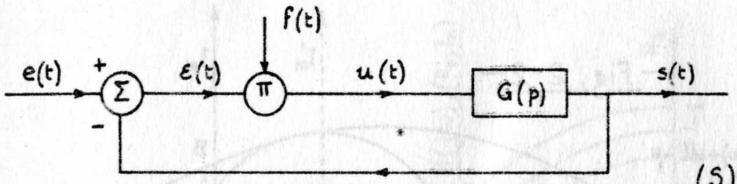

$$H(p) = [G(p)]^{-1} \qquad (S)$$

— Fig. 1-1 —

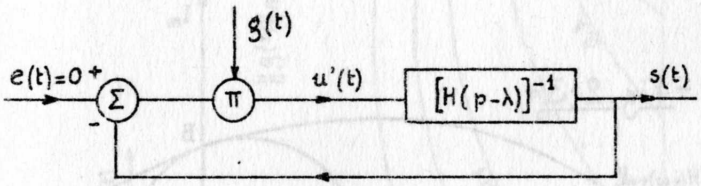

— Fig. 1-2 —

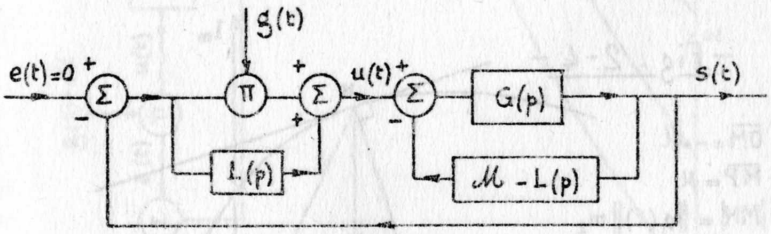

$$g(t) = f(t) - M \qquad (S_m)$$
$$H(t) = [G(p)]^{-1}$$

— Fig. 2-1 —

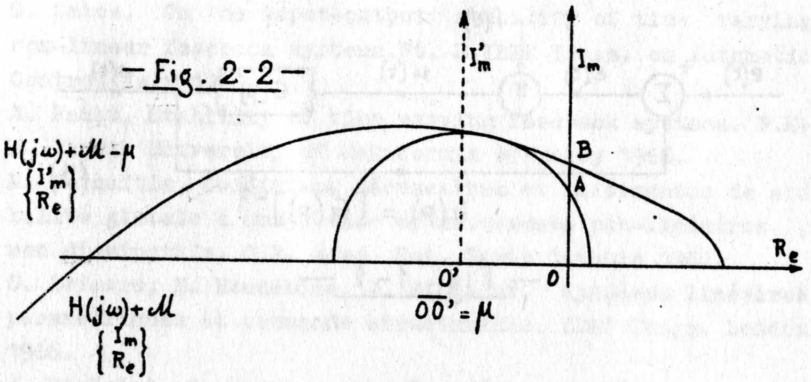

-Fig. 2-2-

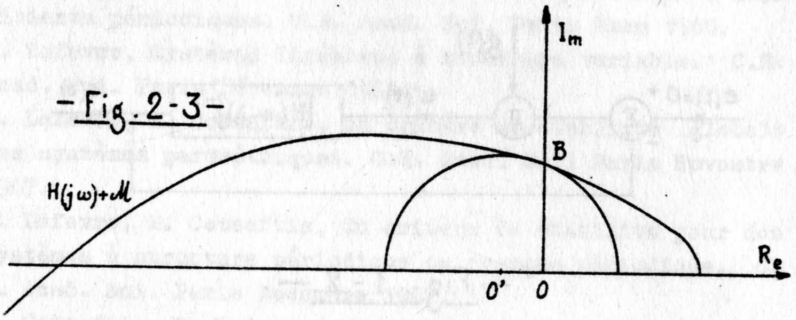

-Fig. 2-3-

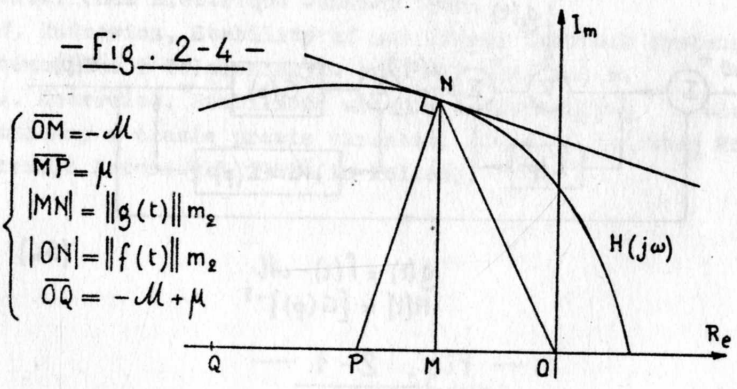

-Fig. 2-4-

$$\begin{cases} \overline{OM} = -M \\ \overline{MP} = \mu \\ |MN| = \|g(t)\|_{m_2} \\ |ON| = \|f(t)\|_{m_2} \\ \overline{OQ} = -M + \mu \end{cases}$$

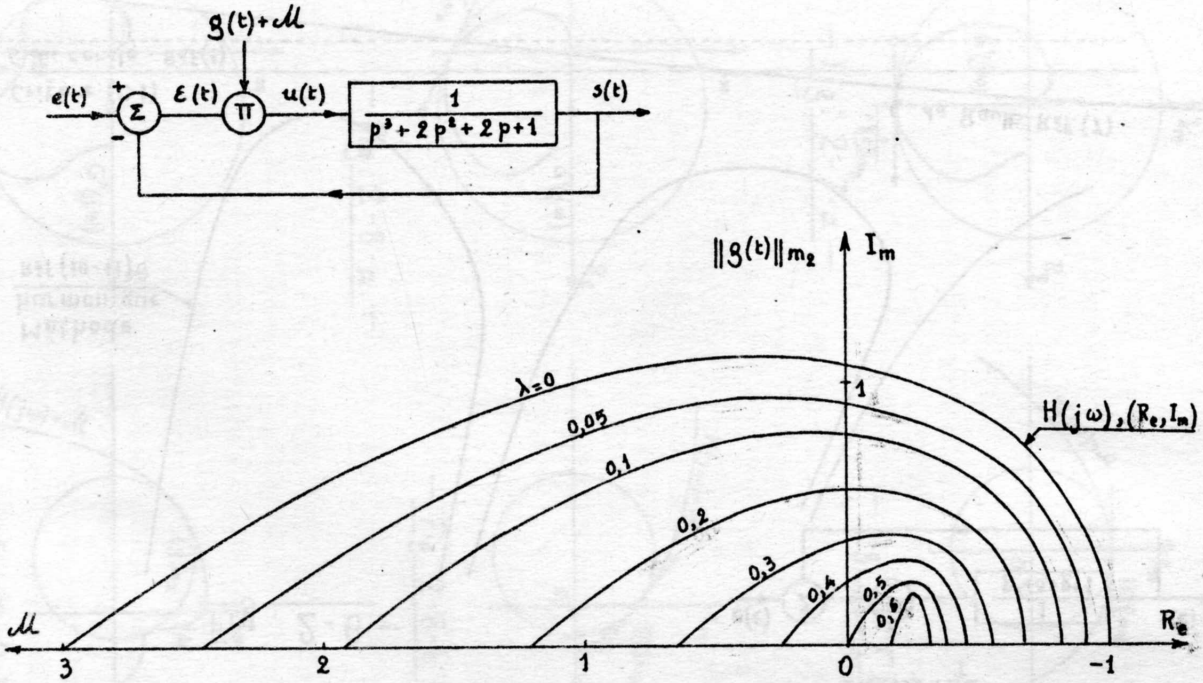
g(t)+M
e(t)
+
-
Σ
ε(t)
ΠΠ
u(t)
1
p³+2p²+2p+1
s(t)
‖g(t)‖m₂
Im
λ=0
0,05
0,1
0,2
0,3
0,4
0,5
0,6
1
H(jω), (Re, Im)
M
3
2
1
0
-1
Re

— Fig. 2-5 —

- Fig. 2-6 -

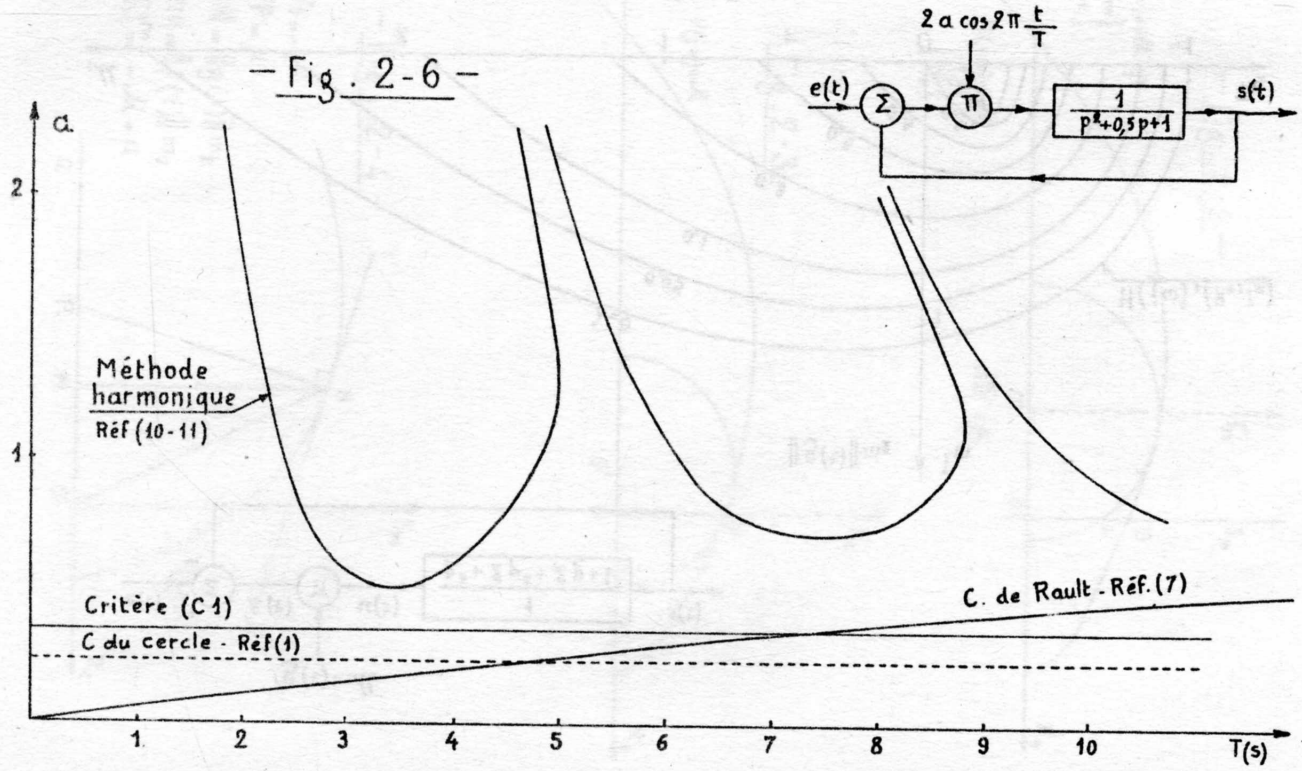
2 a cos 2π t/T
e(t)
Σ
Π
1/(p²+0,5p+1)
s(t)
a.
2
1
Méthode harmonique
Réf (10-11)
Critère (C 1)
C du cercle - Réf(1)
C. de Rault - Réf. (7)
1
2
3
4
5
6
7
8
9
10
T(s)

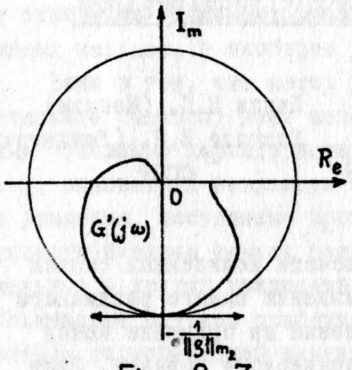

— Fig. 2-7-a —

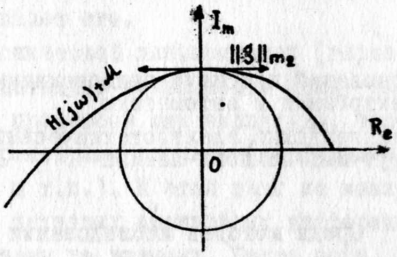

— Fig. 2-7-b —

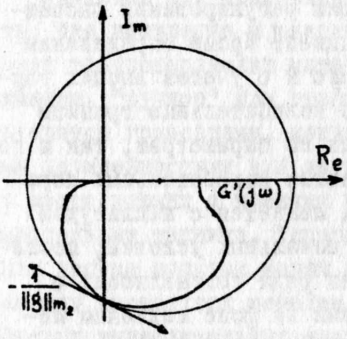

— Fig. 2-8-a —

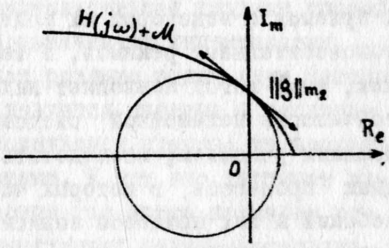

— Fig. 2-8-b —

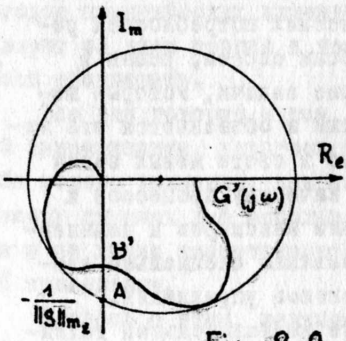

— Fig. 2-9-a —

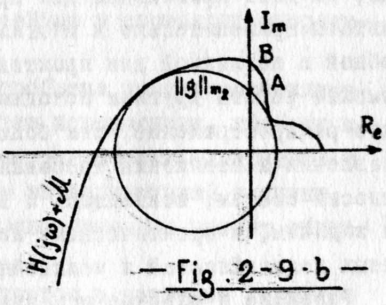

— Fig. 2-9-b —

РАЗВИТИЕ МЕТОДА ГАРМОНИЧЕСКОЙ ЛИНЕАРИЗАЦИИ

Московский институт радиотехники, электроники и автоматики
Ленинградский электротехнический институт им.Ульянова-Ленина

Попов Е.П. (Москва)
Хлыпало Е.И. (Ленинград)
СССР

Среди методов исследования и расчета нелинейных систем автоматического регулирования и управления самого различного назначения нашел широкое распространение на практике метод гармонической линеаризации или гармонического баланса. Этот метод удачно сочетает учет основных специфических нелинейных свойств, недоступных линейной теории, с возможностью применения хорошо знакомых из линейной теории регулирования расчетных приемов с некоторой их модернизацией.[1] Кроме определения автоколебательных режимов, в том числе и с учетом высших гармоник, этот метод позволяет находить колебательные границы устойчивости нелинейной системы, как по параметрам, так и по начальным условиям; исследовать качество колебательных переходных процессов, в которых частота меняется с амплитудой колебаний и вид процесса зависит от начальных условий; исследовать сложные процессы, состоящие из ряда составляющих с различными порядками частот (колебания на фоне медленно меняющихся составляющих и т.п.) с учётом нелинейной взаимосвязи между ними, когда несправедлив принцип суперпозиции решений.[2]

Несмотря на приближенность, а иногда и нестрогость метода, он дает правильные для практических потребностей результаты применительно к многим классам систем, решая в удобной и наглядной для практики форме задачи, которые невозможно решить другими методами. Этим и объясняется его широкое распространение, тем более, что в свете новых задач управления и повышения требований к качеству процессов и точности систем, повысилось и внимание инженеров к нелинейным задачам, к практическому использованию специально введенных нелинейностей и нелинейных законов управления.

Развитие и широкое использование вычислительной техни-

ки отнюдь не уменьшает практическое значение подобных приближенных методов, а наоборот усиливает его.

Дело в том, что метод гармонической линеаризации (гармонического баланса) дает непосредственно зависимости между такими основными характеристиками процессов как амплитуды, частоты, показатели затухания и параметрами системы (коэффициенты усиления, постоянные времени и т.п.). К этой цели не может привести никакое точное решение исходных нелинейных дифференциальных и других уравнений системы во времени. Более того, в большинстве случаев приближенное решение задач, получаемое методом гармонической линеаризации, нельзя заменить другими более точными, хотя бы и сложными, алгоритмами для использования вычислительной техники.

Учитывая это принципиальное обстоятельство, можно сказать, что появление и развитие вычислительной техники способствует распространению метода гармонической линеаризации. А именно, "ручное" или графическое решение задач этим методом становится громоздким, когда исследуется система с несколькими нелинейностями или когда исследуется процесс из нескольких составляющих с разными частотами. И тут нас выручает вычислительная техника. Теперь имеется уже много примеров решения весьма сложных задач в промышленных научно-исследовательских институтах методом гармонической линеаризации на цифровых вычислительных машинах типа М-20 и др. с воплощением результатов решения в реальных нелинейных системах управления.

Многолетний опыт показал, что возможности решения этим методом практических инженерных задач значительно шире, чем говорит об этом теория и чем мы сейчас в состоянии теоретически обосновать.

Все это говорит о том, что проблема метода гармонической линеаризации, казалось бы давно исчерпанная, требует к себе нового внимания, как по линии разработки алгоритмов в сложных случаях для использования вычислительной техники, так и по линии теоретического обоснования для разных областей применения.

В связи с этим, неизбежным является и развитие прикладной стороны метода гармонической линеаризации в различных

направлениях.

В данном сообщении пойдет речь о новой форме представления гармонически линеаризованного эквивалента для неоднозначных нелинейностей с гистерезисными петлями, которые часто встречаются на практике. Эта новая форма позволяет исправить существенную некорректность, появляющуюся в некоторых задачах при формальном применении метода в старой записи.

Гармонически линеаризованное выражение для неоднозначных нелинейностей

$$y = F(x) \tag{1}$$

с гистерезисными петлями принято записывать в форме

$$y = [a(A) + \frac{b(A)}{\omega} p]x, \qquad b(A) < 0, \tag{2}$$

где A, ω - амплитуда и частота колебаний, $a(A)$ и $b(A)$ - коэффициенты:

$$a = \frac{1}{\pi A}\int_0^{2\pi} F(A\sin\psi)\sin\psi d\psi, \quad b = \frac{1}{\pi A}\int_0^{2\pi} F(A\sin\psi)\cos\psi d\psi. \tag{3}$$

В результате в передаточной функции разомкнутой системы появляется полюс, расположенный в правой полуплоскости (меняющий свое положение при изменении амплитуды колебаний). По терминологии линейной теории регулирования получается эквивалентное линеаризованное неминимальнофазовое звено.

Часто при замыкании системы это не влечет за собой никаких последствий и все выкладки метода идут нормально. Однако есть класс систем, в которых это приводит к отрицательному знаку некоторых коэффициентов характеристического уравнения, что должно было бы свидетельствовать о неустойчивости искомых колебаний, в то время как они оказываются на самом деле устойчивыми. Решение же для амплитуды и частоты колебаний получается при этом правильным.

Пример такой системы дан на рис.1. Динамика системы описывается уравнениями

$$\varepsilon = g_1 - g_2, \quad u_3 = \frac{k_3}{1+T_2 p}(u_2 - u_{oc}), \quad R = k_4 u_4.$$

$$u_1 = k_1 \varepsilon, \quad u_{oc} = k_{oc} p \Omega, \quad q_2 = \frac{k_5}{p} \Omega,$$

$$u_2 = \frac{k_2 u_1}{1 + T_1 p}, \quad u_4 = F(u_3) = a(A) u_3 + \frac{b(A)}{\omega} p u_3,$$

$$k = k_1 k_2 k_3 k_4 k_5, \qquad k_6 = k_3 k_4 k_{oc}.$$

Передаточная функция части схемы, охваченной контуром обратной связи, имеет вид

$$W_1(p) = \frac{\Omega}{u_2} = \frac{k_3 k_4 \left[a(A) + \frac{b(A)}{\omega} p\right]}{1 + T_2 p + k_6 \left[a(A) + \frac{b(A)}{\omega} p\right] p}.$$

Передаточная функция разомкнутой системы будет

$$W(p) = \frac{k \left[a(A) + \frac{b(A)}{\omega} p\right]}{p(1 + T_1 p)\left\{1 + T_2 p + k_6 p \left[a(A) + \frac{b(A)}{\omega} p\right]\right\}}.$$

Характеристическое уравнение рассматриваемой системы имеет вид

$$W(p) + 1 = 0$$

или

$$A_0 p^4 + A_1 p^3 + A_2 p^2 + A_3 p + A_4 = 0.$$

Коэффициенты характеристического уравнения будут

$$A_0 = T_1 k_6 \frac{b(A)}{\omega},$$

$$A_1 = T_1 T_2 + T_1 k_6 a(A) + k_6 \frac{b(A)}{\omega},$$

$$A_2 = T_1 + T_2 + k_6 a(A),$$

$$A_3 = 1 + k \frac{b(A)}{\omega}, \quad A_4 = k a(A).$$

Согласно (2) коэффициент A_0 будет отрицательным. Может оказаться отрицательным также и коэффициент A_3, в то время как остальные коэффициенты заведомо положительны.

Это является следствием неудачного выбора формулы эквивалентного гармонически линеаризованного выражения (2), которая

обычно в гармоническом балансе применяется. Сохранив тот же правильный окончательный результат решения для амплитуды и частоты, можно избежать указанной некорректности промежуточного выражения (характеристического уравнения), если для нелинейного звена (1) с неоднозначной петлевой нелинейностью гистерезисного типа принять форму эквивалентной гармонически линеаризованной передаточной функции инерционного звена в виде

$$y = \frac{k_*(A)}{1+T_*(A)p}x . \qquad (4)$$

Новые коэффициенты гармонической линеаризации $k_*(A)$ и $T_*(A)$, т.е. зависящие от искомой амплитуды колебаний коэффициент усиления и постоянная времени инерционного звена, эквивалентного нелинейному звену с гистерезисными петлями, могут быть выражены через прежние коэффициенты гармонической линеаризации, $a(A)$ и $b(A)$ тождественным образом.

В случае периодических колебаний, когда $p=j\omega$, из требуемого тождества

$$\frac{k_*}{1+T_* j\omega} = a + \frac{b}{\omega} j\omega \qquad (b<0)$$

вытекает

$$\frac{k_*}{1+T_*^2\omega^2} = a(A), \quad \frac{k_* T_* \omega}{1+T_*^2\omega^2} = -b(A),$$

откуда

$$T_* = \frac{-b(A)}{\omega a(A)}, \quad k_* = \frac{a^2(A)+b^2(A)}{a(A)}, \qquad (5)$$

где $b(A)<0$, причем $a(A)$ и $b(A)$ определяются формулами (3).

В случае затухающих и расходящихся колебаний эквивалентное гармонически линеаризованное выражение для неоднозначной

петлевой нелинейности $F(x)$ вместо (2) обычно применяется в виде

$$y=\left[a(A)-\frac{\xi}{\omega}b(A)+\frac{b(A)}{\omega}p\right]x, \qquad (6)$$

где ξ для затухающих колебаний <0 и $\xi>0$ для расходящихся.

В этом случае, когда $p=\xi+j\omega$, из требуемого тождества

$$\frac{k_*}{1+T_*(\xi+j\omega)}=a-\frac{\xi}{\omega}b+\frac{b}{\omega}(\xi+j\omega)$$

вытекает

$$\frac{k_*(1+T_*\xi)}{(1+T_*\xi)^2+T_*^2\omega^2}=a(A),\quad \frac{k_*T_*\omega}{(1+T_*\xi)^2+T_*^2\omega^2}=-b(A),$$

откуда

$$\omega T_*=\frac{-b(A)}{a(A)+\frac{\xi}{\omega}b(A)},\quad k_*=\frac{a^2(A)+b^2(A)}{a(A)+\frac{\xi}{\omega}b(A)},$$

где $b(A)<0$, причем $a(A)$ и $b(A)$ определяются прежними формулами (3).

В случае сложных процессов, когда колебания наложены на медленно меняющуюся составляющую, приближенное решение вместо $x=A\sin\omega t$ ищется в форме $x=x^0+x^*$, где $x^*=A\sin\omega t$, а обычная форма гармонической линеаризации вместо (2) имеет вид

$$y=F^0(A,x^0)+\left[a(A,x^0)+\frac{b(A,x^0)}{\omega}p\right]x^*, \qquad (8)$$

где

$$\left.\begin{aligned} F^{\circ} &= \frac{1}{2\pi}\int_0^{2\pi} F(x^{\circ}+A\sin\psi)\,d\psi, \\ a &= \frac{1}{\pi A}\int_0^{2\pi} F(x^{\circ}+A\sin\psi)\sin\psi\,d\psi, \\ b &= \frac{1}{\pi A}\int_0^{2\pi} F(x^{\circ}+A\sin\psi)\cos\psi\,d\psi. \end{aligned}\right\} \qquad (9)$$

При этом уравнение нелинейной системы

$$Q(p)x + R(p)F(x) = N(p)f(t), \qquad (10)$$

где $f(t)$ медленно меняющееся по сравнению с частотой колебаний ω внешнее воздействие, разбивается после гармонической линеаризации на два нелинейно взаимосвязанных уравнения

$$Q(p)x^{\circ} + R(p)F^{\circ}(A,x^{\circ}) = N(p)f(t), \qquad (11)$$

$$Q(p)x^{*} + R(p)\left[a(A,x^{\circ}) + \frac{b(A,x^{\circ})}{\omega}p\right]x^{*} = 0. \qquad (12)$$

В этом случае новую форму эквивалентной передаточной функции можно применить в уравнении (12), т.е. стоящее там выражение в квадратных скобках можно заменить на

$$\frac{k_{*}(A,x^{\circ})}{1+T_{*}(A,x^{\circ})p},$$

причём

$$T_{*} = \frac{-b(A,x^{\circ})}{\omega a(A,x^{\circ})}, \qquad k_{*} = \frac{a^{2}(A,x^{\circ})+b^{2}(A,x^{\circ})}{a(A,x^{\circ})},$$

где a и b определяются формулами (9), $b<0$.

Аналогично можно поступать и для вынужденных колебаний, когда в правой части уравнения нелинейной системы (10) имеет-

ся

$$f(t)=B\sin\omega t \quad \text{или} \quad f(t)=f^0(t)+B\sin\omega t.$$

Опишем расчет с использованием новой формы гармонической линеаризации для указанного выше примера нелинейной системы (рис.1).

Для рассматриваемого вида неоднозначной нелинейности с гистерезисными петлями выражения для коэффициентов гармонической линеаризации имеют вид

$$a=\frac{2h}{\pi A}\left(\sqrt{1-\frac{c^2}{A^2}}+\sqrt{1-\frac{m^2c^2}{A^2}}\right),$$

$$b=-\frac{2ch}{\pi A^2}(1-m), \qquad \text{при } A\geq c,$$

где A – амплитуда колебаний напряжения u_3. Например, для численных значений параметров нелинейного звена: $h=110\,в$, $c=24\,в$, $m=0{,}2$, графики коэффициентов гармонической линеаризации представлены на рис.2. По графикам рис.2 с использованием формул (5) легко могут быть построены зависимости эквивалентных параметров k_* и ωT_* от амплитуды колебаний, которые представлены на рис.3.

Следует иметь в виду, что формулы гармонической линеаризации, а, следовательно, и графики рис.3 имеют смысл только при $A>c$. Поэтому величина T_* ограничена. Как видно из кривых рис.3, с увеличением амплитуды A постоянная времени T_* уменьшается, что для данной нелинейности равносильно уменьшению влияния гистерезисных петель при больших амплитудах колебаний.

С учётом формулы (4) для эквивалентной передаточной функции динамика системы (рис.1) опишется уравнениями:

$$\varepsilon=g_1-g_2, \quad u_3=\frac{k_3}{1+T_2p}(u_2-u_{oc}), \quad u_{oc}=k_{oc}p\Omega,$$

$$u_1=k_1\varepsilon, \quad u_4=\frac{k_*}{1+T_*p}u_3, \quad g_2=\frac{k_5\Omega}{p},$$

$$u_2=\frac{k_2}{1+T_1p}u_1, \quad \Omega=k_4u_4.$$

Передаточная функция части схемы, охваченной обратной связью, имеет вид

$$W_1 = \frac{k_3 k_4 k_*}{(1+T_2 p)(1+T_* p) + k_6 k_*}, \quad k_6 = k_3 k_4 k_{oc}.$$

Передаточная функция разомкнутой системы будет

$$W = \frac{k k_*}{p(1+T_1 p)[(1+T_2 p)(1+T_* p) + k_6 k_* p]}, \quad k = k_1 k_2 k_3 k_4 k_5.$$

Характеристическое уравнение нелинейной гармонически линеаризованной системы получит вид:

$$A_0 p^4 + A_1 p^3 + A_2 p^2 + A_3 p + A_4 = 0,$$

где

$$A_0 = T_1 T_2 T_*,$$
$$A_1 = T_1 T_2 + T_1 T_* + T_2 T_* + T_1 k_6 k_*,$$
$$A_2 = T_1 + T_2 + T_* + k_6 k_*,$$
$$A_3 = 1, \quad A_4 = k k_*.$$

Как видим, здесь все коэффициенты характеристического уравнения, в отличие от прежнего, положительны.

Допустим, целью дальнейшего расчета системы является построение диаграммы качества нелинейных переходных процессов [1], которая дает возможность для каждого значения выбираемого параметра системы и амплитуды колебаний определить показатель затухания переходного процесса ξ и частоту колебаний ω. В качестве выбираемого параметра примем коэффициент усиления линейной части системы $k = k_1 k_2 k_3 k_4 k_5$.

Для решения поставленной задачи введем в характеристическое уравнение гармонически линеаризованной системы вместо p значение $p = \xi + j\omega$. В результате получим уравнение вида

$$X(A, \omega, \xi, k) + jY(A, \omega, \xi, k) = 0.$$

Поскольку выбираемый параметр k входит только в коэффициент A_4, то в этом уравнении после выделения вещественной и мнимой частей параметр k войдёт только в состав вещественной части X. Поэтому на основании выражения

$$Y(A,\omega,\xi)=0$$

можно найти зависимости $\xi(A)$ для различных значений $\omega=const$ и подставив их в выражение

$$X(A,\omega,\xi,k)=0,$$

найти отсюда зависимости $k(A)$ для различных $\omega=const$. Это дает нам сразу линии $\omega=const$ на искомой диаграмме качества нелинейных переходных процессов в системе координат (k,A), а найденные ранее зависимости $\xi(A)$ при разных $\omega=const$, дадут при этом возможность нанести основную часть диаграммы качества в виде линий $\xi=const$ в той же системе координат.

Аналогично этому частному примеру легко переложить все задачи решаемые на практике методом гармонической линеаризации при различных неоднозначных нелинейностях с гистерезисными петлями, используя предложенную здесь более корректную новую форму записи эквивалентной передаточной функции. При этом с целью облегчения практических расчетов для всех конкретных видов нелинейностей могут быть заранее составлены формулы и графики новых коэффициентов гармонической линеаризации $k_*(A)$ и $\omega T_*(A)$, подобно тому, как они существуют сейчас для коэффициентов $a(A)$ и $b(A)$, а также и в более сложных случаях, когда в них появляется дополнительно зависимость от отношения $\frac{\xi}{\omega}$ или от постоянной составляющей x^0.

Литература:

I. Попов Е.П., Пальтов И.П. Приближенные методы исследования нелинейных автоматических систем. Физматгиз, Москва, 1960 (Имеются издания в переводах на английском и немецком языках).

2. Попов Е.П. Разделение нелинейного управляемого процесса по частотам. Известия АН СССР. Техническая кибернетика. № 5 1968 г.

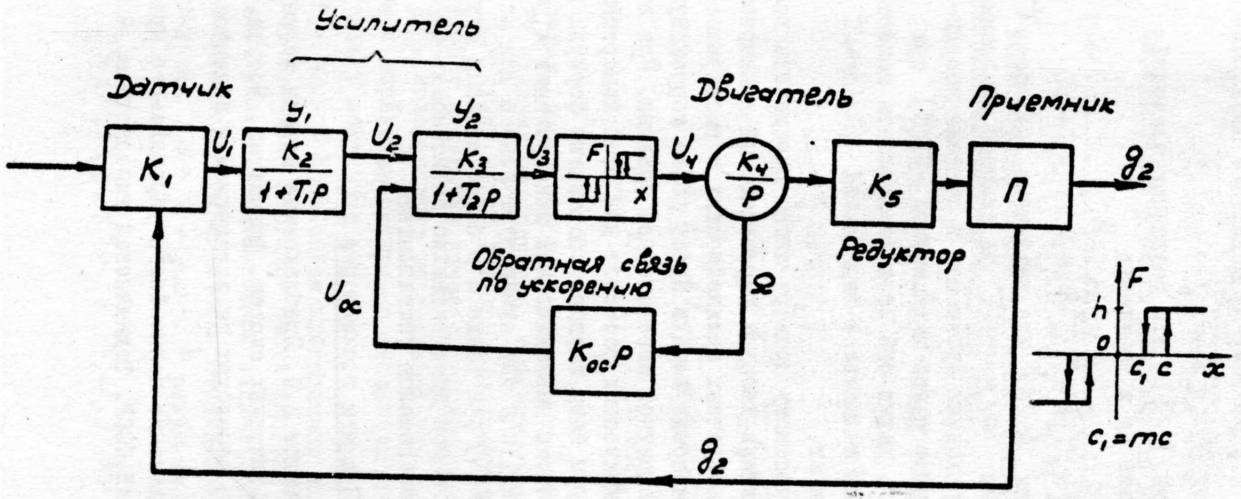
Усилитель
Датчик
Двигатель
Приемник
y_1
y_2
U_1
U_2
U_3
U_4
K_1
$\frac{K_2}{1+T_1P}$
$\frac{K_3}{1+T_2P}$
F
x
$\frac{K_4}{P}$
K_5
П
ϑ_2
Обратная связь по ускорению
$U_{ос}$
Ω
$K_{ос}P$
Редуктор
F
h
0
c_1
c
x
$c_1 = mc$
ϑ_2

Рис. 1

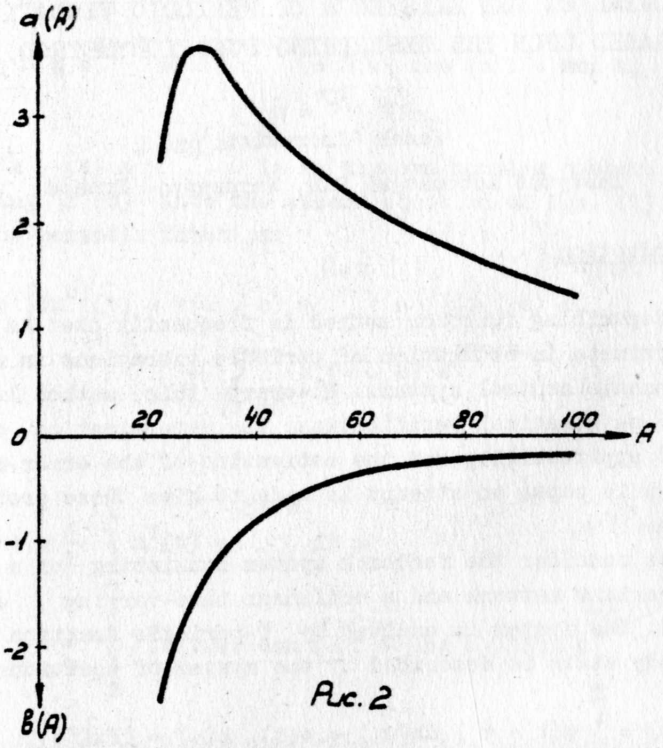
a (A)
3
2
1
0
-1
-2
20
40
60
80
100
A
B(A)

Рис. 2

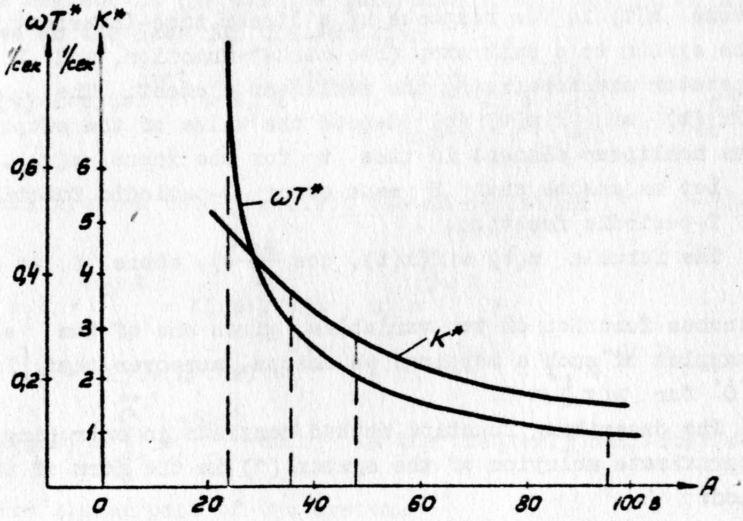
ωT*
1/сек
K*
1/сек
0,6
0,4
0,2
6
5
4
3
2
1
ωT*
K*
0
20
40
60
80
100 в
A

Рис. 3

THEOREMS ON THE EXISTENCE OF PERIODIC VIBRATIONS BASED UPON THE DESCRIBING FUNCTION METHOD

by

Jacek Kudrewicz

Instytut Automatyki PAN, Warszawa, Poland

1. Introduction

The describing function method is frequently used as a tool in approximate investigation of periodic vibrations in nonlinear automatic control systems. However, this method lacks a thorough mathematical verification, the determination of the range of applicability and the estimation of the error involved . In this paper an attempt is made to give these problems a solution.

Let us consider the feedback system consisting of a linear time-invariant network and a nonlinear time-varying element (Fig. 1). The system is excited by T-periodic function $z(t)$. The staedy state is described by the system of equations:

$$x(t) = \int_0^\infty u(t-\tau)\, dh(\tau) + z(t), \quad u(t) = \left[Fx\right](t) \qquad (1)$$

where $h(t)$ is the response of a linear time-invariant part of the system to a unit step (Heaviside) function, and F is the operator characterizing the nonlinear element. The symbols $\left[Fx\right](t)$ or $\left[F\,x(\tau)\right](t)$ denote the value of the output of the nonlinear element in time t for the input $x(\tau)$.

Let us assume that F maps every T-periodic function into a T-periodic function.

The formula $u(t) = f(x(t), \cos\frac{2\pi t}{T})$, where f is a continuous function of two variables, gives one of the simplest examples of such a mapping. We assume, moreover, that $\left[Fx\right](t) \equiv 0$ for $x(\tau) \equiv 0$.

The describing function method consists in searching for an approximate solution of the system (1) in the form of the function:

$$x^{o}(t) = a\, e^{j\omega t} + \bar{a}\, e^{-j\omega t} = 2|a| \cos(\omega t + \arg a), \qquad (2)$$

$$\omega = 2\pi / T,$$

where $a = |a|\, e^{j \arg a}$ is an unknown complex number. By substituting $x^{o}(t)$ into the second equation of Eqs. (1) we obtain the periodic function:

$$u^{o}(t) = \left[Fx^{o}\right](t) = v(\omega, a)\, e^{j\omega t} + \bar{v}(\omega, a)\, e^{-j\omega t} + \sum_{|n| \neq 1} u_n(\omega, a)\, e^{jn\omega t}, \qquad (3)$$

where

$$v(\omega, a) = \frac{1}{T} \int_0^T u^{o}(t)\, e^{-j\omega t}\, dt =$$

$$= \frac{1}{T} \int_0^T \left[F(2|a| \cos(\omega\tau + \arg a))\right](t)\, e^{-j\omega t}\, dt \qquad (4)$$

is referred to as describing function for nonlinearity F.

If we neglect in (3) all the harmonics except the first one, and if we do the same for the function

$$z(t) = z_1\, e^{j\omega t} + \bar{z}_1\, e^{-j\omega t} + \sum_{|n| \neq 1} z_n\, e^{jn\omega t} \qquad (5)$$

after substitution into the first one of equations (1) we obtain

$$a\, e^{j\omega t} + \bar{a}\, e^{-j\omega t} = K(j\omega)\, v(\omega, a)\, e^{j\omega t} + K(-j\omega)\, \bar{v}(\omega, a)\, e^{-j\omega t} + z_1\, e^{j\omega t} + \bar{z}_1\, e^{-j\omega t} \qquad (6)$$

where $K(j\omega) = \int_0^{\infty} e^{-j\omega t}\, dh(t)$ is the frequency characteristic of the linear part of the system.

From the approximate identity (6) (which holds for all t) we obtain the relation

$$a = K(j\omega)\, v(\omega, a) + z_1 \qquad (7)$$

The approximate values of the amplitude $2|a|$ and phase-shift $\arg a$ of the periodic vibrations in system (1) are obtained from Eq. (7).

Since usually it is not difficult to find the function $v(\omega, a)$ for a given operator F and to solve Eq. (7) with respect to a, the method presented above is often used for approximate estimation of periodic vibrations in nonlinear feedback systems. An attempt shall be made to determine the conditions under which the existence of a solution of Eq. (7) implies the existence of a periodic solution $x(t)$ of Eq. (1), and to estimate how far does $x(t)$ lie from the approximate solution (2).

2. The Idea of a Mathematical Verification of the Describing Function Method

We shall search for the solution of Eq. (1) in the form of a Fourier series $x(t) \sim \sum_n x_n e^{jn\omega t}$, where $x_{-n} = \bar{x}_n$. A one to one correspondence allways exists between the function $x(t)$ and the sequence $\{x_0, x_1, x_2, \ldots\}$ of its Fourier coefficients. Therefore we can replace Eq. (1) by the system of equations

$$x_n = K(jn\omega)u_n(\omega; x_0, x_1, x_2, \ldots) + z_n, \quad n = 0,1,2,3,\ldots \qquad (8)$$

where

$$u_n(\omega; x_0, x_1, x_2, \ldots) = \frac{1}{T}\int_0^T \left[F\Big(\sum_p x_p e^{jp\omega\tau}\Big)\right](t)\, e^{-jn\omega t}\, dt \qquad (9)$$

are Fourier coefficients of the function $u(t) = \left[Fx(\tau)\right](t)$ dependent on all the Fourier coefficients of the function $x(t)$.

It is easy to see that

$$v(\omega, a) = u_1(\omega; 0, a, 0, 0, \ldots) \tag{10}$$

where $v(\omega, a)$ is the describing function given by (4).

Assume that $K(j\omega) \neq 0$ and rewrite the system of equations (8) in the form of two systems. The first of them contains the equation with $n = 1$, only.

After some easy transformations it becomes

$$\frac{x_1 - z_1}{K(j\omega)} - v(\omega, x_1) = u_1(\omega; x_0, x_1, x_2, \ldots) + \\ - u_1(\omega; 0, x_1, 0, 0, \ldots) \tag{11}$$

The second one contains all remaining equations

$$x_n = K(jn\omega)\, u_n(\omega; x_0, x_1, x_2, \ldots) + z_n, \quad n = 0,2,3,4,\ldots \tag{12}$$

If $K(jn\omega) = 0$ for $n = 0, 2, 3, 4, \ldots$, the solution of system (11), (12) has the form: $x_n = z_n$ for $n \neq 1$ and $x_1 = a^*$, where a^* satisfies Eq. (7). It can be expected that if $K(jn\omega)$ for $n = 0, 2, 3, 4, \ldots$ is sufficiently small, the function $x(t) = \sum_n x_n e^{jn\omega t}$, whose Fourier coefficients satisfy the system (11), (12), is close in a particular sense, to the function

$$x^*(t) = 2|a^*| \cos(\omega t + \arg a^*) + \sum_{|n|\neq 1} z_n e^{jn\omega t} \tag{13}$$

To veryfy this hypothesis we shall solve the system (11), (12) by the method to follow:

We fix x_1 and apply to Eq. (12) the contraction-mapping fixed-point theorem to find all the remaining coefficients $x_n = x_n(\omega, x_1)$ for $n = 0, 2, 3, 4, \ldots$. These coefficients depend obviously on the fixed value x_1 and on the parameter ω. Substituting $x_n = x_n(\omega, x_1)$, $n = 0, 2, 3, 4, \ldots$ into Eq. (11) we obtain one equation with unknown x_1 in a complex domain. To solve this equation we can use the theory of vector

field on a plane, derived by Krasnoselski [1].

The assumptions, under which the method sketched above is applicable, will be formulated below in the theorems giving the range of applicability of the describing function method and the estimation of the error involved.

3. Theorem for the Nonautonomous Systems

Let X and Y be two Banach spaces of T-periodic functions, and let us assume that the function $\cos(\omega t + \varphi)$, $\omega = 2\pi/T$, belongs to both spaces X and Y, and denote by δ_X and δ_Y the norms of this function in X and Y, respectively, assuming further that δ_X and δ_Y do not depend on the parameter φ.

Let the operator A given by:

$$[Au](t) = \int_0^\infty u(t-\tau)\, dh(\tau) = \sum_n K(jn\omega)\, u_n\, e^{jn\omega t} \qquad (14)$$

where $u(t) = \sum_n u_n e^{jn\omega t}$, be the linear and continuous mapping of the space Y into X. For the particular spaces X and Y we can easily give the conditions for the function h(t) or for the sequence $\{K(jn\omega)\}$, under which $A \in [Y \to X]$. For example, if $\operatorname{Var}_{[0,\infty)} h < \infty$ then $A \in [C_T \to C_T]$, where C_T is the space of the continuous T-periodic functions with the norm $\|u\| = \sup_t |u(t)|$. If $\sum_n |K(jn\omega)|^2 < \infty$, then $A \in [L_T^2 \to l_T]$, where L_T^2 and l_T are Banach spaces with norms

$$\|u\|_Y = \sqrt{\frac{1}{T}\int_0^T |u(t)|^2\, dt} \quad \text{and} \quad \|u\|_X = \sum_n |u_n|,$$

respectively, where u_n are the Fourier coefficients of u(t).

The norm $\|A^0\|_{Y \to X}$ of the operator

$$\left[A^{0}u\right](t) = \sum_{|n|\neq 1} K(jn\omega)\, v_n\, e^{jn\omega t} \tag{15}$$

will play an important role in the further considerations. This norm characterises the "selectivity" of the linear part of the system (1); the lower is $\|A^{0}\|_{Y\to X}$ the higher the selectivity.

Let $z(t)$ be an element of the space X in which we consider the ball $\|x - x^{*}\|_X \leqslant r$ with a given radius r and center in the point $x^{*} = x^{*}(t)$ given by (13). Let us now assume that the nonlinear operator F maps the ball $\|x - x^{*}\|_X \leqslant r$ into the space Y and satisfies the Lipschitz condition

$$\|Fx_\alpha - Fx_\beta\|_Y \leqslant \alpha(r)\|x_\alpha - x_\beta\|_X \tag{16}$$

moreover $F(\theta_X) = \theta_Y$, where θ_X and θ_Y are zero elements in X and Y, respectively.

Now, let us return to Eq. (7). Let a^{*} be an isolated solution of this equation. If Eq. (7) has no solution in the circle $|s - a^{*}| \leqslant r_1$ of the complex plane s other than in point a^{*}, the function

$$\Phi(s) = \frac{s - z_1}{K(j\omega)} - v(\omega, a) \tag{17}$$

maps the complex plane s into itself,

$$\Phi(a^{*}) = 0, \text{ and } \quad |\Phi(s)| > 0 \quad \text{for} \quad 0 < |s - a^{*}| \leqslant r_1$$

Theorem 1. If the function $\Phi(s)$ maps one to one a neighbourhood of the point a^{*} into a neighbourhood of zero (e. g. the Jacobian of Φ is different from zero in point a^{*}), and if there exist positive numebrs r and r_1 such that $|\Phi(s)| > 0$ for $0 < |s - a^{*}| \leqslant r_1$ and

$$\|A^{0}\|_{Y\to X}\, \alpha(r)\,(r + \|x^{*}\|_X) \leqslant$$

$$\leqslant \min\left\{ r - 2\delta_X r_1,\ \frac{2\delta_Y}{\alpha(r)} \min_{|s-a^*|=r_1} |\Phi(s)| \right\} \qquad (18)$$

then Eq. (1) has in the space X at least one solution $x(t)$ in the neighbourhood of the approximate solution $x^*(t)$, viz.,

$$\|x - x^*\|_X \leqslant 2\delta_X r_1 + \|A^0\|_{Y \to X}\, \alpha(r)\, (r + \|x^*\|_X) \qquad (19)$$

The idea of the proof of this theorem has been given in Section 2. The theorem gives the conditions sufficient for the existence of a periodic solution of Eq. (1). The assumptions are expressed in terms of the describing function $v(\omega, s)$ for nonlinearity F and frequency characteristic $K(j\omega)$ of the linear part of the system. The formula (19) gives an estimation of the error involved in the describing function method.

To be able to use Theorem 1, we must choose the spaces X and Y so that the operators A and F have the demanded properties.

4. Example: A System with a Switch

Let us consider a system with a switch described by the integral equation:

$$x(t) = \int_0^\infty \operatorname{sign}\left[x(t-\tau)\right] k(\tau)\, d\tau + 2z \cos \omega t, \qquad z > 0 \qquad (20)$$

By applying the describing function method to Eq. (20) we obtain the approximate solution

$$x^*(t) = 2|a^*| \cos(\omega t + \arg a^*) \qquad (21)$$

where a^* satisfies the equation

$$\Phi(a) \quad \frac{a - z}{K(j\omega)} - \frac{2}{\pi} e^{j \arg a} = 0 \qquad (22)$$

The solution of Eq. (22) is shown in fig. 2.

We shall use Theorem 1 to verify the results obtained. With this in view we introduce the space X of T-periodic functions, with a bounded first derivative and the norm

$$\|x\|_X = \sup_t \max\left\{|x(t)|, \frac{1}{\omega}|\dot{x}(t)|\right\} \tag{23}$$

and the space Y of integrable functions with the norm

$$\|u\|_Y = \frac{1}{T}\int_0^T |u(t)|\,dt, \quad T = \frac{2\pi}{\omega} \tag{24}$$

It can be shown that the operator $[Fx](t) = \operatorname{sign}\dot{x}(t)$ maps the ball $\|x - x^*\|_X \leqslant r$ (where x^* is defined by (21)) contained in X, into the space Y, and that it satisfies the Lipschitz condition (16) with the constant

$$\alpha(r) = \frac{2}{\pi}\left(\sqrt{2|a^*|^2 - 9r^2} - r\right)^{-1} \tag{25}$$

for $r < \frac{2a^*}{\sqrt{10}}$.

In turn

$$[A^o u](t) = \sum_{|n|\neq 1} K(jn\omega)\, u_n\, e^{jn\omega t} \tag{26}$$

is the continuous mapping of the space Y into X provided that its norm

$$\|A^o\|_{Y\to X} \leqslant \max\left\{\sup_t \left|\sum_{|n|\neq 1} K(jn\omega)\, e^{jn\omega t}\right|, \sup_t \left|\sum_{|n|\neq 1} n\,K(jn\omega)\, e^{jn\omega t}\right|\right\} \tag{27}$$

is a bounded value.

Since $\delta_X = 1$, $\delta_Y = 4$ and $\|x^*\|_X = 2|a^*|$, all the values in the inequality (18) are already defined.

It is easy to verify that the Jacobian of the transformation

$$\Phi(s) = \frac{s - z}{K(j\omega)} - \frac{2s}{\pi|s|}$$

is different from zero in point $s = a^{*}$, provided $|a^{*}| \neq \frac{2}{\pi} |K(j\omega)|$ and $|a^{*}| \neq 0$.

Let us fix the values r and r_1 taking for example $r = \frac{|a^{*}|}{2}$ and $r_1 = \frac{|a^{*}|}{8}$. If $|\Phi(s)| > 0$ for $0 < |s - a^{*}| \leqslant r_1$, then by theorem 1 the inequality

$$\|A^{0}\|_{Y \to X} \leqslant \frac{|a^{*}|}{8} \min \left\{ 1,\ 40 \min_{8|s-a^{*}| = |a^{*}|} \left| \frac{s - z}{K(j\omega)} - \frac{2s}{\pi |s|} \right| \right\} \tag{28}$$

is the sufficient condition for the existence of a periodic solution of Eq. (20) in space X.

The example given above shows how by a convenient choice of spaces X and Y, the theorem 1 can be used for a system with an element having a "discontinuous" characteristic.

5. Autonomous Systems

The system (1) iscalled autonomous or stationary when the operator F is stationary, i.e. when it is commutative with the time shift operator

$$\left[F\, x(\tau + p)\right](t) = \left[F\, x(\tau)\right](t + p) \quad \text{for every } p \tag{29}$$

and when $z(t) = z_0$ is a constant. The formulae

$$\left[F_1 x\right](t) = f(x(t)), \quad \left[F_2 x\right](t) = g(x(t), \dot{x}(t), x(t - t_0))$$

where f and g are continuous functions, are examples of the stationary operators.

The equation

$$x(t) = \int_0^{\infty} \left[Fx\right](t - \tau)\, dh(\tau) \tag{30}$$

with $z = 0$ and $\left[Fx\right](t) \equiv 0$ for $x(\tau) \equiv 0$, may be studied instead of Eq. (1) without affecting the general considerations.

For autonomous systems theorem 1 is worthless bacause Eq. (7) does not have isolated solutions. Hence, the describing

function method must be modified here.

It is easy to see that if $x(t)$ is a solution of Eq. (30) then for every real number p the function $x(t + p)$ is also a solution. Thus, if we find the solution $x(t)$ of the form

$$x(t) = 2x_1 \cos \omega t + \sum_{|n|\neq 1} x_n e^{jn\omega t}, \quad x_1 > 0 \qquad (31)$$

then by shifting the argument we can easily obtain a whole family of solutions.

The describing function method is reduced in this case to finding an approximate solution in the form

$$x^{*}(t) = 2a^{*} \cos \omega^{*} t, \quad a^{*} > 0, \quad \omega^{*} > 0 \qquad (32)$$

where the amplitude $2a^{*}$ and frequency ω^{*} of vibrations are found from the equation

$$a = K(j\omega)\, v(\omega, a) \qquad (33)$$

The difference between the describing function method for nonautonomous and autonomous systems consists in that in the first case $\omega = 2\pi/T$ is a known value and $|a^{*}|$ and $\arg a^{*}$ are found from Eq. (7), whereas in the second case the amplitude $2a^{*}$ and frequency ω^{*} are sought for, but the phase is established by $\arg a^{*} = 0$.

The verification of the describing function method for autonomous systems is reduced to the examination of the dependence between Eq. (33) and the system (11), (12) with $z_n = 0$ for $n = 0, 1, 2, \ldots$. The idea of proceeding is the same as for nonautonomous systems, but now x_1 and ω are the unknown real positive numbers. Since ω is unknown, some additional assumption as to the continuity of all operators with respect to ω are needed here.

6. Theorem for Autonomous Systems

Let X and Y be two Banach spaces of complex number sequences

$$\xi = \{x_0, x_1, x_2, \ldots\}, \qquad \eta = \{u_0, u_1, u_2, \ldots\} \tag{34}$$

the first two elements being real. These spaces will be chosen to suit the given operator F. Let δ_X and δ_Y be the norms of vector $\delta = \{0, 1, 0, 0, 0, \ldots\}$ in the spaces X and Y, respectively.

Let us assume that the function $h(t)$ has a bounded variation for $t \in [0,\infty)$. The frequency characteristic $K(j\omega)$ is then a uniform continuous function for $\omega \in (-\infty,\infty)$. The operation $\xi = A_\omega \eta$ given by

$$x_n = K(jn\omega)u_n \quad \text{for} \quad n = 0, 1, 2, 3, \ldots \tag{35}$$

and dependent on the positive parameter ω shall be regarded as the mapping of the space Y into X. The norm $\|A^0_\omega\|_{Y \to X}$ of the operator

$$A^0_\omega \eta = \{K(0)u_0, 0, K(j\omega)u_1, K(2j\omega)u_2, K(3j\omega)u_3, \ldots\} \tag{36}$$

characterizes the selectivity of the linear part of the system.

The nonlinear operation $\eta = U_\omega \xi$ defined by equalities

$$u_n = u_n(\omega; x_0, x_1, x_2, \ldots) =$$
$$= \frac{1}{T}\int_0^T \left[F\left(x_0 + 2\mathrm{Re}\sum_{p=1}^{\infty} x_p e^{jp\omega\tau}\right)\right](t)\, e^{-jn\omega t}\, dt \tag{37}$$

and dependent on the parameter $\omega = 2\pi/T$ shall be treated as the mapping of the space X into Y. The equalities (37) are the same as in (9) and the identity (10) is also satisfied.

In the theorem given below the transformation

$$\Phi(\omega, x) = \frac{x}{K(j\omega)} - v(\omega, x) \tag{38}$$

of the quarter of plane $x > 0, \omega > 0$ into a complex plane will play an important role. If the point (ω^*, a^*) satisfies Eq. (33), then $\Phi(\omega^*, a^*) = 0$. Let us fix two positive numbers $\Omega < \omega^*$ and $r_1 < a^*$, and denote by l the border of the rectangle $|\omega - \omega^*| \leqslant \Omega$, $|x - a^*| \leqslant r_1$ (fig. 3).

Theorem 2. Let r, r_1, Ω be fixed positive numbers. Suppose that:

(1) $K(j\omega) \neq 0$ for $\omega \in [\omega^* - \Omega, \omega^* + \Omega]$.

(2) For every fixed $\omega > 0$ and $\eta \in Y$ we have

$$\left\| \left\{ 0, 0, \ldots, 0, K(jN\omega)u_N, K[j(N+1)\omega]\, u_{N+1}, \ldots \right\} \right\|_X \to 0$$

for $N \to \infty$

(3) For every $\omega \in [\omega^* - \Omega, \omega^* + \Omega]$ the operator A_ω defined by (35) is a linear bounded mapping of the space Y into X.

(4) For every $\omega \in [\omega^* - \Omega, \omega^* + \Omega]$ the operator U_ω defined by (37) maps the ball $\|\xi - a^* \delta\|_X \leqslant r$ of the space X (with the centre in point $\{0, a^*, 0, 0, 0, \ldots\}$ and with a radius r) into the space Y. Furthermore, the operator U_ω is continuous with respect to ω, and satisfies the Lipschitz condition

$$\|U_\omega \xi_1 - U_\omega \xi_2\|_Y \leqslant \alpha(r, \Omega) \|\xi_1 - \xi_2\|_X \tag{39}$$

(5) In the rectangle $|\omega - \omega^*| \leqslant \Omega$, $|x - a^*| \leqslant r_1$ there exists one and only one solution (ω^*, a^*) of Eq. (33), and $\Phi(\omega, x)$ maps one to one a neighbourhood of the point (ω^*, a^*) into a neighbourhood of zero of the complex plane.

(6) The inequality

$$q(r, \Omega) \leqslant \min \left\{ r - \delta_X r_1, \frac{\delta_Y}{\alpha(r, \Omega)} \min_{(\omega, x) \in 1} \left| \frac{x}{K(j\omega)} + \right. \right.$$
$$\left. \left. - v(\omega, x) \right| \right\} \tag{40}$$

holds, and

$$q(r, \Omega) = \sup_{\omega - \omega^* \ \Omega} \left\| A^0_\omega \right\|_{Y \to X} \alpha(r, \Omega)(r + \delta_X a^*) \tag{41}$$

Under these assumptions Eq. (30) has a periodic solution

$$x(t) = x_0 + 2x_1 \cos \omega t + 2 \sum_{n=2}^{\infty} \operatorname{Re} (x_n e^{jn\omega t}) \tag{42}$$

for which the following estimations hold

$$|\omega - \omega^*| < \Omega, \quad |x_1 - a^*| < r_1, \quad \left\|\{x_0, 0, x_2, x_3, \ldots\}\right\|_X \leqslant q(r, \Omega) \tag{43}$$

The proof of this theorem is analogous to that for theorem 1. However, a certain complication arises due to the necessity of examining the continuity of operators A_ω and U_ω with respect to ω. A particular case of theorem 2 specially suited for the given operator F characterizing the nonlinear part of the system is given below.

7. Example: System with Nonlinearity of the Type f(x)

We search for a periodic solution of the integral equation

$$x(t) = \int_0^\infty f\left[x(t - \tau)\right] dh(\tau), \quad \operatorname*{Var}_{[0,\infty)} h < \infty \tag{44}$$

where f(x) satisfies the Lipschitz condition

$$|f(x_1) - f(x_2)| \leqslant \alpha |x_1 - x_2|$$

and f(0) = 0. The describing function for nonlinearity f does not depend on ω, and is a real function:

$$v(a) = \frac{1}{T}\int_0^T f(2a \cos \omega t)\, e^{-j\omega t}\, dt = \frac{1}{\pi}\int_0^\pi f(2a \cos \tau) \cos \tau \, d\tau \tag{45}$$

If ω^* and a^* satisfy Eq. (33), which in this case is reduced to

$$\operatorname{Im} K(j\omega) = 0, \quad a = \left|K(j\omega)\right| v(a) \tag{46}$$

the function $x^*(t) = 2a^* \cos \omega^* t$ is referred to as approximate solution of Eq, (44) (fig. 4).

To estimate the error of this approximation we shall use theorem 2. Let $X = Y = l^2$ be the Banach space of the se-

quences with the norm

$$\|\xi\| = \sqrt{x_0^2 + 2\sum_{n=1}^{\infty} |x_n|^2} = \sqrt{\frac{1}{T}\int_0^T |x(t)|^2 \, dt} \qquad (47)$$

where $x(t) = x_0 + 2\mathrm{Re}\sum_{n=1}^{\infty} x_n e^{jn\omega t}$, $\omega = \frac{2\pi}{T}$.

Theorem 3. Let Ω and r_1 be fixed positive numbers. We assume that only one solution (ω^*, a^*) of Eq. (46) exists in the rectangle $|\omega - \omega^*| \leqslant \Omega$, $|a - a^*| \leqslant r_1$, and

$$\left.\frac{d\,\mathrm{Im}\,K(j\omega)}{d\omega}\right|_{\omega=\omega^*} \neq 0 \quad \text{and} \quad \left. v(a^*) - a^* \frac{dv(x)}{dx}\right|_{x=a^*} \neq 0 \qquad (48)$$

If $K(j\omega) \neq 0$ for $|\omega - \omega^*| \leqslant \Omega$, and if the inequality

$$\alpha \max\left\{|K(0)|, \sup_{\omega > 2(\omega^* - \Omega)} |K(j\omega)|\right\} \leqslant \frac{\min_{(\omega,x)\in l} \left|\frac{x}{K(j\omega)} - v(x)\right|}{\min_{(\omega,x)\in l} \left|\frac{x}{K(j\omega)} - v(x)\right| + (r_1 + a^*)\alpha} \qquad (49)$$

holds, where l is the border of the rectangle $|\omega - \omega^*| \leqslant \Omega$, $|x - a^*| \leqslant r_1$, then Eq. (44) has a periodic solution in the form (42), for which we have the estimations $|\omega - \omega^*| < \Omega$ and $|x_1 - a^*| < r_1$ and

$$\sqrt{x_0^2 + 2\sum_{n=2}^{\infty} |x_n|^2} \leqslant \frac{2}{\alpha} \min_{(\omega,x)\in l} \left|\frac{x}{K(j\omega)} - v(x)\right| \qquad (50)$$

Full proofs of the theorems presented here and a number of examples of application are given in the book "Frequency Methods in the Theory of Nonlinear Dynamic Systems" (in Polish) by the present author, to be published in 1969.

References

1. Krasnoselski M.A.: Vector Field on the Plane (in Russian) . Moscow 1963.
2. Rozenvasser E.N.: On Application of Integral Equations in the Theory of Nonlinear Vibartions (in Russian). Proc. 2nd USSR Conf. on Pure and Applied Mechanics, Moscow 1965.
3. Kudrewicz J.: Contribution to the Theory of Describing Function. 4th Conf. on Nonlinear Oscillations, Prague 1967.

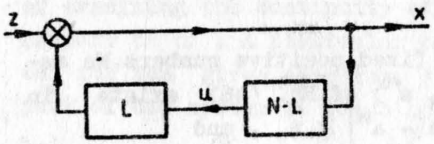

Fig. 1. System described by Eq. (1)

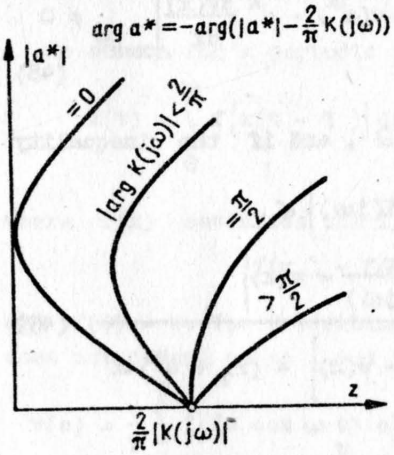

Fig. 2. Solution of Eq. (22)

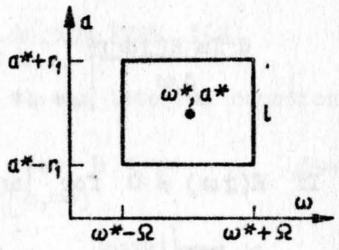

Fig. 3. Neighbour-hood of point (ω^*, a^*) satisfying Eq. (33)

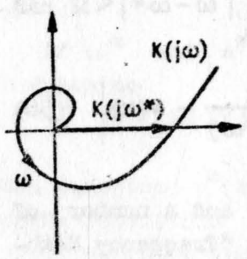

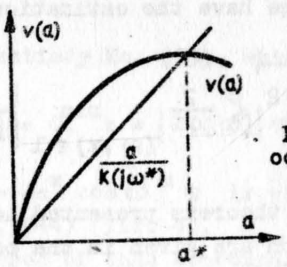

Fig. 4. Graphic method of solving Eq. (46)

STEADY STATE ANALYSIS OF NONLINEAR SYSTEMS AND MULTIPLE INPUT DESCRIBING FUNCTIONS /M.I.D.F./

Ronald G. Sea
Dept. of Electrical Engineering
Illinois Institute of Technology
Chicago, Illinois 60616
U.S.A.

André G. Vacroux
Assistant Professor
Dept. of Electrical Engineering
Illinois Institute of Technology
Chicago, Illinois 60616
U.S.A.

I. INTRODUCTION

The Describing Function technique[1] has been used for many years to study the steady state behavior of nonlinear feedback systems. Extensions of the basic technique have been made in order to analyze various phenomena such as the stimulation or quenching of limit cycles by an external sinusoidal signal[2], subharmonic oscillations[3,4], jump phenomena[5,6], stability of oscillations[3], signal stabilization of a forced system[3] and other effects. The describing functions used to analyze each of these situations have several common features. The input to the nonlinearity is always assumed to have the form

$$x = \sum_{m=1}^{M} E_m \cos(\omega_m t + \varphi_m) \qquad (1)$$

where E_m, ω_m and φ_m are respectively the amplitude, the frequency and the phase of the m^{th} component in the input.

In each case, the describing function K_{eq} is the complex quantity relating the input and output components at a given frequency, e.g. if the component of frequency ω_m of the output is given by: $a\cos(\omega_m t + \varphi_m) + b\sin(\omega_m t + \varphi_m)$, the corresponding describing function is $K_{eq} = (a-jb)/E_m$. Expressions for such describing functions have been previously derived[1,2,3,8] only for cases in which three or fewer frequency components are present in the input to the nonlinearity. In each of these cases, the describing function only gives information about a frequency component of the output which is also present in the input. In general the output of a nonlinearity contains not only the input frequencies but all their integer combinations as well.

The present paper deals, in part, with the more general problem of computing the amplitude of any frequency component in the output of a nonlinearity with an input given by equation (1). As a particular case, the Multiple Input Describing Function (M.I.D.F.) is derived. The M.I.D.F. is a generalization (for any number of inputs) of the formulas which were previously developed for single, dual, and triple input

describing functions[1,2,8]. Several algorithms are presented to accomplish the computations of the output. One of these algorithms permits a very rapid computation of the output amplitudes when these amplitudes are to be computed for many combinations of input amplitudes. In addition, it is also directly applicable to cases in which the nonlinearity is defined empirically by a set of input-output data points.

An efficient method of computing output amplitudes when the input frequencies are harmonically related is also presented. As an application, the relationship between the Dual Input Describing Function (D.I.D.F.) for harmonically related input frequencies[3], and the D.I.D.F. for non harmonically related input frequencies[2] is established. A few sample curves obtained by using the proposed method are given and an example is presented.

II. MULTIPLE FOURIER SERIES EXPANSION

If a nonlinear device has an input given in the form of equation (1), its output can be expanded in an M-dimensional Fourier series. To simplify notation, introduce M variables θ_i defined by

$$\theta_i = \omega_i t + \varphi_i, \quad i = 1,2,\ldots,M \tag{2}$$

If the output, y, of the nonlinearity is a single valued function of the input:

$$y = f(x) \tag{3}$$

the Fourier series expansion of the output is represented by

$$y = \sum_{n_1=-\infty}^{\infty} \cdots \sum_{n_M=-\infty}^{\infty} \frac{V_{n_1 \ldots n_M}}{2} \exp\left(jn_1\theta_1 + \ldots + jn_M\theta_M\right) \tag{4}$$

where the coefficients $V_{n_1 \ldots n_M}$ are given by

$$V_{n_1 \ldots n_M} = \frac{2}{(2\pi)^M} \int_{-\pi}^{\pi} \cdots \int_{-\pi}^{\pi} f\left(\sum_{m=1}^{M} E_m \cos\theta_m\right) \cdot \exp\left(-jn_1\theta_1 - \ldots - jn_M\theta_M\right) d\theta_1 \cdots d\theta_M \tag{5}$$

A typical component in the output y, given by equation (4), can be written as

$$\bar{y} = \frac{V_{\bar{n}_1 \ldots \bar{n}_M}}{2} \exp\left(j\bar{n}_1\theta_1 + \cdots + j\bar{n}_M\theta_M\right) + \frac{V_{-\bar{n}_1 \ldots -\bar{n}_M}}{2} \exp\left(-j\bar{n}_1\theta_1 - \cdots - j\bar{n}_M\theta_M\right) \tag{6}$$

if at least one n_i is different from zero. If all the n_i are equal to zero, then the D.C. component $\frac{V_{0\ldots0}}{2}$ is obtained.

Considering equation (5), and noticing that $f(\sum_{m=1}^{M} E_m \cos\theta_m)$ is an even function of each θ_m, it can be seen that only the cosine part of each exponential contributes to the integral. Thus $V_{n_1\ldots n_M}$ depends only on the absolute value of each index n_i, and equation (6) becomes

$$\bar{y} = V_{\bar{n}_1\ldots\bar{n}_M} \cos(\bar{n}_1\theta_1 + \ldots + \bar{n}_M\theta_M) \tag{7}$$

or

$$\bar{y} = V_{\bar{n}_1\ldots\bar{n}_M} \cos\left[(\bar{n}_1\omega_1+\ldots+\bar{n}_M\omega_M)\, t + (\bar{n}_1\varphi_1 + \ldots + \bar{n}_M\varphi_M)\right] \tag{8}$$

It can now been seen that the main problem in finding the output of a nonlinearity is the calculation of the coefficients $V_{\bar{n}_1\ldots\bar{n}_M}$. Several methods to this effect are given in part III. It should be pointed out that these methods are valid for the computation of these coefficients regardless of whether or not the input frequencies are commensurate (e.g. harmonically related).

The importance of relations between the different input frequencies can be easily seen from equation (8): If the frequencies ω_i of the input were not all independent, different combinations of integers n_i would give rise to different components of amplitudes $V_{n_1\ldots n_M}$ at the same output frequency, all of which should be summed to get the total output amplitude at that frequency. This important case is investigated separately in part IV.

In describing function analysis there is need only for low order coefficients such as $V_{100\ldots0}$, $V_{010\ldots0}$, ..., etc., except when the input frequencies are harmonically related. The formulas for the describing function terms are special cases of the formulas to be derived below.

III. METHODS OF COMPUTING AMPLITUDES

Direct Approach

Since $V_{n_1\ldots n_M}$ is defined by equation (5), the most direct approach is to perform a numerical integration. However this method is not suitable when the number of input frequencies is large, since one must carry out an M-fold integration, and each additional input frequency multiplies the computing time by the number of points used for the new frequency. This method should be avoided for cases with more than two input components.

Power Series Approach

When the nonlinearity can be described by a power series, there exists an algebraic formula for the amplitude of any frequency component. Let the input-output characteristic be described by

$$y = \sum_{n=0}^{\infty} a_n x^n \tag{9}$$

it has been shown by Sea[9] that, for this representation of the nonlinearity, $V_{n_1 \cdots n_M}$ is given by

$$V_{n_1 \cdots n_M} = 2 \sum_{L=0}^{\infty} a_{N+2L} (N+2L)! \sum_{q_1} \cdots \sum_{q_M} \prod_{p=1}^{M} \frac{(\frac{1}{2}E_p)^{|n_p|+2q_p}}{(q_p + |n_p|)!\, q_p!} \tag{10}$$

where the inner summation is an M-fold summation over all non negative integers $q_1, \ldots, q_M$ such that $q_1 + \ldots + q_M = L$. The quantity $N = |n_1| + \ldots + |n_M|$ is called the "order" of the output component of amplitude $V_{n_1 \cdots n_m}$. This method is very advantageous if the nonlinearity can be approximated by a low degree polynominal; however since the number of terms for which $q_1 + \ldots + q_m = L$ increases rapidly as L increases, this method is not very satisfactory for nonlinearities which require many terms in their power series expansion.

Fourier Transform Approach

General Case This approach requires only that the nonlinear function f(x) have a Fourier Transform F(ju) where

$$f(x) = \frac{1}{2\pi} \int_{-\infty}^{+\infty} F(ju)\, e^{jux}\, du \tag{11}$$

Substituting equation (11) into equation (5) and interchanging the order of integration yields

$$V_{n_1 \cdots n_M} = \frac{1}{\pi} \int_{-\infty}^{\infty} F(ju) \left[\frac{1}{2\pi} \int_{-\pi}^{\pi} e^{juE_1 \cos\theta_1} e^{-jn_1\theta_1}\, d\theta_1 \right] \cdots \left[\frac{1}{2\pi} \int_{-\pi}^{\pi} e^{juE_M \cos\theta_M} e^{-jn_M\theta_M} d\theta_M \right] du \tag{12}$$

Noting that the integrals inside the brackets are representations of Bessel functions of the first kind, i.e.

$$j^{|n|} J_{|n|}(juE) = \frac{1}{2\pi} \int_{-\pi}^{\pi} e^{juE\cos\theta}\, e^{-jn\theta}\, d\theta$$

Equation (12) takes the general form (first given by Rice[10]):

$$V_{n_1 \cdots n_M} = \frac{j^N}{\pi} \int_{-\infty}^{\infty} F(ju) \left[\prod_{i=1}^{M} J_{|n_i|}(E_i u) \right] du \tag{13}$$

where $N = |n_1| + |n_2| + \ldots + |n_M|$.

Application to Multiple Input Describing Functions. A particular case of equation (13) which is of major interest for control engineers is obtained by considering only one component in the output, say the component which corresponds to the input of amplitude E_1 and frequency ω_1; in that case $n_1 = 1$, $n_i = 0$ for $i = 2,3\cdots M$; thus $N = 1$, and equation (13) becomes

$$V_{10\cdots0} = \frac{j}{\pi} \int_{-\infty}^{+\infty} F(ju)\, J_1(E_1u)\, J_0(E_2u)\, J_0(E_3u)\cdots J_0(E_Mu)\, du \qquad (14)$$

If it is furthermore assumed that none of the input frequencies are harmonically related, $V_{10\cdots0}$ is the amplitude of the output component of frequency ω_1, which permits the definition of the Multiple Input Describing Function for the signal of frequency ω_1:

$$M.I.D.F. = \frac{j}{\pi E_1} \int_{-\infty}^{+\infty} F(ju)\, J_1(E_1u)\, J_0(E_2u)\, J_0(E_3u)\cdots J_0(E_Mu)\, du \qquad (15)$$

Note that equation (15) generalizes (for M independent inputs) the well known formulas for single, dual, and triple input describing functions[1,2,8].

In spite of the fact that equation (15) generalizes, for an arbitrary number of inputs, previously known results, it is important to remember that it is only a particular case of equation (13). In its general form equation (13) not only allows the determination of the amplitudes of the components of the output which are also present in the input, but it also yields the amplitudes of the components of the output which correspond to frequencies not present in the input. These components are intermodulation terms generated by the nonlinearity. Closed form solutions for equation (13) are difficult to find. Solutions for certain cases have been obtained[2], but in general the equation must be integrated numerically.

Fourier Series Approach

This approach is conceptually closely related to that of the previous section, but has several computational advantages. Instead of expressing $f(x)$ in terms of its Fourier Transform, one expands it into a Fourier Series over the interval $[-E_o, E_o]$:

$$f_p(x) = \sum_{n=-\infty}^{+\infty} c_n \exp\left(j\frac{n\pi x}{E_o}\right) \qquad (16)$$

This may be done for any single valued nonlinearity, including one which is only known empirically by a set of data points on its input-output curve. Since $f_p(x) = f(x)$ for $|x| \leq E_o$, one may replace $f(x)$ by $f_p(x)$ in equation (5), provided that the peak value of the input is not greater than E_o. That is:

$$E_1 + E_2 + \ldots + E_M \leq E_o \qquad (17)$$

Substituting equation (16) into equation (5) and interchanging the order of summation and integration gives

$$V_{n_1 \cdots n_M} = 2 \sum_{n=-\infty}^{\infty} c_n \left[\frac{1}{2\pi} \int_{-\pi}^{\pi} \exp\left(j \frac{n\pi E_1}{E_o} \cos\theta_1 - j n_1 \theta_1\right) d\theta_1 \right] \cdots \left[\frac{1}{2\pi} \int_{-\pi}^{\pi} \exp\left(j \frac{n\pi E_M}{E_o} \cos\theta_M - j n_M \theta_M\right) d\theta_M \right] \tag{18}$$

Recognizing once again the terms in brackets as integral representations of Bessel functions, equation (18) becomes

$$V_{n_1 \cdots n_M} = 2j^N \sum_{n=-\infty}^{\infty} c_n \left\{ \prod_{p=1}^{M} J_{|n_p|}\left(\frac{n\pi E_p}{E_o}\right) \right\} \tag{19}$$

where $N = |n_1| + |n_2| + \cdots + |n_M|$

If now the expansion of equation (16), is replaced by an expansion of $f(x)$ in sine and cosine series:

$$f_p(x) = a_0 + \sum_{n=1}^{\infty} a_n \cos\left(\frac{n\pi x}{E_o}\right) + \sum_{n=1}^{\infty} b_n \sin\left(\frac{n\pi x}{E_o}\right) \tag{20}$$

then the amplitudes $V_{n_1 \cdots n_M}$ of the output components are respectively given by

$$V_{n_1 \cdots n_M} = 2(-1)^{\frac{N-1}{2}} \sum_{n=1}^{\infty} b_n \left\{ \prod_{p=1}^{M} J_{|n_p|}\left(\frac{n\pi E_p}{E_o}\right) \right\}, \text{ for N odd} \tag{21}$$

and

$$V_{n_1 \cdots n_M} = 2(-1)^{\frac{N}{2}} \sum_{n=0}^{\infty} a_n \left\{ \prod_{p=1}^{M} J_{|n_p|}\left(\frac{n\pi E_p}{E_o}\right) \right\}, \text{ for N even} \tag{22}$$

If values of the $V_{n_1 \cdots n_M}$ are desired for many different values of the input amplitudes E_i, the calculations can be simplified by quantizing these amplitudes, i.e. requiring each E_i to have the form

$$E_i = \frac{L_i}{L_o} E_o \;, \quad L_i = 0, 1, 2, \ldots, L_o \tag{23}$$

Then the equations (21) and (22) become respectively

$$V_{n_1 \cdots n_M} = 2(-1)^{\frac{N-1}{2}} \sum_{n=1}^{\infty} b_n \left\{ \prod_{p=1}^{M} J_{|n_p|}\left(\frac{n\pi L_p}{L_o}\right) \right\}, \text{ for N odd} \tag{24}$$

and

$$V_{n_1 \cdots n_M} = 2(-1)^{\frac{N}{2}} \sum_{n=0}^{\infty} a_n \left\{ \prod_{p=1}^{M} J_{|n_p|}\left(\frac{n\pi L_p}{L_o}\right) \right\}, \text{ for N even} \tag{25}$$

If the Fourier Series in equation (20) is truncated so that the upper

limit of summation is K, then in equations (24) and (25) the only arguments for which the Bessel functions need be evaluated are $0, \frac{\pi}{L_o}, 2\frac{\pi}{L_o}, \cdots, K L_o (\frac{\pi}{L_o})$. The Bessel functions for each of these $KL_o + 1$ different arguments can be computed and stored before the computation of $V_{n_1 \cdots n_M}$ begins, thus saving a great deal of computing time.

Using this technique, the values of a four input D.F. (for the limiter of Fig. 1) were computed for 3675 different combinations of input amplitudes in 10 minutes on the IBM 360 digital computer. This is an average of only 0.16 second per value, which is much faster than the computation by other methods such as numerical integration of equation (5) or (13). For this example, 50 terms in the Fourier series for f(x) were used and L_o was 100. Thus, 5001 values of Bessel functions of orders zero and one were computed and prestored prior to the computation of the 3675 values of the D.F. This required 2 minutes of the total computing time. If the Bessel functions had been computed each time they were used, it would have been necessary to compute them 735,000 times, which would have required several hours. This clearly shows the advantages gained by quantizing the input amplitudes (as in equation 23) and precomputing the Bessel functions as described above.

IV COMPUTATION OF OUTPUT AMPLITUDES IN THE CASE OF RELATED INPUT FREQUENCIES.

It was shown in Part II that the terms in the output of a nonlinearity were given by expressions of the form of equation (8). The frequency of each such term was

$$\bar{\omega} = \bar{n}_1 \omega_1 + \cdots + \bar{n}_M \omega_M \tag{26}$$

If the input frequencies are not incommensurate, the set of integers $\bar{n}_1, \cdots, \bar{n}_M$ giving the frequency $\bar{\omega}$ is not unique. To see this, suppose that the input frequencies are related by an equation of the form

$$k_1 \omega_1 + \cdots + k_M \omega_M = 0 \tag{27}$$

where the k_i are positive or negative integers or zero and any common integer factor has been divided out. Assume also for the sake of simplicity that only one such relation exists. Multiplying equation (27) by an arbitrary integer λ, and adding to equation (26) yields:

$$\bar{\omega} = (\bar{n}_1 + \lambda k_1) \omega_1 + \cdots + (\bar{n}_M + \lambda k_M) \omega_M \tag{28a}$$

or

$$\bar{\omega} = n_1 \omega_1 + \cdots + n_M \omega_M \tag{28b}$$

Thus for every integer value of λ there is a different set of integer multipliers $n_1,\ldots,n_M$ giving the same output frequency $\bar{\omega}$. There follows that all the terms of the form of equation (8) for which $n_i = \bar{n}_i + \lambda k_i$, $i = 1,2,\ldots,M$ must be summed in order to obtain the total output at frequency $\bar{\omega}$. The result is

$$\bar{y} = \sum_{\lambda=-\infty}^{\infty} V_{\bar{n}_1+\lambda k_1,\ldots,\bar{n}_M+\lambda k_M} \cos\left[\bar{\omega}t + (\bar{n}_1\varphi_1+\ldots+\bar{n}_M\varphi_M) + \lambda(k_1\varphi_1+\ldots+k_M\varphi_M)\right] \tag{29}$$

Letting $\bar{\varphi} = \bar{n}_1\varphi_1+\ldots+\bar{n}_M\varphi_M$

$$\varphi_o = k_1\varphi_1+\ldots+k_M\varphi_M$$

Equation (29) can be written in terms of its sine and cosine components

$$\bar{y} = \bar{a}\cos(\bar{\omega}t+\bar{\varphi}) + \bar{b}\sin(\bar{\omega}t+\bar{\varphi}) \tag{30}$$

where

$$\bar{a} = \sum_{\lambda=-\infty}^{+\infty} V_{\bar{n}_1+\lambda k_1,\ldots,\bar{n}_M+\lambda k_M}\cos(\lambda\varphi_o) \tag{31}$$

$$\bar{b} = -\sum_{\lambda=-\infty}^{+\infty} V_{\bar{n}_1+\lambda k_1,\ldots,\bar{n}_M+\lambda k_M}\sin(\lambda\varphi_o) \tag{32}$$

In the derivation of equation (29) it was assumed that only one constraint existed among the input frequencies; an example of this is the case in which one of the input frequencies is a harmonic of another. These results have been generalized to allow more than one constraint. The general formulas for any number of constraints are notationally cumbersome, but conceptually similar to the above formulas. For each constraint a different multiplier λ_j is used, and equation (29) becomes a multiple summation over all the λ_j's. In the cases in which only a few constraints exist (for instance the case of a system with a fundamental, a third and a fifth harmonic, i.e. two constraints) it is easy to derive directly the relation which would replace equation (29), so a general formula for an arbitrary number of constraints is not really needed.

It should be emphasized, that the methods given in part III for computing the $V_{n_1\ldots n_M}$ are applicable whether or not the input frequencies are related. If they are unrelated, equation (8) gives the output at any particular frequency. If they are related by a constraint of the form of equation (27), then equation (29) must be used to compute the output at a given frequency. In practice, as the example below will illustrate, only a few terms of the summations of equations (31) and (32) are generally needed

for the numerical computation of $\bar{a}$ and $\bar{b}$.

Example: Dual Input Describing Functions and Application to the Analysis of Subharmonic Oscillations of a Third order System.

To illustrate the above results, the Dual Input Describing Function (D.I.D.F.) for harmonically related signals will be derived, compared with the D.I.D.F. for unrelated frequencies, and used to analyze a closed loop system in which the subharmonics may be generated. It must be pointed out that the solution of this problem is not new and has been given in a less general form by West.[3]

Calculation of the D.I.D.F for related input frequencies. Assume that the input to the nonlinearity has the form

$$x = E_1 \cos \omega_1 t + E_2 \cos(\omega_2 t + \varphi_2)$$

where ω_2 is the k^{th} harmonic of ω_1 and φ_2 represents the phase shift. Thus $k\omega_1 - \omega_2 = 0$ and $\varphi_b = -\varphi_2$; then equations (31) and (32) become

$$\bar{a} = \sum_{\lambda=-\infty}^{\infty} V_{\bar{n}_1+\lambda k, \bar{n}_2-\lambda} \cos(\lambda\varphi_2)$$

$$\bar{b} = \sum_{\lambda=-\infty}^{\infty} V_{\bar{n}_1+\lambda k, \bar{n}_2-\lambda} \sin(\lambda\varphi_2)$$

and the k^{th} subharmonic describing function is defined as

$$K_1 = \frac{\bar{a} - j\bar{b}}{E_1} \qquad \text{where } \bar{n}_1 = 1,\ \bar{n}_2 = 0 \text{ or}$$

$$K_1 = \frac{1}{E_1} \sum_{\lambda=-\infty}^{\infty} V_{1+k\lambda,-\lambda} \cos(\lambda\varphi_2) \quad -j\,\frac{1}{E_1} \sum_{\lambda=-\infty}^{\infty} V_{1+k\lambda,-\lambda} \sin(\lambda\varphi_2) \tag{33}$$

Denoting the terms entering equation (33) by

$$D(E_1,E_2) = \frac{V_{10}}{E_1} \tag{34}$$

$$P_\lambda(E_1,E_2) = \frac{V_{1+k\lambda,-\lambda} + V_{1-k\lambda,\lambda}}{E_1} \tag{35}$$

$$Q_\lambda(E_1,E_2) = \frac{V_{1-k\lambda,\lambda} - V_{1+k\lambda,-\lambda}}{E_1} \tag{36}$$

equation (33) can be written in the form

$$K_1(E_1,E_2,\varphi_2) = D(E_1,E_2) + \sum_{\lambda=1}^{\infty} P_\lambda(E_1,E_2) \cos(\lambda\varphi_2) + j \sum_{\lambda=1}^{\infty} Q_\lambda(E_1,E_2) \sin(\lambda\varphi_2) \tag{37}$$

It is seen from equation (37) that the D.I.D.F. for the k^{th} subharmonic is expressed as a Fourier series in φ_2 (phase shift), and that

each coefficient in the series depends only on E_1 and E_2. This describing function is evaluated by computing the terms in equations (34) to (36) by any of the methods given in part III.

Relations between the D.I.D.F.'s for related and unrelated input frequencies Consider the D.I.D.F. for related frequencies given by equation (33). It can be seen that its first term, which is defined by equation (34), represents the D.I.D.F. for asynchronous (unrelated) frequencies[2]. This shows that if the D.I.D.F. for related frequencies is averaged over a full period of φ_2, the result is equal to the D.I.D.F. for unrelated frequencies.

Application to a problem involving a third subharmonic The third subharmonic describing function for the ideal limiter of Fig. 1 was computed using the above techniques. It was found that the first three terms in the series of equation (37) were sufficient to compute K_1 because the contributions to the output signal decreased rapidly for increasing values of λ.

Figure 2 shows the curves of $D(E_1,E_2)$ for the ideal limiter of Fig. 1. The corresponding curves of $P_1(E_1,E_2)$ and $Q_1(E_1,E_2)$ are shown in Figs. 3 and 4. The curves for the higher order coefficients are not shown, but these were found to be considerably smaller. The effect of the phase on the real and imaginary parts of $K_1(E_1,E_2,\varphi_2)$ is shown in Figs. 5 and 6.

In examining the third subharmonic response of the system of Fig. 7, which include the limiter of Fig. 1, computer generated plots of $-1/K_1$ are used, since the criterion for sustained third subharmonic oscillation is: $-1/K_1 = G(j\omega_1) = G(j\omega_2/3)$. The plots of $-1/K_1$ are shown for $E_2 = 1.5$, 1.0, and 0.5 in Figs. 8,9, and 10, respectively, with the Nyquist plot of $G(j\omega)$ superimposed. The intersections of the $-1/K_1$ loci with the Nyquist plot represent possible third subharmonic oscillations. In general, there is more than one solution for a given value of E_2 and ω_2. Stability of the subharmonic oscillation for each solution is determined by usual methods[3,4].

For this example, the third subharmonic D.I.D.F. was computed for 1029 combinations of E_1, E_2, and φ_2. A 33 term Fourier Series expansion of $f(x)$, for $-20 \leq x \leq 20$, was used. For the evaluation of equation (37), the first three terms in each summation were used. The computing time was 2 minutes for the Bessel Functions and 8 minutes for the 1029 values of the D.I.D.F., using an IBM 360 mod 40 digital computer. The time required by previously used techniques would have been considerably greater. In this example, the method of separately computing and prestoring the Bessel Functions (as described above) was used to reduce the computing time.

CONCLUSION

The output of a single valued nonlinearity subjected to any number of input sine waves has been investigated. Exact formulas and numerical approximations for the amplitude of any frequency component in the output have been given for both the case of incommensurate input frequencies and that of commensurate (e.g. harmonically related) frequencies. The formulas for Multiple Input Describing Functions (M.I.D.F.) are special cases.

Although each of the formulas derived here is of general theoretical importance, the numerical method based on the Fourier Series expansion of the nonlinearity is particularly promising because it permits the computation of an output amplitude or an M.I.D.F. in a very short time. This is essential when the computation is to be repeated for many different values of the input amplitudes. The computational efficiency and generality of the methods which have been presented should facilitate the further investigation of nonlinear steady state phenomena.

REFERENCES

1. L.C. Goldfarb, "On Some Nonlinear Phenomena in Regulatory Systems", Avtomatika i Telemekhanika, Vol. 8, No. 5, pp. 349-383, Sept. 1947.
2. J.E. Gibson and R. Sridhar, "A New D.I.D.F. and an Application to the Stability of Forced Nonlinear Systems", Sec. 9, Proc. Joint Automatic Conference (JACC), New York, June, 1962.
3. J.C. West, J.L. Douce, and R.K. Livesley, "The Dual-Input Describing Function and Its Use in the Analysis of Nonlinear Feedback Systems", Proc. IEE, Vol. 103, Part B, pp. 463-474, 1956.
4. R. Oldenburger and R.E. Nicholls, "Stability of Subharmonic Oscillations in Nonlinear Systems", Trans. ASME, pp. 116-120, March, 1964.
5. H. Hatanaka, "The Frequency Responses and Jump Resonance Phenomena of Nonlinear Feedback Control Systems", Trans. ASME, pp. 236-242, June, 1963.
6. J.C. Hill, "Closed Loop Response of Nonlinear Systems by a Functional Transformation Approach", IRE Trans. A.C., pp. 39-44, July, 1962.
7. R. Oldenburger and R.C. Boyer, "Effects of Extra Sinusoidal Inputs to Nonlinear Systems", ASME J. Basic Engrg., pp. 559-570, December, 1962.
8. T.L. Setchfield and A.F.D'Souza, "Triple Input Describing Function and Applications to the Stability of Nonlinear Systems", ASME Winter Meeting, Pittsburgh, 1967.
9. R. Sea, "An Algebraic Formula for Amplitudes of Intermodulation Products Involving an Arbitrary Number of Frequencies", Proc. IEEE, pp. 1388-1389, August, 1968.
10. S.O. Rice, "Mathematical Analysis of Random Noise", Bell System Tech. J., Vol. 24, pp. 46-155, 1945.

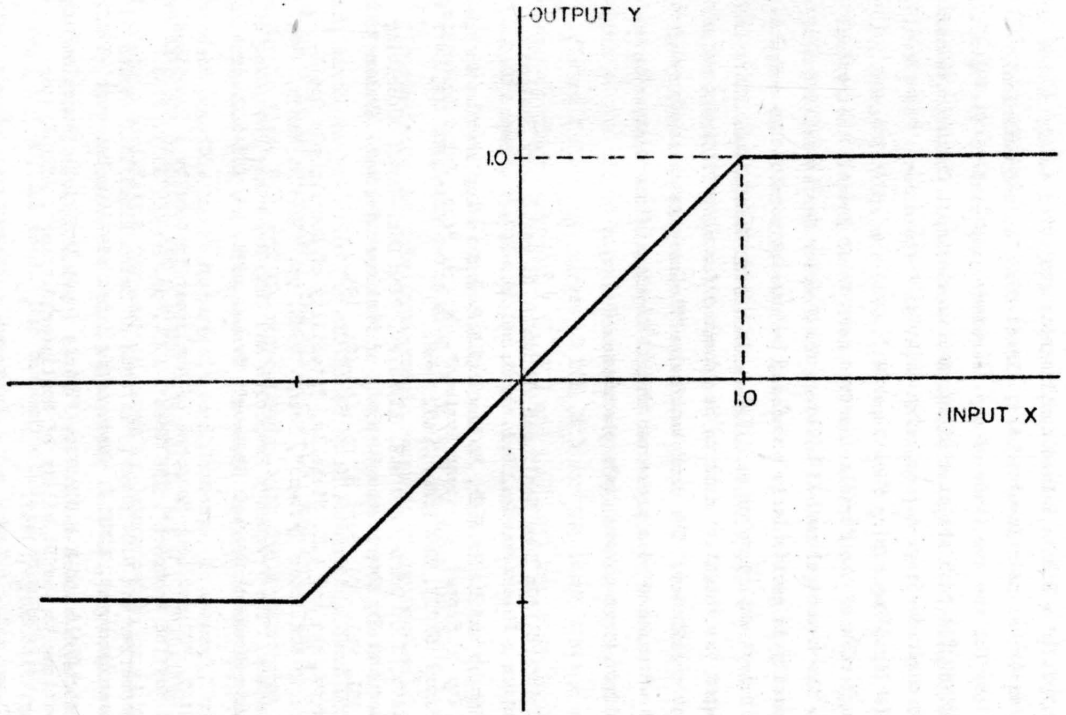

FIGURE 1. INPUT-OUTPUT CURVE OF ODD NONLINEARITY (IDEAL LIMITER)

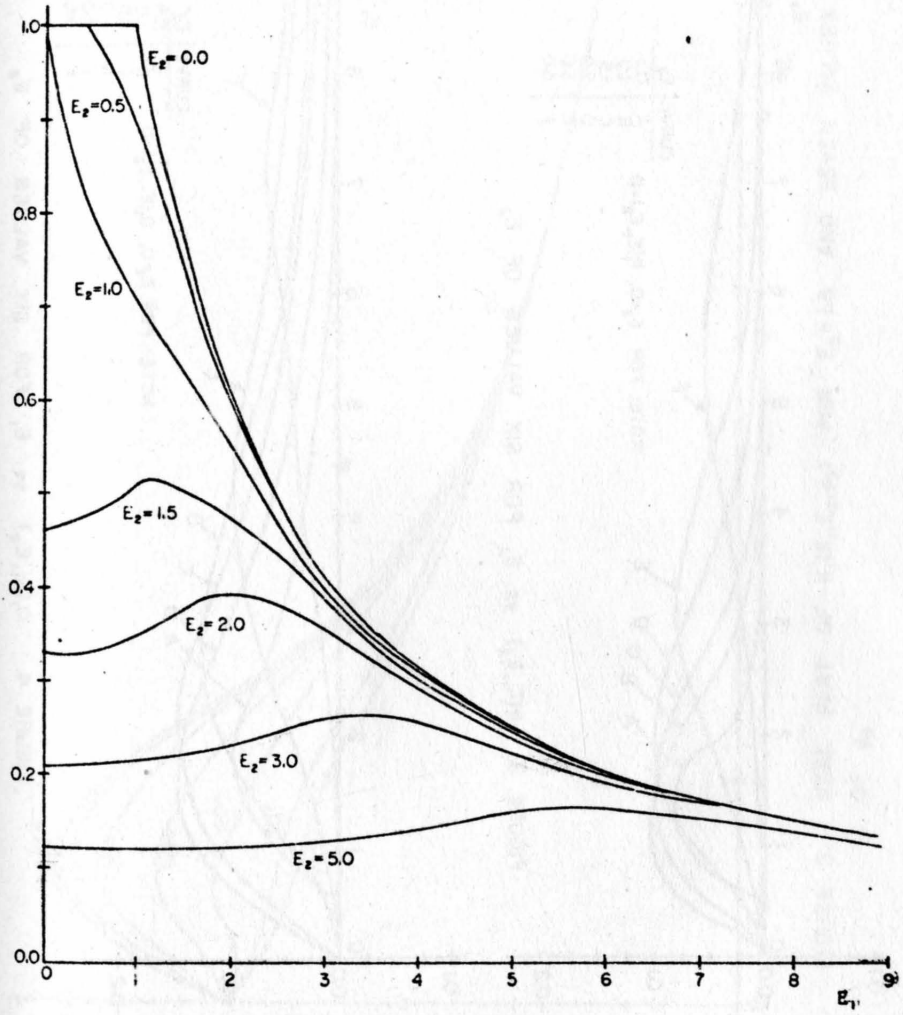

FIGURE 2: $D(E_1, E_2)$ vs E_1 FOR SEVEN VALUES OF E_2

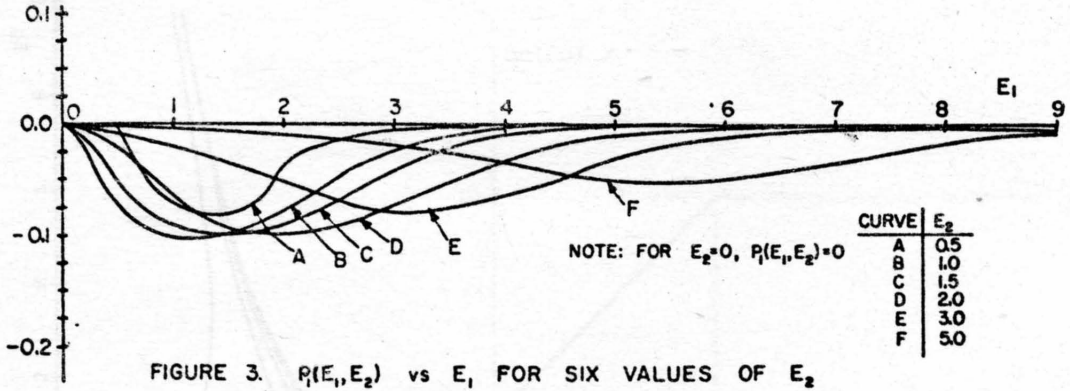

FIGURE 3. $P_1(E_1, E_2)$ vs E_1 FOR SIX VALUES OF E_2

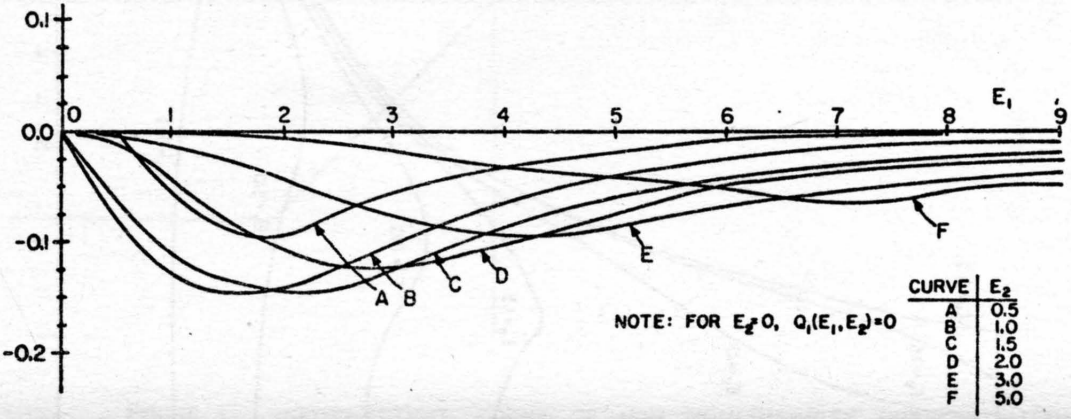

FIGURE 4. $Q_1(E_1, E_2)$ vs E_1 FOR SIX VALUES OF E_2

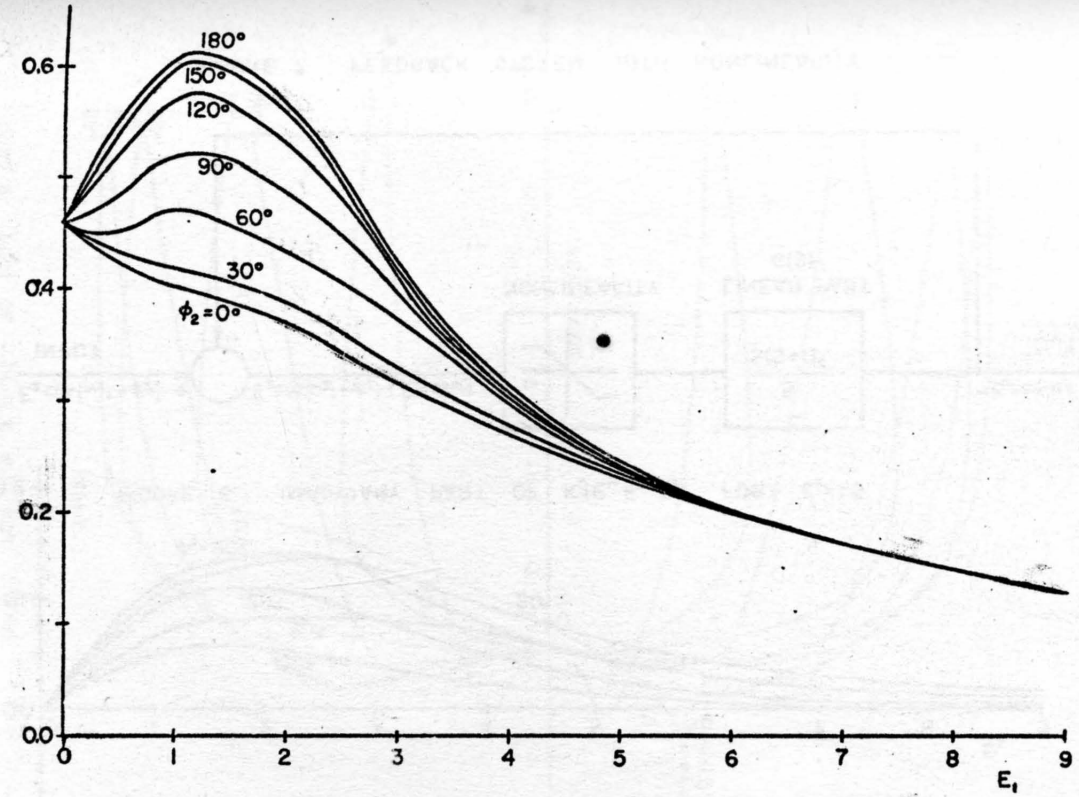

FIGURE 5. REAL PART OF $K_1(E_1, E_2, \phi_2)$ FOR $E_2 = 1.5$ AND SEVEN VALUES OF ϕ_2

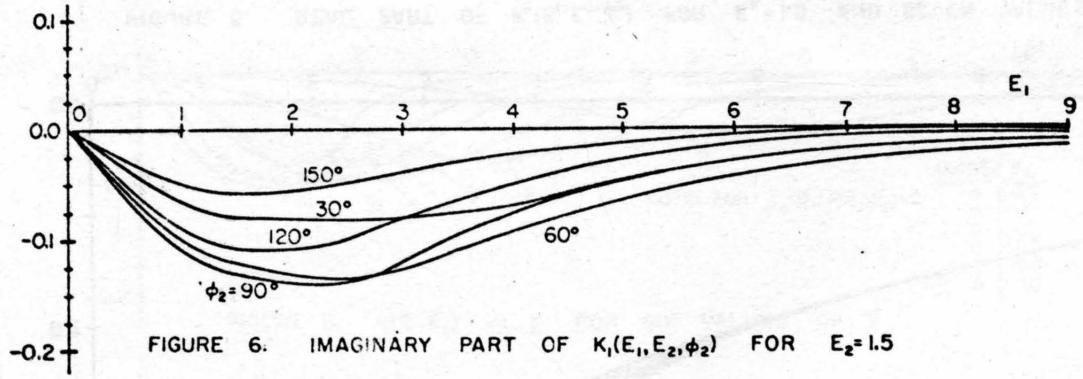

FIGURE 6. IMAGINARY PART OF $K_1(E_1, E_2, \phi_2)$ FOR $E_2 = 1.5$

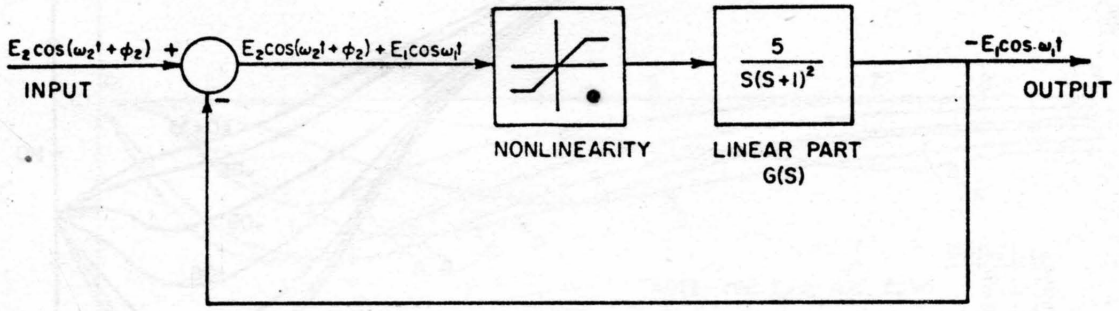

FIGURE 7. FEEDBACK SYSTEM WITH NONLINEARITY

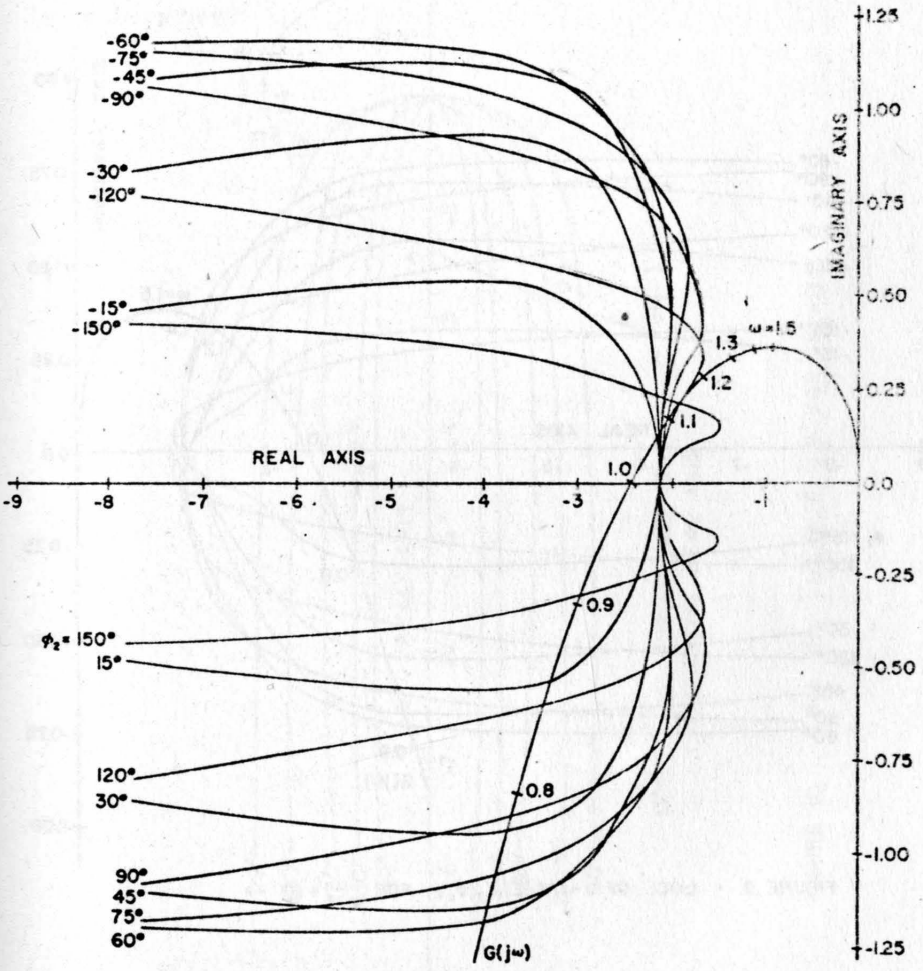

FIGURE 8. LOCI OF $-1/K_1(E_1, E_2, \phi_2)$ FOR $E_2 = 1.5$

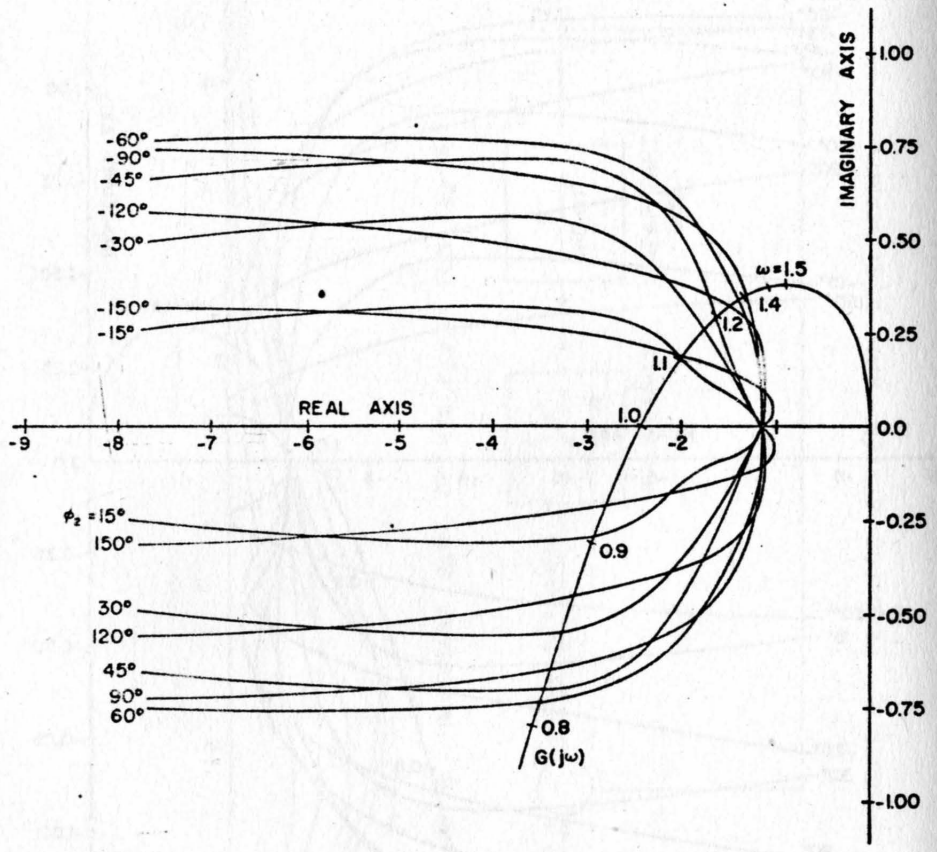

FIGURE 9. LOCI OF $-1/K_1(E_1,E_2,\phi_2)$ FOR $E_2 = 1.0$

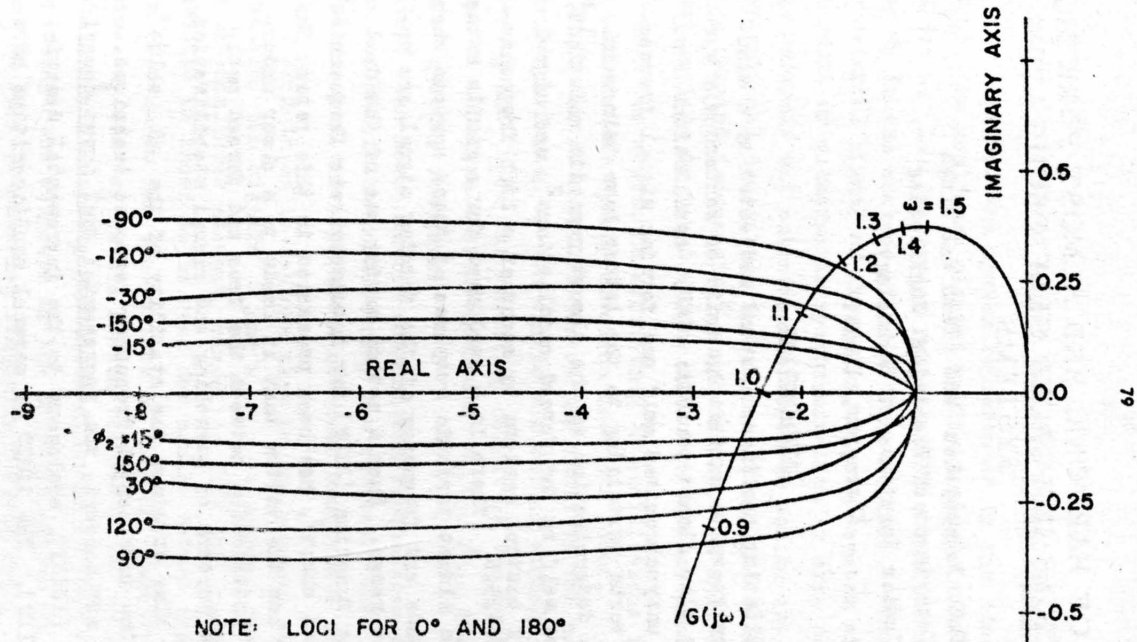

NOTE: LOCI FOR 0° AND 180° LIE ALONG REAL AXIS

FIGURE 10. LOCI OF $-1/K_1(E_1, E_2, \phi_2)$ FOR $E_2 = 0.5$

ANALYSIS OF HARMONIC AND ALMOST PERIODIC OSCILLATIONS IN FORCED SELF OSCILLATING SYSTEMS

P.K. Rajagopalan and Yash Pal Singh
Department of Electrical Engineering
Indian Institute of Technology,
Kharagpur, India.

Introduction

Self oscillating nonlinear systems subjected to a sinusoidal input are known to exhibit harmonic or subharmonic synchronization or else almost periodic (AP) oscillations resulting from the unsynchronized self and forcing signal frequencies. Earlier works pertaining to the latter have been mainly confined to the determination of the almost periodic solutions[1,2], quenching of the self by the forced oscillations[2], and signal stabilization of control systems by means of a high frequency forcing signal[3,4,5,6]. There is a real need for a simple method of analysing the almost periodic response of these systems when both the amplitude and frequency of the forcing signal are varied over a wide range. Such a method making use of the dual input describing function (DIDF) for incommensurate frequencies[6] and the universal chart[7], has been presented in this paper. The proposed method has the virtue that it leads to a clear understanding of the interaction between the free and forced oscillations and the process of quenching and signal stabilization.

The paper also examines the stability of the AP solutions by using the incremental frequency response technique. This leads to a new concept, the incremental dual input describing function (IDIDF), analogous to the incremental describing function (IDF). The IDIDF of several nonlinearities have been evaluated. Criteria for determining the stability of solutions are also presented. The application of the proposed method has been illustrated by investigating the behaviour of the van der Pol equation and a third order relay system.

Analysis of Almost Periodic Oscillations

Consider the system represented by the block diagram of Fig.1, the nonlinear element having a single valued odd characteristic. Let the system exhibit self oscillation at a frequency w_s in the absence of an external signal. When forced with an external signal of frequency w_f, the system will exhibit harmonic or subharmonic synchronization or else AP oscillations. The harmonic and subharmonic responses can be evaluated by the conventional describing function (DF) and the DIDF for integrally related frequencies[8], respectively. An analysis of the AP oscillations is based on the following assumptions :

(i) The system is exhibiting AP oscillations i.e. harmonic or subharmonic synchronization does not occur.

(ii) The AP oscillations at the input to the nonlinearity are approximated by two finite sinusoidal signals of frequencies w_s and w_f. The resulting output of the nonlinearity will consist of signals of frequencies w_s, w_f, pw_s, qw_f and $(\pm pw_s + qw_f)$ p and q being integers.

(iii) The harmonic and combination frequencies generated in the output of the nonlinearity are ignored. This assumption implies that the amplitudes of these components are small.

From these it follows that in the absence of any synchronization, the signals x_f and x_s do not undergo any phase shift in the nonlinear element, since the DIDF for incommensurate frequencies is known to be real for single valued nonlinear elements[6,9]. Hence for the purpose of finding components of frequencies w_s and w_f in the system response, the original system can be represented by the block diagrams of Figs 2 and 3, representing the response of the original system at the forcing and the self-oscillation frequency respectively, N_f and N_s being the respective DIDF'S. From these we obtain :

$$\frac{(C_f)}{(R_f)} = \frac{N_f\,(G)\,(jw_f)}{1 + N_f (G)(jw_f)} \qquad (1)$$

and

$$N_s\,(G)(jw_s) = -1 \qquad (2)$$

Since N_s is always real for single valued nonlinearities, it follows from eqn.2 that the phase angle contributed by $G(jw_s)$ must be 180°. Assuming for the present that only one value of w_s satisfies this phase angle requirement, the following two conditions have to be satisfied:

(i) The frequency of self oscillation, w_s, is constant and consequently:

(ii) The DIDF, N_s, for the self oscillation signal is also constant and is given by:

$$N_s = \frac{1}{|G(jw_s)|} \qquad (3)$$

Since N_s is a function only of the amplitudes X_f and X_s, it follows that when X_f changes, X_s must so adjust itself as to satisfy the condition for the constancy of N_s. Thus for the given system, as X_f varies, X_s takes a definite permissible value and there will be a definite value of N_f for each value of X_f. In other words, the N_s = constant condition leads to a unique N_f/X_f characteristic for the system of Fig.2, X_s being known at each point of the characteristic. This characteristic may be considered as an "Equivalent Describing Function" for the purpose of finding the response at the forcing frequency in the system of Fig.2.

Thus, the analysis of the AP oscillation has been reduced to a problem of finding the forced harmonic response of a system having a nonlinearity for which the gain/input characteristic is the N_f/X_f characteristic drawn for the condition N_s = constant. Once the response at the frequency w_f is determined, the response at the frequency w_s is also known, X_s being known at each point on the N_f/X_f characteristic. Thus the two most significant components in the system response can be determined in a direct manner. The expressions for the N_f/X_f characteristic for a constant N_s, have been derived in Appendix I for several nonlinearities.

If the self oscillations are quenched and the system is synchronized to the forcing frequency, w_f, the input to the nonlinearity can be approximated by a pure sinusoid and the response can be evaluated by the DF analysis. Hence for this case

the problem reduces to that of finding the response of the system of Fig.2, the N_f/X_f characteristic being the conventional describing function characteristic.

Hence the component of frequency w_f in the response of the system can be analysed as the response of the system of Fig. 2, where the gain/input characteristic for the "nonlinear element" is:

(i) The N_f/X_f characteristic drawn for a constant N_s, for the case when self oscillations are present, and

(ii) The N/X_f characteristic for the case when the self oscillations have been quenched.

In other words the gain/input characteristic for the forcing signal is constituted by the two above mentioned parts, the solutions corresponding to the first and the second parts being the AP and the harmonic oscillations respectively. It will be seen that this unified approach gives a clear picture of the transitions from the AP to harmonic oscillations and vice versa.

The response of the system of Fig.2 can be obtained by any one of the several well known methods for finding the closed loop frequency response of nonlinear systems. Of all these methods, the universal chart method[7], being the most convenient when solutions are required over a range of frequencies and amplitudes of the input signals, has been used in this paper. A brief account of the universal chart and its application is included in Appendix 2.

Stability of the Harmonic Solutions

Incremental Describing Function

The solutions obtained by the foregoing analysis can occur in a physical system provided they are stable. The stability of a harmonic solution can be investigated from the open loop frequency response of the system, under the assumed forced condition, for a forcing signal of infinitesimal amplitude, the resulting Nyquist locus being termed as the incremental frequency response locus[8]. When the input to a nonlinear element is

sinusoidal, the gain for the incremental signal is the IDF, M_i. A detailed investigation of the IDF leads to the following two important cases[10]:

(i) When the incremental signal has the same frequency as the finite signal, and

(ii) When the incremental signal is different from that of the finite signal.

For the first case, the IDF for a single valued nonlinearity is complex and is given by :

$$\textcircled{M_i} = (N + \frac{1}{2} X \frac{\partial N}{\partial X}) + \frac{1}{2} X \frac{\partial N}{\partial X} e^{-j2\varphi} \qquad (4)$$

where N is the DF for the finite signal X, and φ the phase of the incremental signal with respect to the finite signal. Clearly, as the angle φ varies, the $\textcircled{M_i}$ phasor traces a circle of radius ($\frac{1}{2} X \frac{\partial N}{\partial X}$), centred at ($N + \frac{1}{2} X \frac{\partial N}{\partial X}$). For the second case the IDF is real and is given by :

$$M_i = (N + \frac{1}{2} X \frac{\partial N}{\partial X}) \qquad (5)$$

Incremental Frequency Response

A typical incremental frequency response locus, $\textcircled{M_i}\textcircled{G}(jw)$, shown in Fig. 4, is composed of:

(i) A locus $(N + \frac{1}{2} X \frac{\partial N}{\partial X}) \textcircled{G}(jw)$, which is similar to the $\textcircled{G}(jw)$ locus { with an associated gain $a_o = N + \frac{1}{2} X \frac{\partial N}{\partial X}$ } for all frequencies other than w_f.

(ii) A circle of radius $(\frac{1}{2} X \frac{\partial N}{\partial X}) \left|\textcircled{G}(jw_f)\right|$ centered at the point corresponding to the frequency w_f on the plot (i).

Stability Criteria

From this two conditions for the stability of forced oscillations are deduced:

(i) The linear system obtained after replacing the nonlinear element by a gain a_o ($= N + \frac{1}{2} X \frac{\partial N}{\partial X}$) must be stable.

(ii) The distance of the critical point from the w_f point on the $a_o \textcircled{G}(jw)$ plot must be greater than $\frac{1}{2} X \frac{\partial N}{\partial X} \left|\textcircled{G}(jw_f)\right|$.

The second stability condition can be shown to be equi-

valent to $\frac{dR}{dX} \geqslant 0$, and while working with the universal chart corresponds to the N curve (considered for increasing X) cutting the θ_l curves in the direction of increasing θ_l. The first condition can be verified by marking, on the N curve, a point C at which $a_o (= N + \frac{1}{2} X \frac{\partial N}{\partial X})$ is equal to a critical gain for the linear system. C is a point of demarcation between stable and unstable values of X. Hence a solution will be stable provided:

(i) The θ_l curve intersects the N curve on the stable side of the critical point C, and

(ii) the N curve (for increasing X) cuts the θ_l curve in the direction of increasing θ_l i.e. from inside to outside.

Stability Of Almost Periodic Solutions

Incremental Dual Input Describing Function

Proceeding along similar lines we arrive at the conclusion that the stability of the almost periodic oscillations can also be investigated using the incremental frequency response technique. To do this we have to define and determine the gain of an incremental signal for the case when the input to the nonlinear element consists of two finite sinusoidal signals of incommensurate frequencies. This is termed as the incremental DIDF (IDIDF) and is defined as :

$$\left(N_i\right) = \frac{\left(\Delta Y\right)}{\left(\Delta X\right)} \qquad (6)$$

where $\left(\Delta Y\right)$ represents the additional component of frequency w in the output for an incremental signal of this frequency represented by the phasor $\left(\Delta X\right)$ at the input.

When the frequencies of the finite signals at the input are w_f and w_s, the following important cases arise:

(i) $w = w_f$
(ii) $w = w_s$
(iii) w being non integrally related to w_f and w_s
(iv) w being an integral multiple of w_f or w_s.

(i) IDIDF for $w = w_f$.

The phasor diagram of Fig.5 shows the input phasor $\left(A_f\right)$,

and the corresponding output (Y_f) being in phase with (X_f) and of magnitude $Y_f (= X_f N_f)$ The Fig. also shows an increment (ΔX_f) $(= \Delta X_f . e^{j\varphi})$. The resulting component of frequency w_f at the input to the nonlinearity is the sum of (X_f) and (ΔX_f), and has an amplitude $X_f + \Delta X_f \cos\varphi$, ΔX_f being infinitesimal. As the amplitude of the signal of frequency w_f increases from X_f to $(X_f + \Delta X_f \cos\varphi)$, the DIDF for this signal increases from N_f to $(N_f + \frac{\partial N_f}{\partial X_f} \Delta X_f \cos\varphi)$. The increased output is represented by the phasor $(Y_f) + (\Delta Y_f)$ being in phase with $(X_f) + (\Delta X_f)$. Taking (X_f) as the reference, we obtain :

$$(Y_f) + (\Delta Y_f) = (X_f + \Delta X_f e^{j\varphi})(N_f + \frac{\partial N_f}{\partial X_f} \Delta X_f \cos\varphi)$$

Neglecting terms involving higher powers of X_f, eliminating (Y_f) and substitution in eqn. 6 finally yields:

$$(N_1')_{w=w_f} = (N_f + \frac{1}{2} X_f \frac{\partial N_f}{\partial X_f}) + \frac{1}{2} X_f . \frac{\partial N_f}{\partial X_f} e^{-j2\varphi} \qquad (7)$$

Therefore, as the angle φ varies, the $(N_1')_{w=w_f}$ phasor traces a circle, Fig.6, centered at $(N_f + \frac{1}{2} X_f \frac{\partial N_f}{\partial X_f})$ and of radius $\frac{1}{2} X_f \frac{\partial N_f}{\partial X_f}$, and is known in terms of the DIDF of the nonlinearity.

(ii) IDIDF for $w = w_s$

Proceeding along similar lines, it can be shown that:

$$(N_1')_{w=w_s} = (N_s + \frac{1}{2} X_s \frac{\partial N_s}{\partial X_s}) + \frac{1}{2} X_s \frac{\partial N_s}{\partial X_s} e^{-j2\varphi} \qquad (8)$$

φ being the angle of the incremental phasor with respect to the phasor (X_s). As the angle φ varies the $(N_1')_{w=w_s}$ phasor also traces a circle whose centre and radius are known in terms of the DIDF of the nonlinearity.

(iii) IDIDF when w is nonintegrally related to w_f and w_s.

A general method of determining the IDIDF is described in Appendix 3, and yields the interesting result:

$$N_1' = Y_{0,0}' = N_s + \frac{1}{2} X_s \frac{\partial N_s}{\partial X_s} = N_f + \frac{1}{2} X_f \frac{\partial N_f}{\partial X_f} \qquad (9)$$

(iv) IDIDF when w is an integral multiple of w_f or w_s

It is seen from Appendix 3, that:

$$\left(\mathcal{N}_1'\right)_{w=nw_f} = Y'_{0,0} - \frac{Y_{2n,0}}{2} e^{-j2\varphi}$$
$$\text{and} \qquad (10)$$
$$\left(\mathcal{N}_1'\right)_{w=nw_s} = Y'_{0,0} - \frac{Y'_{0,2n}}{2} e^{-j2\varphi}$$

Cases may arise where N_s and N_f are not available in an analytical form. For such cases the IDIDF can be determined by a graphical method equivalent of the method of Appendix 3.

Analytical expressions for the IDIDF of several nonlinearities are derived in Appendix 4.

Incremental Frequency Response

A typical incremental frequency response plot for an almost periodic solution, is shown in Fig.7. It is composed of:

(i) A locus $Y'_{0,0}\mathcal{G}(jw)$ for all frequencies that are non-integrally related to w_f and w_s.

(ii) A circle of radius $\frac{1}{2} X_f \frac{\partial N_f}{\partial X_f} \left|\mathcal{G}(jw_f)\right|$ centered at the $w = w_f$ point of the plot (i).

(iii) A circle of radius $\frac{1}{2} X_s \frac{\partial N_s}{\partial X_s} \left|\mathcal{G}(jw_s)\right|$ centered at the $w = w_s$ point of the plot (i).

The circles centered at nw_f and nw_s have radii $\frac{Y'_{2n,0}}{2}\left|\mathcal{G}(jnw_f)\right|$ and $\frac{Y'_{0,2n}}{2}\left|\mathcal{G}(jnw_s)\right|$ respectively which are small and are ignored.

Stability Criteria

From the incremental frequency response plot the following conditions for the stability of forced AP oscillations are obtained:

(i) The linear system obtained after replacing the nonlinear element by a gain $Y'_{0,0}\left(= M_s + \frac{1}{2} X_s \frac{\partial N_s}{\partial X_s} = N_f + \frac{1}{2} X_f \frac{\partial N_f}{\partial X_f}\right)$ must be stable.

(ii) $$\frac{dR_f}{dX_f} \geqslant 0$$

While working with the universal chart, the second condition for the stability of almost periodic oscillation can be seen to

correspond to the N curve (log Y_f/log X_f plot), considered for increasing X_f, cutting the θ_l curves in the direction of increasing θ_l . The first condition can be verified by marking, on the N curve, a point C at which $Y'_{o,o}$ is equal to a critical gain for the linear system. C is a point of demarcation between regions of stable and unstable values of X_f. Hence, a solution will be stable provided:

(i) The θ_l curve intersects the N curve on the stable side of the critical point C, and

(ii) The N curve (for increasing X_f) cuts the θ_l curve in the direction of increasing θ_l i.e. from inside to outside.

Applications

The application of the proposed method is illustrated by determining the forced oscillations of (i) a van der Pol equation and (ii) a third order system incorporating an ideal relay.

Example 1 : Forced Oscillations of the van der Pol Equation.

The equation

$$\frac{d^2x}{dt^2} - \alpha \frac{dx}{dt} + \gamma \frac{d}{dt}(x^3) + w_o^2 = Bw^2 \sin wt \qquad (11)$$

can be represented by the block diagram of Fig. 8, where

$$\textcircled{R} = \frac{B w^2}{(w_o^2 - w^2) - j\alpha w} \qquad (12)$$

$$y = \gamma x^3$$

(a) Self Oscillations

Since the describing function for the cubic nonlinearity is real, the nonlinearity can be looked upon as a variable gain $N \left(= \frac{3}{4}\gamma X^2 \right)$. The root locus, Fig. 9, shows that the system is unstable for small values of X, and indicates stable self oscillations of frequency $w_s = w_o$. The amplitude, X_o, of self oscillations is given by:

$$\frac{3}{4}\gamma X_o^2 = -\frac{1}{G(jw_o)} = \alpha$$

$$\therefore \quad X_o^2 = \frac{4\alpha}{3\gamma} \qquad (13)$$

(b) Forced Harmonic Response

(i) Solutions - When the self oscillations are absent,

the forced harmonic response can be obtained by DF analysis. Taking the phasor $\textcircled{X_f}$ representing the input to nonlinearity as the reference phasor, we obtain :

$$Y_f = -\frac{3}{4}\gamma X_f^3$$

$$\therefore \textcircled{Z_f} = -\frac{3}{4}\gamma X_f^3 \left[\frac{jw_f}{(w_s^2-w_f^2) - j\alpha w_f}\right]$$

Also $\textcircled{R_f} = X_f + \textcircled{Z_f}$

$$\therefore \frac{\textcircled{B}\, w_f^2}{(w_s^2-w_f^2) - j\alpha w_f} = X_f + -\frac{3}{4}\gamma X_f^3 \left[\frac{jw_f}{(w_s^2 - w_f^2) - j\alpha w_f}\right]$$

$$\therefore \frac{B^2 w_f^2}{X_f^2} = \frac{(w_s^2 - w_f^2)^2}{w_f^2} + \alpha^2 \left[1 - \frac{X_f^2}{(4\alpha/3\gamma)}\right]^2 \qquad (14)$$

(ii) Stability

From the root locus, Fig. 9 , we find that the system is stable for associated gains greater than α . Hence from the first stability condition, we obtain :

$$N_1 = -\frac{3}{2}\gamma X_f^2 \geqslant \alpha$$

$$\therefore X_f^2 \geqslant \frac{2\alpha}{3\gamma} \qquad (15)$$

Comparing with eqn. 13, it is seen that the harmonic oscillations will be stable provided the square of the forced amplitude is greater than half the square of the amplitude of the free oscillations. The critical value , X_{fc} , is given by:

$$X_{fc}^2 = \frac{2\alpha}{3\gamma} \qquad (16)$$

Also, the second stability condition $\frac{dR}{dX} \geqslant 0$ can be seen to be equivalent to $-\frac{dB^2}{dX^2} \geqslant 0$ derived by van der Pol[1].

(c) Forced Almost Periodic Response

(i) Solutions.

For this case the frequency of the self oscillation remains fixed at w_o and consequently the DIDF for this signal also remains fixed at α. Hence from Appendix 1, we obtain:

$$N_f = 2\alpha - \frac{9\gamma}{4} X_f^2 \qquad (17)$$

and $X_s^2 = \frac{4\alpha}{3\gamma} - 2X_f^2$ (18)

Hence taking the phasor $\textcircled{X}_f$ representing the signal of the forcing frequency at the input to the nonlinearity as the reference phasor, we obtain for the system of Fig. 8:

$$\frac{\textcircled{B}\ w_f^2}{(w_s^2 - w_f^2) - j\alpha w_f} = X_f + (2\alpha X_f - \frac{9\gamma}{4} X_f^3) \frac{jw_f}{(w_s^2 - w_f^2) - j\alpha w_f}$$

$$\therefore \frac{B^2}{X_f^2} \frac{w_f^2}{} = \frac{(w_s^2 - w_f^2)^2}{w_f^2} + \alpha^2 \left[1 - \frac{3}{(4\alpha/3\gamma)} X_f^2 \right]^2 \quad (19)$$

Also the mean square of the output is obtained from eqn. 18 as:

$$\frac{1}{2}(X_s^2 + X_f^2) = \frac{1}{2}\left\{ \frac{4\alpha}{3\gamma} - X_f^2 \right\} \quad (20)$$

This quantity decreases as X_f increases from 0 to X_{fo}, and has a minimum value $2\alpha/3\gamma$ for $X_f = X_{fo}$.

Eqn.17 also shows that as X_f increases from 0 to X_{fo}, X_s decreases from X_{so} to zero and remains zero for all higher values of X_f.

These results are identical to those obtained by van der Pol[1] by the method of slowly varying gain and phase.

(ii) Stability

From Appendix 4, for $N_s = \alpha$, the IDIDF, N_i' ($= \alpha + \frac{3\gamma}{4} X_s^2$), is seen to be always greater than α. Hence the first stability condition is satisfied by all the possible AP oscillations. Hence the AP oscillations will be stable provided $\frac{dR_f}{dX_f}$ is greater than zero.

For a given B and w_f, eqn. 19 is a cubic in X_f^2. Hence for certain combination of the parameters, this eqn. may have three real roots for X_f^2. In such situations one of the solutions will correspond to $\frac{dB}{dX_f} < 0$ and will be unstable and the AP response will exhibit a jump phenomenon. Hence a jump can take place from one AP state to another AP state, resulting in a jump in X_f, accompanied by a jump in X_s as well as in the mean square value of the response x.

Example 2. Application of the Universal Chart to the Forced Oscillation of the van der Pol equation.

(a) System Characteristics.

Consider the van der Pol equation with the numerical constants, $\alpha = 1$, $= 4/9$ and $w_o = 1$. For this system, $w_s = 1$, $N_s = 1$, $X_{so}^2 = 3$ and $X_{fo}^2 = 1.5$.

The DF for the nonlinearity, $y = \frac{4}{9} x^3$, yields:

$$\log Y_f = 3 \log X_f - \log 3 \qquad (21)$$

For $N_s = 1$, the DIDF for the nonlinearity is obtained from eqn. 30 as:

$$\log Y_f = \log (2X_f - X_f^3) \qquad (22)$$

The transfer function of the linear part is given by :

$$\mathcal{G}(jw) = \left(\frac{jw}{1 - w^2 - jw} \right) \qquad (23)$$

The $\log Y_f / \log X_f$ plot comprising the DF as well as the DIDF (for $N_s = 1$) plot is shown (Curve N) in Fig.10, along with a plot L, of $\log |\mathcal{G}(jw)|$. The phase angle of the linear transfer function is marked along with each frequency on the L curve. The point C marks the critical point on the DF plot.

(b) Solutions

Fig11 illustrates the superposition of the $\Theta_l = 156^\circ$ curve of the universal chart on Fig. 10 for $\log R_f = \bar{1}.90$ at $w = 1.25$. The only intersection of the Θ_l curve with the N curve is the point P on the stable part of the DF. At this intersection the N curve cuts the Θ_l curve from inside to outside. Hence the resulting response is a stable harmonic oscillation with $\log X_f = 0.265$.

The response for a range of variation of R_f can be obtained by repeating this procedure. Fig. 12 shows the solutions for several values of R_f for $w = 1.25$. For $\log R_f = 0.2$ and 0.0 the intersections indicate stable harmonic oscillations with $\log X_f = 0.345$ and 0.30 respectively. For $\log R_f = \bar{1}.8$ and $\bar{1}.4$ the stable intersections are on the DIDF part of the N curve and yield $\log X_f = 0.07$ and $\bar{1}.415$ respectively. The variation of X_s with X_f for the AP oscillations can be obtained from eqn. 26, and is shown in the $\log X_s / \log X_f$ plot of Fig.13. From this, $\log X_s = \bar{1}.71$ and 0.23 for $\log R_f = \bar{1}.8$ and $\bar{1}.4$

respectively. For log $R_f = \bar{1}.61$ there are three intersections of which the middle one corresponding to log $X_f = \bar{1}.94$ is seen to be unstable. The remaining two yield log X_f = 0.0 and $\bar{1}.70$ and log X_s = 0.0 and 0.2 respectively.

Figs. 14 and 15 show the log X_f/log R_f and log X_s/log R_f plots for w_f = 1.25 and 2.0 respectively. At w_f = 1.25 as log R_f is increased X_s decreases and X_f increases steadily. At log R_f = $\bar{1}.65$ a jump takes place resulting in an increase in X_f and a decrease in X_s. As log R_f is further increased X_s decreases to zero and at log $R_f = \bar{1}.88$ a further jump in X_f takes place and the system exhibits forced harmonic response for higher values of R_f. In other words synchronization occurs at log R_f = $\bar{1}.88$. When R_f is decreased from a large value a jump down in X_f takes place at log $R_f = \bar{1}.835$ with a simultaneous building up of X_s. Hence desynchronization takes place at $R_f = \bar{1}.835$.

Example 3. Forced Oscillations of a Third Order System Incorporating an Ideal Relay.

System Characteristics.

Consider the system of Fig.1, where the nonlinear element is an ideal relay (M=1), and the transfer function of the linear element is:

$$G(jw) = \frac{2}{jw(1+jw)^2} \tag{24}$$

The DF of the relay yields:

$$\log Y_f = \log 4 - \log \Pi \tag{25}$$

For this system, w_s = 1.0, $|G(jw_s)|$ = 1.0 and N_s = 1.0. The Y_f/X_f characteristic is given by eqns. 38 and 39 . The log Y_f/log X_f plot is shown (curve N) in Fig.16, along with a plot, L, of log $|G(jw)|$. The phase angle of the linear transfer function is marked along with each freqency along the L curve. The dotted parts of the DF and DIDF plots terminated by the critical points C_1 and C_2 correspond to the IDF(= N_1) and IDIDF (N_1') being greater than 1.0, and lead to unstable solutions.

Solutions

Fig. 17 shows the superposition of the $\theta_l = 170^\circ$ curve of the universal chart for log R_f = 1.35 at w_f = 1.2. The intersection at P_2 indicates a possible stable harmonic solution. The intersection at P_1 indicates a possible stable almost

periodic solution. The intersections Q_1 and Q_2 indicate unstable AP solutions and the intersection Q_3 indicates an unstable harmonic solution.

Fig. 18 shows the solutions for several values of R_f for $w_f = 1.5$. When R_f is increased from 0 onwards the system continues to exhibit AP oscillations till log R_f reaches the value $\bar{1}.8$. At this amplitude, the intersection changes over from DIDF to the DF part of the curve N and hence the system gets synchronized to the forcing frequency and remains synchronized for all higher values of R_f. However, when the amplitude R_f is slowly decreased, the system remains synchronized till log R_f reaches the value $\bar{1}.40$. At this point the response changes over from harmonic to almost periodic with the reappearance of the self oscillations. The values of X_s for the AP solutions can be obtained from the log X_s/log X_f plot of Fig. 13 based on eqns. 38 and 39.

Fig. 19 shows the variation of X_f and X_s with variations in R_f of a frequency 1.5. The quenching and reappearance of the self oscillation frequency signal is brought out very clearly in this diagram.

When the frequency w_f is very high, $X_f \simeq R_f$. Hence the log X_s/log X_f diagram of Fig. 13 becomes identical to the log X_s/log R_f plots. From this it is seen that self oscillations are quenched when log R_f increases beyond $\bar{1}.93$.

Conclusions

In this paper a simple method of analysing the almost periodic oscillations of nonlinear systems has been presented. Such oscillations occur when unsynchronized free and forced oscillations are present in the response of the system. It has been shown that for systems incorporating a single valued element the DIDF for the component at the input frequency is to be determined for the constraint that the DIDF for the signal of the self oscillation frequency remains a constant. With this constraint, it is possible to treat the component at the forcing frequency as the harmonic response of an 'equivalent system'. Also there a simple relationship is shown to exist

between the amplitudes of the two frequency components in the response. The universal chart method has been employed to eva-luate the forced frequency response as it gives a clear picture of the variation of X_f with variations in R_f. The applica-tion of the method has been illustrated by analysing the response of (i) the van der Pol equation, and (ii) a third order system incorporating an ideal relay.

The stability of the almost periodic oscillations has been studied by making use of the incremental frequency response technique. For this a new concept, the incremental dual input describing function has been developed. Expressions for the IDIDF for several well known nonlinearities have been derived and several of its interesting properties have been studied.

Simplified criteria for the stability of the AP oscillations have been obtained and employed to interpret the stability of the solutions obtained from the universal chart.

The method has been able to clearly bring out the variation of X_f and X_s with variation in the amplitude of the forcing signal at the input to the system. For the van der Pol equation it has clearly brought out the transition from the drift to periodic motion[11]. For the relay system the existance of a finite magnitude of X_s just before quenching[6] by a high frequency signal is also made evident.

Acknowledgement

The authors are grateful to Prof. N. Kesavamurthy for his keen interest in this work and for many valuable discussions. The authors also thank their colleagues Dr. V. Balaramamurty and Mr. T.R. Padmnabhan for many suggestions and help in the preparation of the paper.

References

1. van der Pol, B.: 'Forced oscillations in a circuit with nonlinear resistance. (Receiption with reactive triode)', The London, Edinburg, and Dublin Philosophical magazine and journal of science, 1927,3, pp. 65-80.

2. Minorsky, N.: 'Nonlinear oscillations', (Van Nostrand, 1962)
3. Oldenburger, R.: 'Signal stabilization of a control system', Trans. ASME, 1957, 69, pp.1869-1872
4. Oldenburger, R., and Liu, C.C.: 'Signal stabilization of a control system', Trans. AIEE, 19, 78, pt. II, pp.96-100.
5. Oldenburger, A., and Nakada, T.: 'Signal stabilization of self oscillating systems', IRE Trans. on automatic control, 1961, AC-6, pp.319-325.
6. Oldenburger, R., and Boyer, R.C.: 'Effects of extra sinusoidal inputs to nonlinear systems', Trans. ASME (JBE) 1962, 84, D, pp.559-570.
7. Singh, Yash Pal : 'Graphical method for finding the closed-loop frequency response of nonlinear feedback control systems', Proc. IEE, 1965, 112, No.11, pp. 2165-2170.
8. West, J.C., Douce, J.L., and Livesley, R.K.: 'The dual input describing function and its use in the analysis of nonlinear feedback systems', Proc. IEE, 1956, 103, pt.B, pp.463-474.
9. Rajagopalan, P.K., and Singh, Yash Pal: 'The complete dual input response of nonlinear elements', (Companion paper being sent to the IVth Congress of I.F.A.C.)
10. Rajagopalan, P.K., and Singh, Yash Pal: 'The incremental describing function and its application to the stability of forced nonlinear systems', (Paper being prepared for publication)
11. Cartwright, M.L.: 'Forced oscillations in nearly sinusoidal systems', JIEE, 1948, 95, pt.III, pp.88-96
12. Gibson, J.E.: 'Nonlinear automatic control', (McGraw-Hill, 1963).

Appendix I

N_f/X_f Characteristics for a Constant N_s

Expressions for the N_f/X_f characteristics for a constant N_s for several nonlinear elements are derived below:

1. Cubic

For a cubic nonlinearity $y = x^3$, the DIDF's for incommen-

surate frequencies are given by:

$$N_s = \frac{3}{4}\left\{X_s^2 + 2X_f^2\right\} \tag{24}$$

and

$$N_f = \frac{3}{4}\left\{X_f^2 + 2X_s^2\right\} \tag{25}$$

X_s and X_f being the amplitudes of the two inputs. From eqn.24 we obtain

$$X_s^2 = \frac{4}{3} N_s - 2X_f^2 \tag{26}$$

Substituting this in eqn.25, and simplifying we obtain:

$$N_f = 2N_s - \frac{9}{4} X_f^2 \tag{27}$$

For $X_s = 0$,

$$N_f = \frac{3}{4} X_f^2 \tag{28}$$

These N_f/X_f characteristics are plotted in Fig.20. The two characteristics intersect at the point C, hence equating the two gains, the value of X_{fc} is given by :

$$2N_s - \frac{9}{4} X_{fc}^2 = \frac{3}{4} X_{fc}^2$$

$$\therefore \quad X_{fc}^2 = \frac{2}{3} N_s \tag{29}$$

Substituting this value in eqn.26, we find

$$X_{sc}^2 = \frac{4}{3} N_s - \frac{4}{3} N_s = 0$$

Hence at the point C, even for the N_f/X_f characteristics (for constant N_s), the value of X_s is zero.

Hence as X_f is increased from zero, the gain N_f decreases from the value $2N_s$, till X_f attains a value X_{fc} (eqn.29). At this point, the signal X_s, which decreases with increase in X_f, (eqn.26), disappears and for higher values of X_f, the gain N_f follows the describing function plot. The dotted part of the constant N_s curve corresponds to imaginary values of X_s and may be ignored.

Summarizing, for N_s = Constant

$$N_f = 2N_s - \frac{9}{4} X_f^2$$

$$\therefore \quad Y_f = X_f . N_f = 2N_s . X_f - \frac{9}{4} X_f^3 \tag{30}$$

$$X_{fc}^2 = \frac{2}{3} N_s$$

At, $X_f = X_{fc}$, $\quad N_f = \frac{N_s}{2}$

2. Quintic

For the quintic characteristics, $y = x^5$, the DIDF's for incommensurate frequencies are given by :

$$N_s = \frac{5}{8} X_s^4 + \frac{15}{4} X_s^2 X_f^2 + \frac{15}{8} X_f^4 \qquad (31)$$

and $$N_f = \frac{15}{8} X_s^4 + \frac{15}{4} X_s^2 X_f^2 + \frac{5}{8} X_f^4 \qquad (32)$$

For a constant N_s, X_s is given by:

$$\frac{5}{8} X_s^4 + \frac{15}{4} X_s^2 X_f^2 + \frac{15}{8} X_f^4 - N_s = 0$$

$$\therefore X_s^2 = -3X_f^2 \pm \sqrt{6X_f^4 + \frac{8N_s}{5}}$$

For real X_s, only the positive sign is admissible,

$$\therefore X_s^2 = \sqrt{6 X_f^4 + \frac{8N_s}{5}} - 3X_f^2 \qquad (33)$$

Substituting in eqn. 32 and simplifying , we obtain:

$$N_f = 3N_s + \frac{35}{2} X_f^4 - \frac{15}{2} X_f^2 \sqrt{6X_f^4 + \frac{8}{5} N_s} \qquad (34)$$

For $X_s = 0$;

$$N_f = \frac{5}{8} X_f^4 \qquad (35)$$

These two N_f/X_f characteristics are plotted in Fig.21, and intersect at C. The X_f for this point can be obtained by substituting $X_s = 0$ in eqn. 33, giving :

$$X_{fc}^4 = \frac{8}{15} N_s \qquad (36)$$

Hence, as X_f is increased from zero, the gain N_f decreases from the value $3N_s$, till X_f reaches the value X_{fc}. At this point the signal X_s, which decreases on increasing X_f disappears. For higher values of X_f, the gain N_f follows the describing function plot. The dotted part of the constant N_s curve corresponds to imaginary values of X_s, and may be ignored. Also for $X_f = X_{fc}$,

$$N_f = \frac{N_s}{3} \qquad (37)$$

3. Ideal relay.

(a) $X_f \leqslant X_s$

For the ideal relay the DIDF's for incommensurate frequencies are given by[12] :

$$N_s = \frac{8M}{\pi^2 X_s} \textcircled{E}(k)$$

and $$N_f = \frac{8M}{\pi^2 X_s} \cdot \frac{1}{k^2}\left\{\textcircled{E}(k) - (1-k^2)\textcircled{K}(k)\right\}$$

where $k = X_f/X_s$ and is less than 1, and $\textcircled{K}$ and $\textcircled{E}$ are the complete elliptical integrals of the first and second kind respectively.

$$\therefore \frac{N_f}{N_s} = \frac{1}{k^2} \frac{\textcircled{E}(k) - (1-k^2)\textcircled{K}(k)}{\textcircled{E}(k)}$$

$$= \left\{\frac{\textcircled{E}(k) - \textcircled{K}(k)}{k^2} + \textcircled{K}(k)\right\} \frac{1}{\textcircled{E}(k)} = \frac{-\textcircled{D}(k) + \textcircled{K}(k)}{\textcircled{E}(k)}$$

$$\therefore \frac{N_f}{N_s} = \frac{\textcircled{B}(k)}{\textcircled{E}(k)}$$

Hence for a constant N_s, we obtain:

$$X_s = \frac{8M}{\pi^2} \cdot \frac{\textcircled{E}(k)}{N_s}$$

$$X_f = k.X_s$$

$$N_f = \frac{\textcircled{B}(k)}{\textcircled{E}(k)} N_s \qquad (38)$$

$$Y_f = \frac{8M}{\pi^2} k\textcircled{B}(k)$$

where $k = X_f/X_s \leqslant 1$.

(b) $X_f \geqslant X_s$

For this case, the DIDF's for incommensurate frequencies are given by:

$$N_s = \frac{8M}{\pi^2 X_s} \cdot \frac{1}{k}\left\{\textcircled{E}(k) - (1-k^2)\textcircled{K}(k)\right\}$$

and $$N_f = \frac{8M}{\pi^2 X_s} k\textcircled{E}(k)$$

where $k = \frac{X_s}{X_f}$ and is less than 1.

$$\therefore \frac{N_f}{N_s} = \frac{\textcircled{E}(k)}{\textcircled{B}(k)}$$

Hence for a constant N_s, we obtain:

$$X_s = \frac{8M}{\pi^2} \cdot k \frac{\textcircled{B}(k)}{N_s}$$

$$X_f = \frac{8M}{\pi^2} \cdot \frac{\textcircled{B}(k)}{N_s} \qquad Y_f = \frac{8M}{\pi^2} \textcircled{E}(k) \qquad (39)$$

$$N_f = \frac{\textcircled{E}(k)}{\textcircled{B}(k)} \cdot N_s \qquad \text{where } k = X_s/X_f \leqslant 1.$$

As the complete elliptical integrals are tabulated in terms of the parameter k, these results are also expressed in terms of k for ease in computation.

Appendix II

The Universal Chart

A brief account of the universal chart and its application is given below.

Consider the system of Fig.22, For any unity feedback system $r(t) = e(t) + c(t)$. For components of a given frequency in the three quantities, this relationship is expressed in the phasor diagram of Fig.23. The ratio of the amplitudes C and E and the phase angle between them are determined by the linear and the nonlinear transfer functions in the forward loop. Consider the case when the amplitude, R, and the loop phase shift, θ_l , are fixed and C and E take various values. From triangle OAB in Fig.23,

$$\frac{C}{R} = \frac{\text{Sin}(180^\circ - \overline{\theta_l + \theta_o}}{\text{Sin}(180^\circ - \theta_l)}$$

and $$\frac{E}{R} = \frac{\text{Sin}\,\theta_o}{\text{Sin}(180^\circ - \theta_l)}$$

$$\log\left(\frac{C}{R}\right) = \log \text{Sin}\,(\theta_l + \theta_o) - \log \text{Sin}\,\theta_l$$

and $$\log\left(\frac{E}{R}\right) = \log \text{Sin}\,\theta_o - \log \text{Sin}\,\theta_l$$

Clearly, for a fixed θ_l , $\log\left(\frac{C}{R}\right)$ and $\log\left(\frac{E}{R}\right)$ are functions of θ_o only. Plotting $\log\left(\frac{C}{R}\right)$/ $\log\left(\frac{E}{R}\right)$ for a given θ_l (= 166° say), the curve of Fig.24 is obtained. A family of such curves, each for a fixed θ_l is drawn, and is designated as the universal chart, since it has been obtained without any reference to the system characteristics. By shifting the origin of the universal chart to (-log R, -log R) it is transformed into the log C/log E plots for various values of θ_l . For the system of Fig.22,

$$\log E = \log X - \log G_1 \qquad (40)$$

and $$\log C = \log Y + \log G_2$$

where X and Y represent the amplitudes at the input and output respectively, of the nonlinear element and G_1 and G_2 are the

gains of the linear transfer functions for the signal of a certain frequency. For the case when the input to the nonlinearity can be assumed to be sinusoidal, $Y = N.X$, N being the conventional describing function, and the log Y/log X plot is obtained as shown in Fig.25. To predict the response over a range of frequencies, the characteristics of the linear transfer functions are plotted as log G_2/log G_1 as shown by the curve L in Fig. 25. Frequencies w_1, w_2,... and the corresponding phase shifts for a transfer function $G_1(jw)$. $G_2(jw)$ are marked along the curve L in this figure. Considering only single valued nonlinearities, for a chosen frequency, say 4.0, the curve N with O_1 (the point for w = 4.0 on the curve L) as origin represents the log C/log E curve defined by eqn. 40, and the total loop phase shift is 166°. For a given R (=1.25 say) the curve O_1 = 166° of the universal chart with its origin shifted to (-.097, -.097) represents the log C/log E variation. The superposition of these two sets of log C/log E curves is shown in Fig.26, in which the intersections of the 166° curve of the universal chart and the N curve, represent the only points where the loop phase shift and the loop gain conditions represented by eqn.40, are simultaneously satisfied, and give the possible values of the response. This procedure can be repeated for any desired range of R and w.

Appendix III

General Method of Determining the IDIDF of Odd Nonlinear Elements

Consider an odd nonlinearity $y = f(x)$, having an input $x = X_1 \text{ Sin } w_1t + X_2 \text{ Sin } w_2t$, w_1/w_2 being an irrational number. For an incremental input signal x_i, the incremental output is obtained as[10].

$$y_i = x_i \frac{d}{dx}\left\{f(x)\right\} + \frac{x_i^2}{2!}\frac{d^2}{dx^2}\left\{f(x)\right\} + \ldots$$

where $x = X_1 \text{ Sin } w_1t + X_2 \text{ Sin } w_2t$

For an infinitesimal signal x_i:

$$y_i = x_i \frac{d}{dx}\left\{f(x)\right\}$$

When y is an odd function of x, $\frac{dy}{dx}$ is an even func-

tion of x. For the case when $x = X_1 \sin w_1 t + X_2 \sin w_2 t$, $\frac{d}{dx}\{f(x)\}$ can be expressed as :

$$\frac{d}{dx}\{f(x)\} = \sum_{p=-\infty}^{\infty} \sum_{q=0}^{\infty} Y'_{p,q} \cos(\overline{pw_1 + qw_2}\, t)$$

where p and q are either both odd or both even.

$$\therefore\ y_i = x_1 \sum_{p=-\infty}^{\infty} \sum_{q=0}^{\infty} Y'_{p,q} \cos(\overline{pw_1 + qw_2}\, t)$$

The following cases arise:

(i) $x_i = \Delta X \sin(w_1 t + \varphi)$

For this case, terms of frequency w_1 in the incremental output are obtained for p = q = o, and p=2, q = o.

$$\therefore\ \underset{w=w_1}{(N'_1)} = Y'_{o,o} - \frac{Y'_{2,o}}{2} e^{-j2\varphi}$$

(ii) $x_i = \Delta x \sin(w_2 t + \varphi)$

For this case, terms of frequency w_2 in the incremental output are obtained for p = q = o, and p = o, q = 2.

$$\therefore\ \underset{w=w_2}{(N'_1)} = Y'_{o,o} - \frac{Y'_{o,2}}{2} e^{-j2\varphi}$$

(iii) $x_i = \Delta X \sin(nw_1 t + \varphi)$, where n is an integer.

For this case:

$$\underset{w=nw_1}{(N'_1)} = Y'_{o,o} - \frac{Y'_{2n,o}}{2} e^{-j2\varphi}$$

(iv) $x_i = \Delta X \sin(nw_2 t + \varphi)$, where n is an integer:

$$\underset{w=nw_2}{(N'_1)} = Y'_{o,o} - \frac{Y'_{o,2n}}{2} e^{-j2\varphi}$$

(v) $x_i = \Delta X \sin(wt + \varphi)$, $\frac{w}{w_1}$ and $\frac{w}{w_2}$ being irrational

$$N'_1 = Y'_{o,o}$$

From these it can be seen that the centre of the (N'_1) circles is always $Y'_{o,o}$. Comparing the results of (i) and (ii) above with eqns. 7 and 8, we obtain:

$$N_s + \frac{1}{2} X_s \frac{\partial N_s}{\partial X_s} = N_f + \frac{1}{2} \frac{\partial N_f}{\partial X_f} = Y'_{o,o}$$

$$\frac{1}{2} X_s \frac{\partial N_s}{\partial X_s} = \frac{Y'_{2,o}}{2} \qquad (41)$$

$$\frac{1}{2} X_f \frac{\partial N_s}{\partial X_f} = \frac{Y'_{o,2n}}{2}$$

Appendix IV

The expressions for the incremental DIDF of several nonlinearities are derived below:

(1) Cubic.

For the nonlinear characteristics $y = x^3$,

$$N_s = \frac{3}{4}\left\{X_s^2 + 2X_f^2\right\}$$

and $$N_f = \frac{3}{4}\left\{X_f^2 + 2X_s^2\right\}$$

$$\therefore \frac{1}{2} X_s \frac{\partial N_s}{\partial X_s} = \frac{3}{4} X_s^2$$

and

$$\frac{1}{2} X_f \frac{\partial N_f}{\partial X_f} = \frac{3}{4} X_f^2$$

$$\therefore N_s + \frac{1}{2} X_s \frac{\partial N_s}{\partial X_s} = \frac{3}{2}\left\{X_s^2 + X_f^2\right\} = N_f + \frac{1}{2} X_f \frac{\partial N_f}{\partial X_f}$$

$$= N_i'$$

It can be seen that N_i' is always greater that N_s or N_f at any point.

(2) Quintic

For the nonlinear characteristics, $y = x^5$,

$$N_s = \frac{5}{8} X_s^4 + \frac{15}{4} X_s^2 X_f^2 + \frac{15}{8} X_f^4$$

and $$N_f = \frac{5}{8} X_f^4 + \frac{15}{4} X_s^2 X_f^2 + \frac{15}{8} X_s^4$$

$$\therefore \frac{1}{2} X_s \frac{\partial N_s}{\partial X_s} = \frac{10}{8} X_s^4 + \frac{15}{4} X_s^2 X_f^2$$

and $$\frac{1}{2} X_f \frac{\partial N_f}{\partial X_f} = \frac{10}{8} X_f^4 + \frac{15}{4} X_s^2 X_f^2$$

$$\therefore N_s + \frac{1}{2} X_s \frac{\partial N_s}{\partial X_s} = N_f + \frac{1}{2} X_f \frac{\partial N_f}{\partial X_f}$$

$$= \frac{15}{8} X_s^4 + \frac{15}{2} X_s^2 X_f^2 + \frac{15}{8} X_f^4 = N_i'$$

It can be seen that N_i' is always greater than N_s or N_f at point

(3) Ideal Relay

For the ideal relay the following two cases arise:

(i) $X_f \leqslant X_s$ - For this case:

$$N_s = \frac{8M}{\pi^2 X_s} \textcircled{E}(k)$$

and $$N_f = \frac{8M}{\pi^2 X_s} \textcircled{B}(k)$$

where $k = X_f / X_s$ and is less than 1.

$$\therefore -\frac{1}{2} X_s \cdot \frac{\partial N_s}{\partial X_s} = -\frac{4M}{\pi^2} -\frac{1}{X_s}\left\{\textcircled{K}(k) - 2\textcircled{E}(k)\right\}$$

$$\therefore N_s + \frac{1}{2} X_s \frac{\partial N_s}{\partial X_s} = \frac{8M}{\pi^2} \frac{1}{2X_s}\left\{\textcircled{E}(k) + k^2 \textcircled{D}(k)\right\}$$

$$= \frac{4M}{\pi^2} \frac{\textcircled{K}(k)}{X_s}$$

Also $$\frac{1}{2} X_f \frac{\partial N_f}{\partial X_f} = \frac{8M}{\pi^2} \frac{k^2 \textcircled{C}(k)}{2X_s}$$

$$\therefore N_f + \frac{1}{2} X_f \frac{\partial N_f}{\partial X_f} = \frac{4M}{\pi^2} \frac{\textcircled{K}(k)}{X_s}$$

$$\therefore N_i' = N_s + \frac{1}{2} X_s \frac{\partial N_s}{\partial X_s} = N_f + \frac{1}{2} X_f \frac{\partial N_f}{\partial X_f}$$

$$= \frac{4M}{\pi^2} \frac{\textcircled{K}(k)}{X_s}$$

(ii) $X_f \geqslant X_s$ - For this case:

$$N_s = \frac{8M}{\pi^2} \frac{\textcircled{B}(k)}{X_f}$$

and $N_f = \frac{8M}{\pi^2} \frac{\textcircled{E}(k)}{X_f}$ where $k = X_s/X_f \leqslant 1$

$$\therefore -\frac{1}{2} X_s \frac{\partial N_s}{\partial X_s} = \frac{4M}{\pi^2} \frac{k^2 \textcircled{C}(k)}{X_f} \qquad (43)$$

and $$-\frac{1}{2} X_f \frac{\partial N_f}{\partial X_f} = \frac{4M}{\pi^2} \frac{-\textcircled{E}(k) + k^2 \textcircled{D}(k)}{X_f}$$

$$\therefore N_i' = N_s + \frac{1}{2} X_s \frac{\partial N_s}{\partial X_s} = N_f + \frac{1}{2} X_f \frac{\partial N_f}{\partial X_f} = \frac{4M}{\pi^2} \frac{\textcircled{K}(k)}{X_f}$$

From eqn. 43, we find that for a given N_s, N_i' is always greater than N_s for $X_f \geqslant X_s$. For $X_f < X_s$, N_i' is less than N_s for small values of X_f. N_i' is equal to N_s when $(K)(k) = 2(E)(k)$ (From eqn. 43) i.e. for $k = 0.909$. Hence for a N_s = constant characteristics N_i will be less than N_s if $X_f/X_s < 0.909$, and N_i will be greater than N_s for $X_f/X_s > 0.909$.

List of captions to the illustrations

Fig. 1 : Nonlinear System.
Fig. 2 : 'Equivalent Nonlinear System' for Determining the Component of Forcing Frequency.
Fig. 3 : 'Equivalent Nonlinear System' for Representing the Self Oscillations.
Fig. 4 : Incremental Frequency Response for Harmonic Oscillations.
Fig. 5 : Phasor Diagram.
Fig. 6 : IDIDF for $w = w_f$.
Fig. 7 : Incremental Frequency Response for Almost Periodic Oscillations.
Fig. 8 : System Representing the van der Pol Equation.
Fig. 9 : Root Locus Associated with van der Pol Equation.
Fig.10 : System characteristics for Example 2.
Fig.11 : Determination of Response for $w_f = 1.25$ and $\log R_f = \bar{1}.9$.
Fig.12 : Illustrating solutions for several R_f at $w_f = 1.25$.
Fig.13 : $\log X_s/\log X_f$ Plots for Examples 2 and 3.
Fig.14 : $\log X_f/\log R_f$ and $\log X_s/\log R_f$ Plots for $w_f = 1.25$.
Fig.15 : $\log X_f/\log R_f$ and $\log X_s/\log R_f$ Plots for $w_f = 2.0$.
Fig.16 : System characteristics for Example 3.
Fig.17 : Illustrating Solutions for $w_f = 1.2$, $\log R_f = \bar{1}.35$.
Fig.18 : Illustrating Solutions for several R_f at $w_f = 1.5$.
Fig.19 : $\log X_f/\log R_f$ and $\log X_s/\log R_f$ Plots for $w_f = 1.5$.
Fig.20 : N_f/X_f for for $N_s = 1$ For a Cubic Nonlinearity.
Fig.21 : N_f/X_f Plot for $N_s = 1$ For a Quintic Nonlinearity.
Fig.22 : Block Diagram of a General Nonlinear System.
Fig.23 : Phasor Diagram for Forcing Frequency.
Fig.24 : $\log (C/R)/\log (E/R)$ Plot for $\theta_l = 166^\circ$.
Fig.25 : Representation of System Characteristics.
Fig.26 : Illustrating Solutions for a Given R and w.

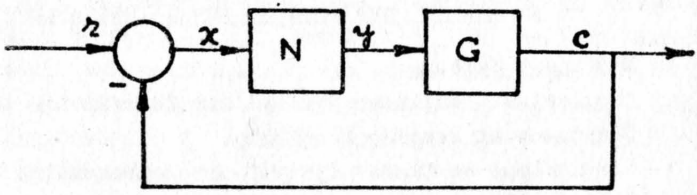

FIG. 1.

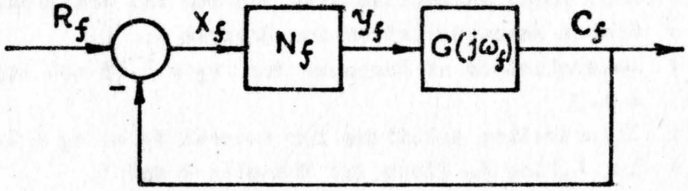

FIG. 2.

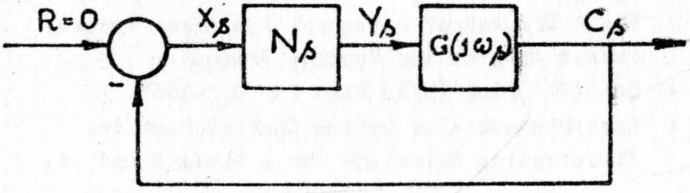

FIG. 3.

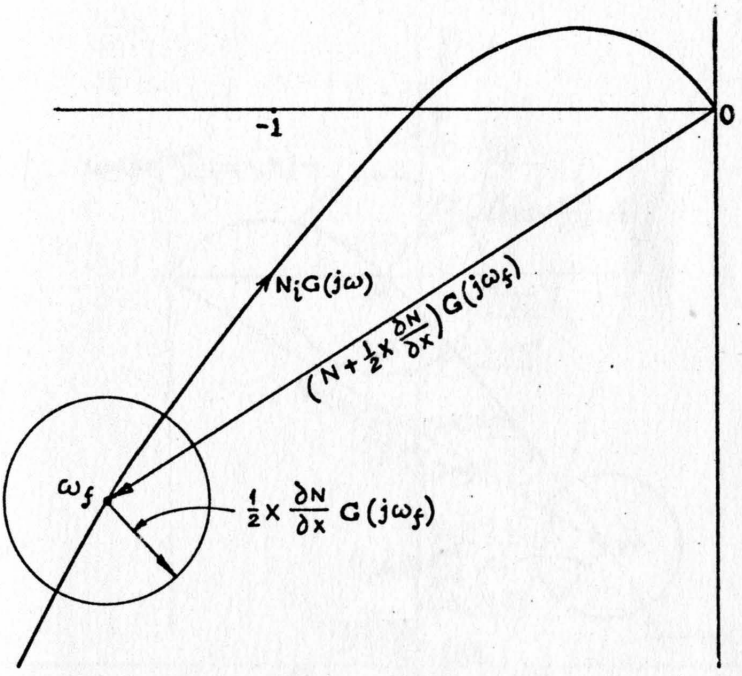

FIG.4.

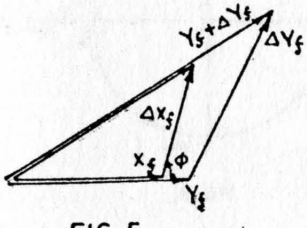

FIG.5.

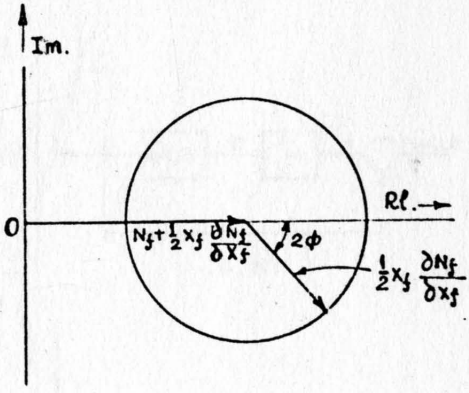

FIG.6.

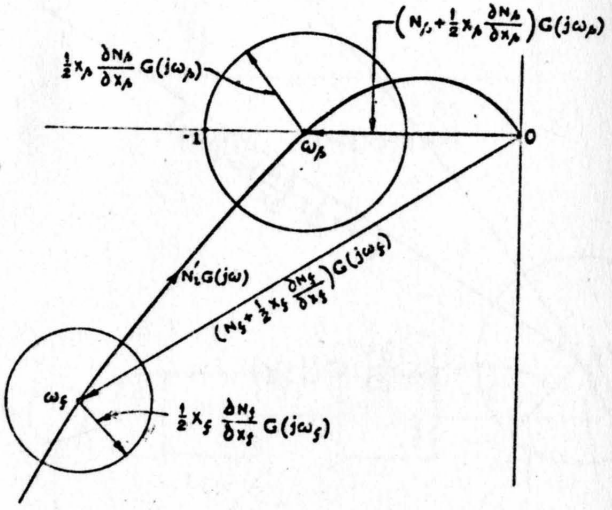

FIG. 7.

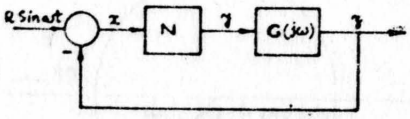

FIG. 8.

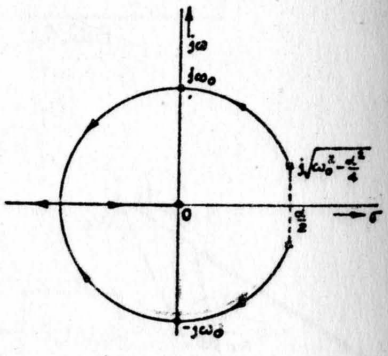

FIG. 9.

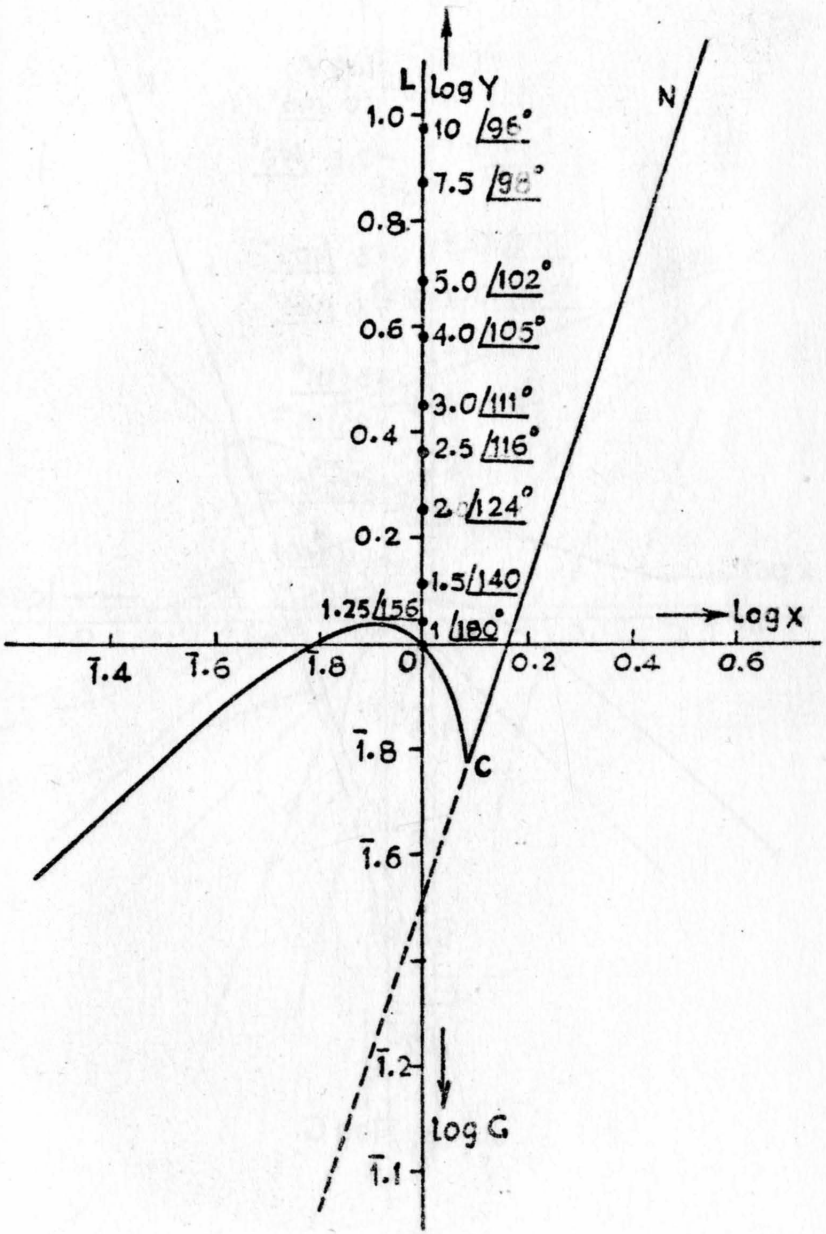
L
log Y
1.0
10 /95°
7.5 /98°
0.8
5.0 /102°
0.6
4.0 /105°
3.0 /111°
0.4
2.5 /116°
2 /124°
0.2
1.5 /140
1.25 /156
1 /180°
N
log X
T.4
T.6
T.8
0
0.2
0.4
0.6
C
T.8
T.6
T.2
log G
T.1

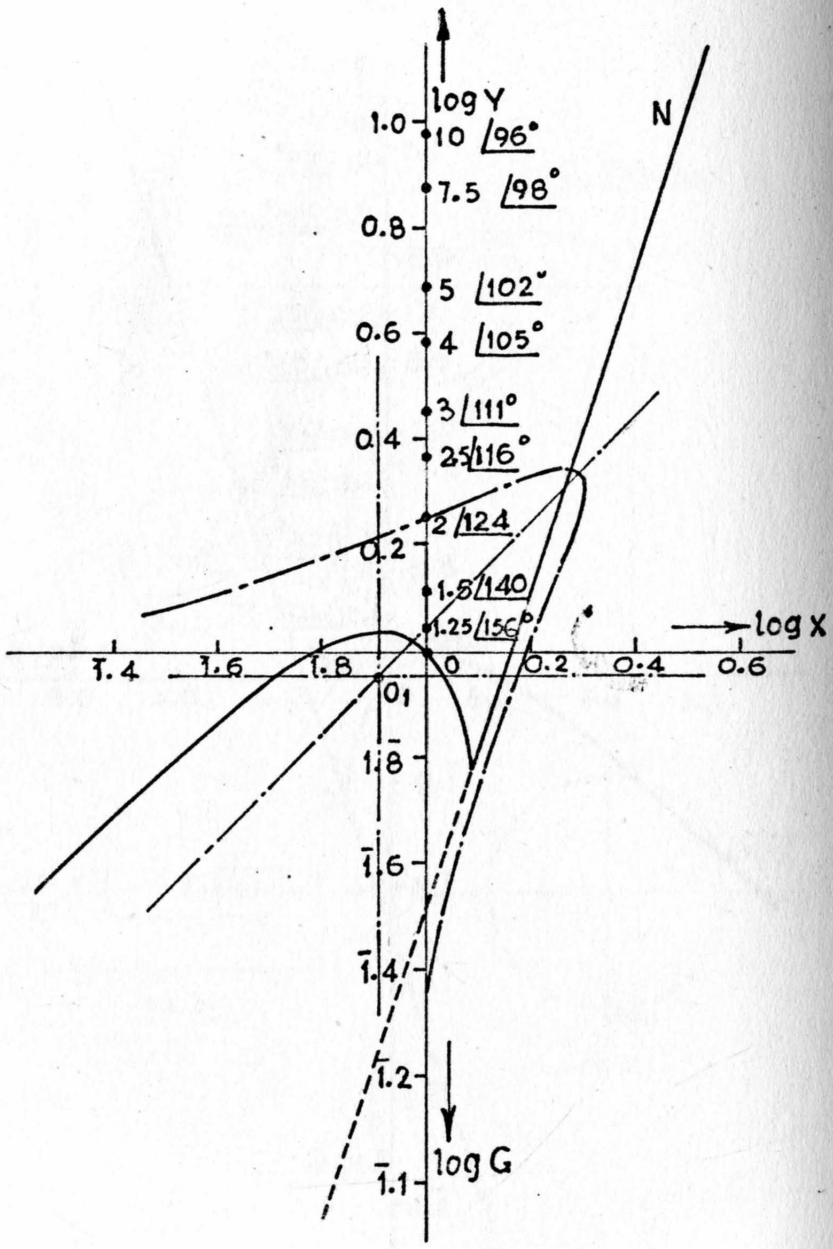
log Y
1.0
10 /96°
7.5 /98°
0.8
5 /102°
0.6
4 /105°
3 /111°
0.4
2.5 /116°
2 /124
0.2
1.5 /140
1.25 /150°
N
log X
T.4
T.6
T.8
0
0.2
0.4
0.6
O1
1.8
1.6
1.4
1.2
1.1
log G

FIG. 11.

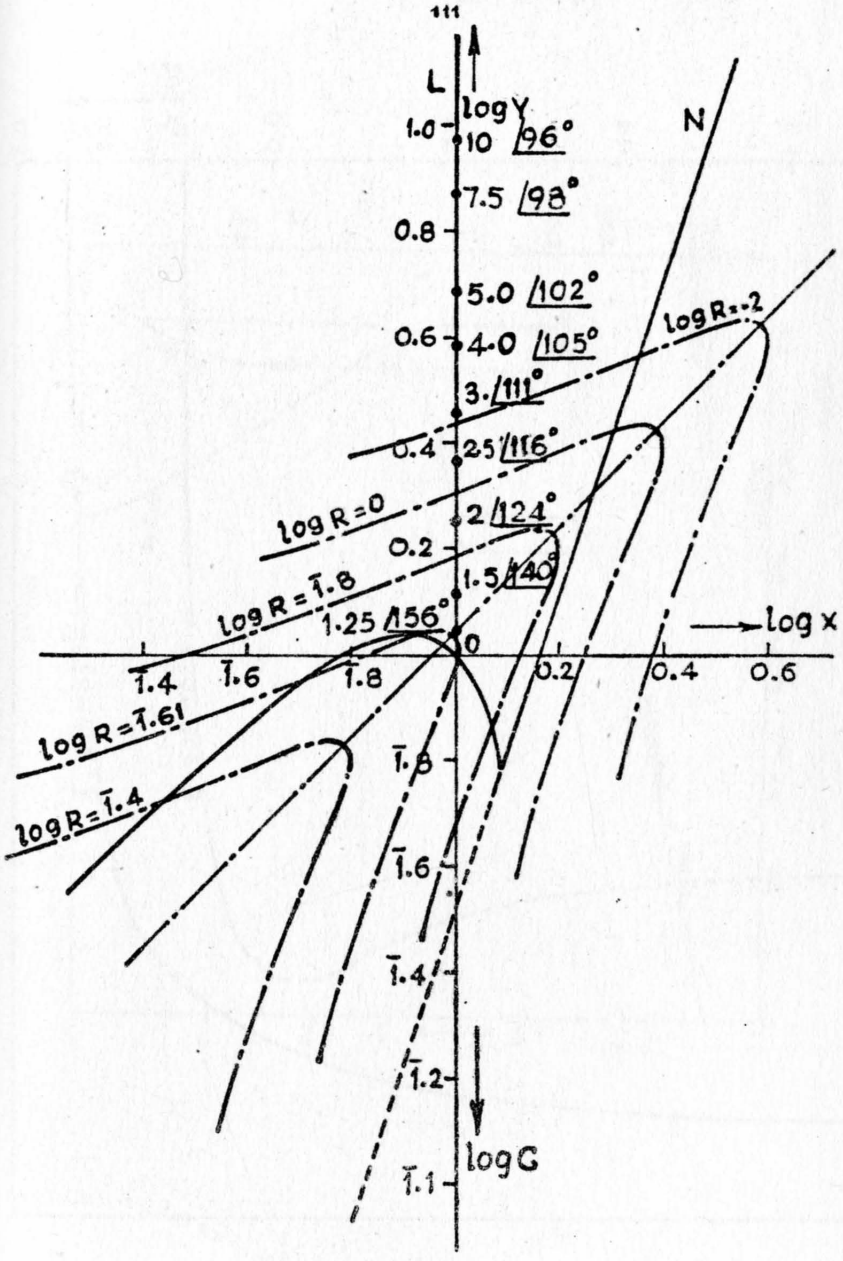
111
L
log Y
1.0
10 /96°
N
7.5 /98°
0.8
5.0 /102°
0.6
4.0 /105°
log R=.2
3. /111°
0.4
2.5 /116°
log R=0
2 /124°
0.2
1.5 /140°
log R=T.8
1.25 /156°
log x
0
T.4
T.6
T.8
0.2
0.4
0.6
log R=T.61
log R=T.4
T.8
T.6
T.4
T.2
T.1
log C

FIG. 12.

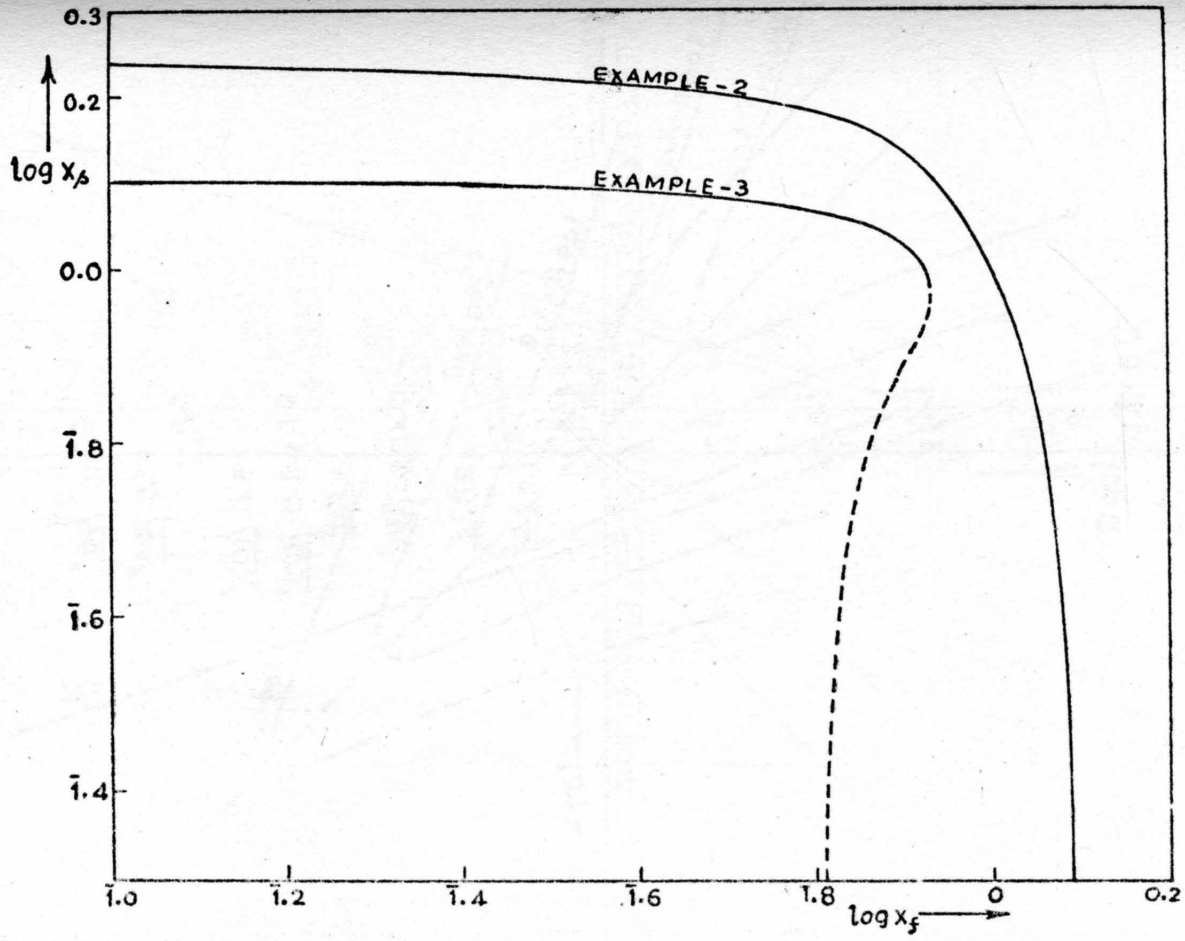
0.3
0.2
log x_b
0.0
$\bar{1}.8$
$\bar{1}.6$
$\bar{1}.4$
EXAMPLE-2
EXAMPLE-3
$\bar{1}.0$
$\bar{1}.2$
$\bar{1}.4$
$\bar{1}.6$
$\bar{1}.8$
0
0.2
log x_f

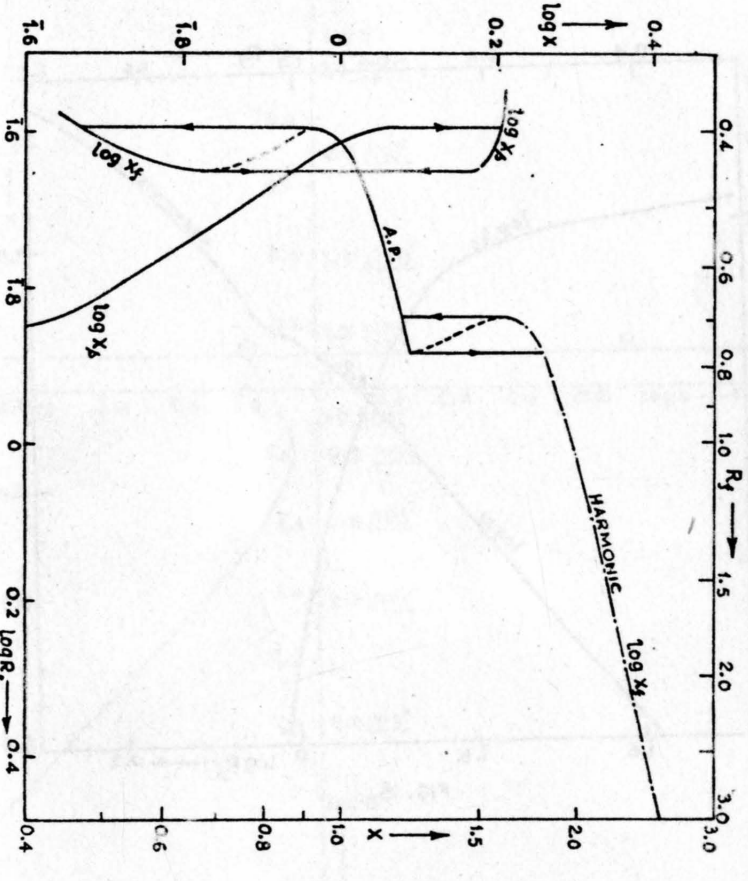
log X
0.4
0.2
0
$\bar{1}.8$
$\bar{1}.6$
log X_4
log X_5
log X_6
A.P.
HARMONIC
log X_4
R_f ⟶
0.4
0.6
0.8
1.0
1.5
2.0
3.0
X ⟶
0.4
0.6
0.8
1.0
1.5
2.0
3.0
0.2 log R_f ⟶ 0.4

FIG. 14.

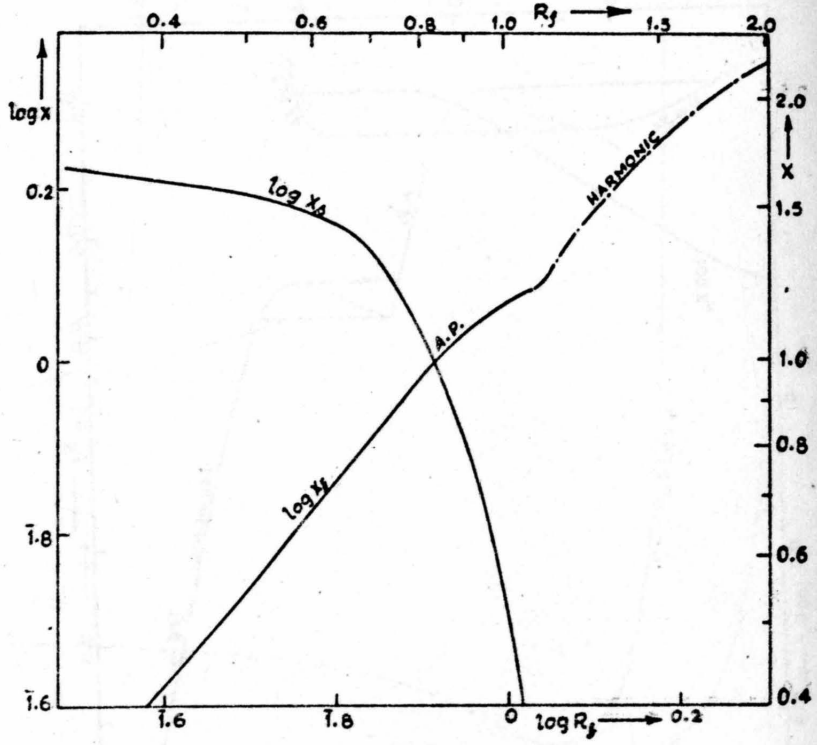
0.4
0.6
0.8
1.0
R_f
1.5
2.0
log x
0.2
0
$\bar{1}.8$
$\bar{1}.6$
log x_b
log x_f
A.P.
HARMONIC
2.0
x
1.5
1.0
0.8
0.6
0.4
$\bar{1}.6$
$\bar{1}.8$
0
log R_f
0.2

FIG. 15.

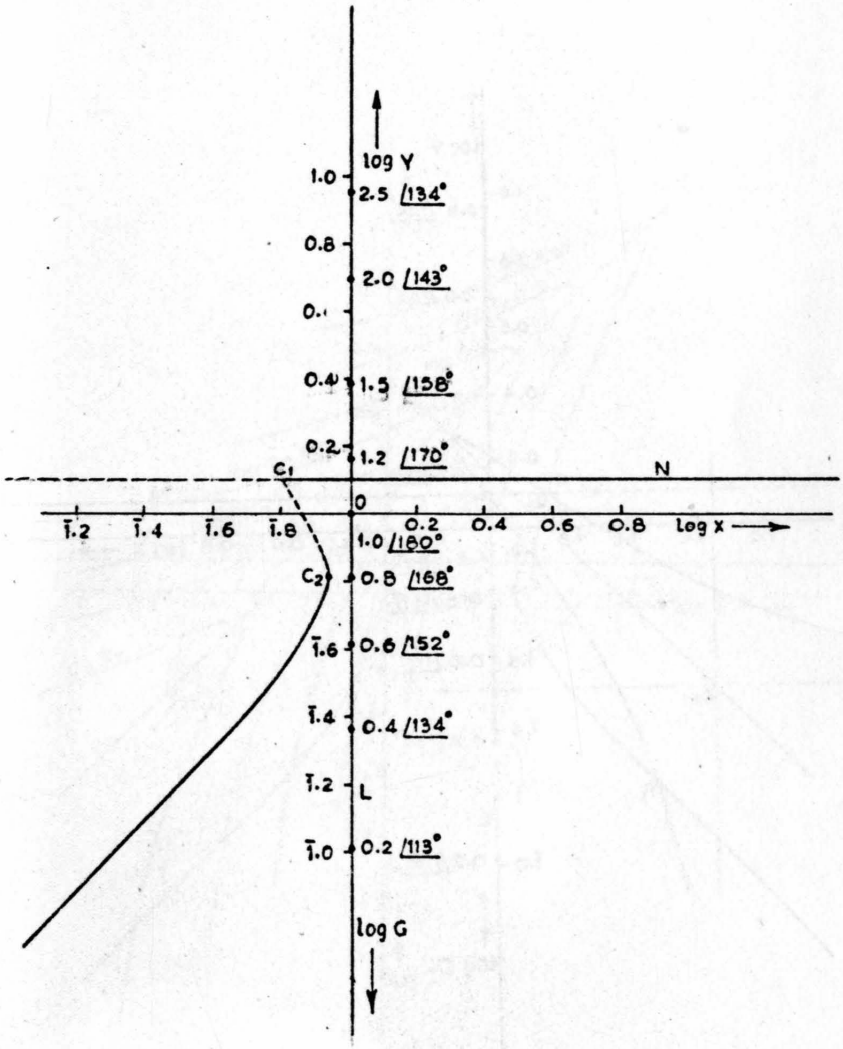
log Y
1.0
2.5 /134°
0.8
2.0 /143°
0.6
0.4
1.5 /158°
0.2
1.2 /170°
C1
N
0
1.2
1.4
1.6
1.8
0.2
0.4
0.6
0.8
log X
1.0 /180°
C2
0.8 /168°
1.6
0.6 /152°
1.4
0.4 /134°
1.2
L
1.0
0.2 /113°
log G

FIG. 16.

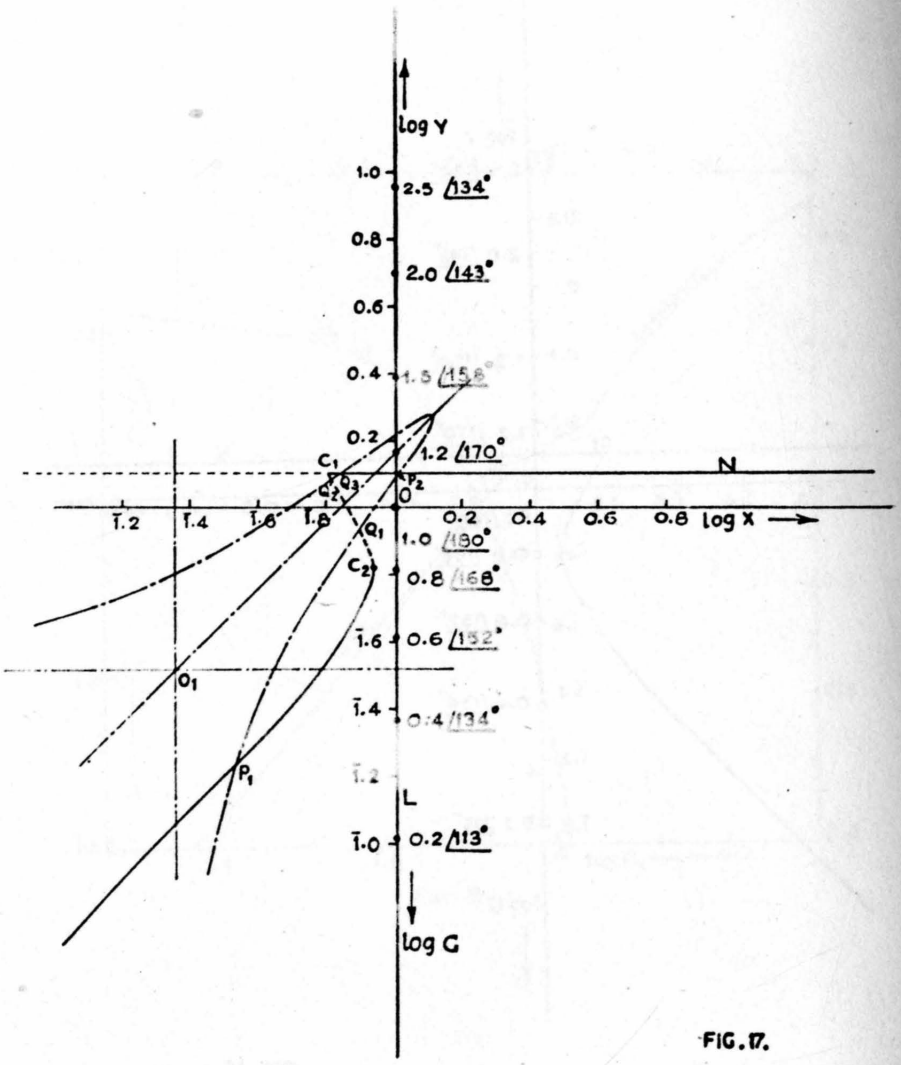
log Y
1.0
2.5 /134°
0.8
2.0 /143°
0.6
0.4
1.5 /158°
0.2
1.2 /170°
N
C1
Q3
C2
P2
O
T.2
T.4
T.6
T.8
Q1
0.2
0.4
0.6
0.8 log X
1.0 /180°
C2
0.8 /168°
T.6
0.6 /152°
O1
T.4
0.4 /134°
P1
T.2
L
T.0
0.2 /113°
log G

FIG. 17.

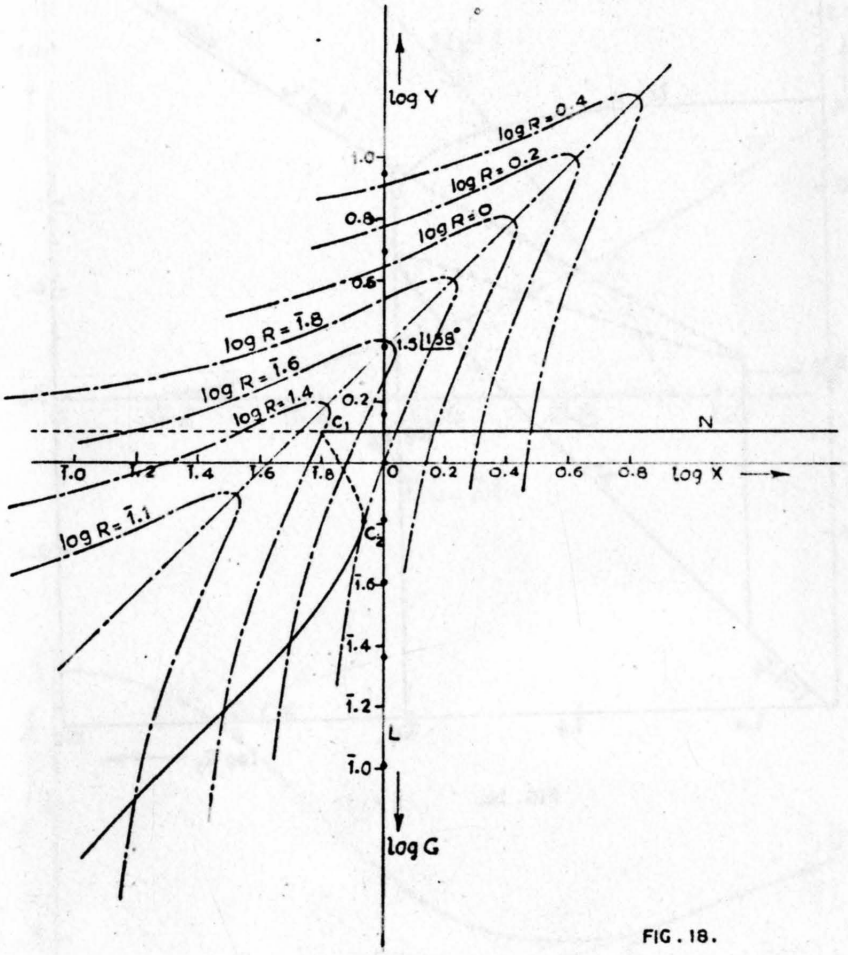
log Y
log R = 0.4
log R = 0.2
log R = 0
log R = $\bar{1}$.8
log R = $\bar{1}$.6
log R = $\bar{1}$.4
log R = $\bar{1}$.1
1.0
0.8
0.6
1.5 | 138°
0.2
N
C_1
$\bar{1}$.0
$\bar{1}$.2
$\bar{1}$.4
$\bar{1}$.6
$\bar{1}$.8
0
0.2
0.4
0.6
0.8
log X
C_2
L
log G

FIG. 18.

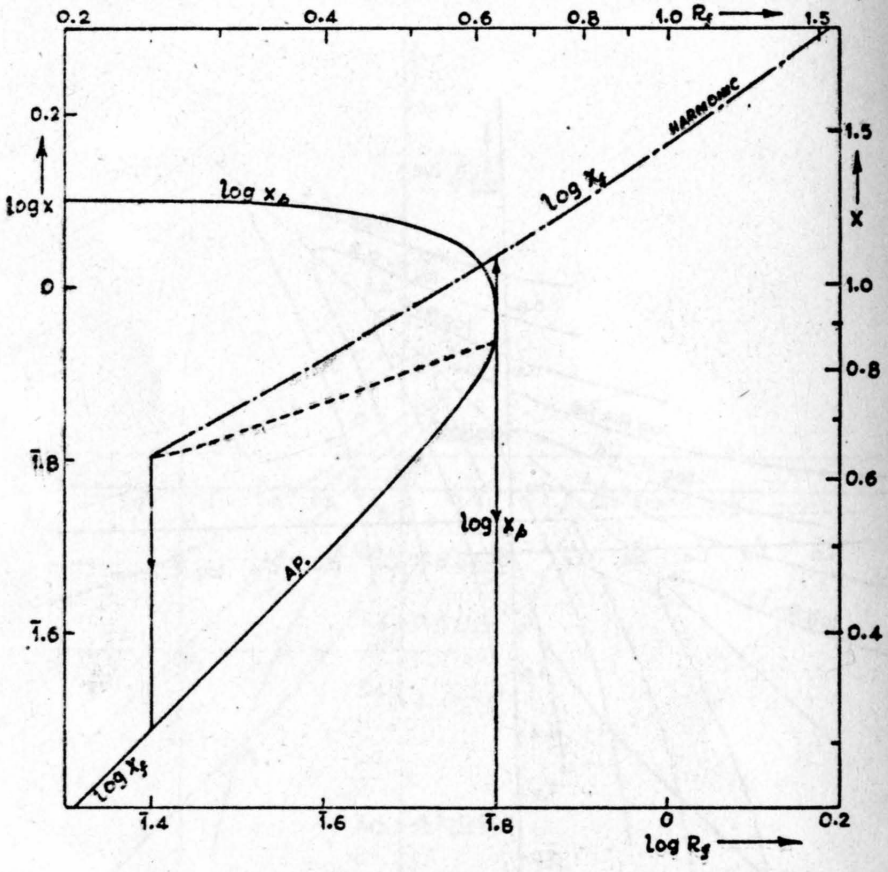
0.2
0.4
0.6
0.8
1.0 R_g
1.5
0.2
log x
0
$\bar{1}.8$
$\bar{1}.6$
HARMONIC
log x_h
log x_f
log x_p
AP.
log x_f
1.5
X
1.0
0.8
0.6
0.4
$\bar{1}.4$
$\bar{1}.6$
$\bar{1}.8$
0
0.2
log R_g

FIG. 19.

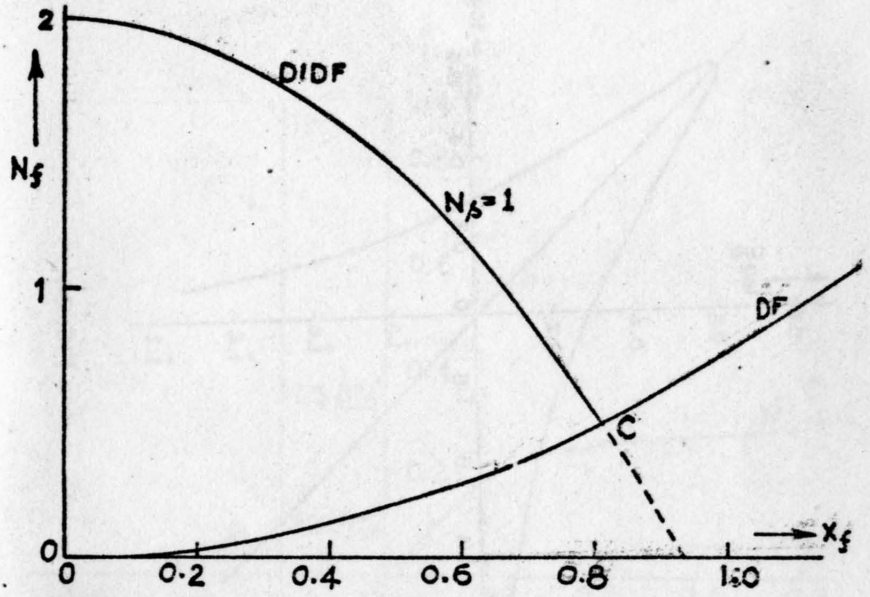
2
N_f
1
0
DIDF
$N_\beta=1$
DF
C
X_f
0
0·2
0.4
0.6
0.8
1·0

FIG. 20.

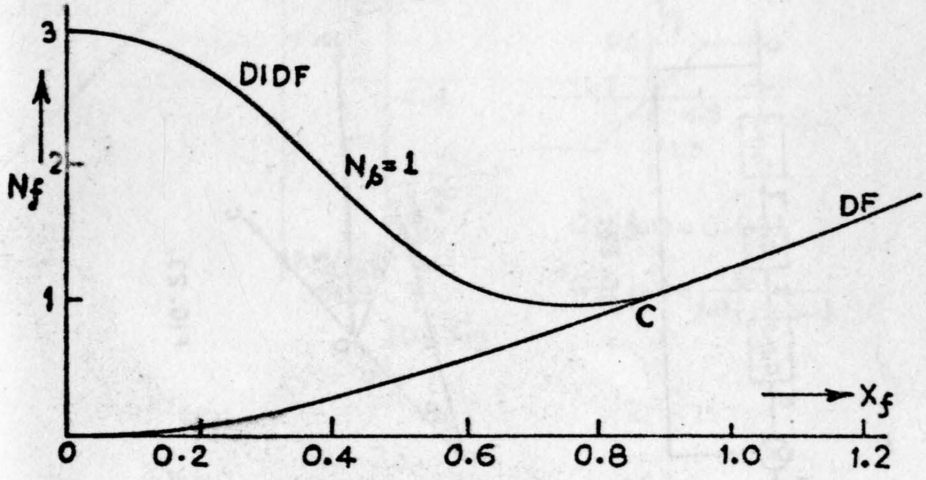
3
N_f
2
1
DIDF
$N_\beta=1$
DF
C
X_f
0
0·2
0.4
0.6
0.8
1.0
1.2

FIG. 21.

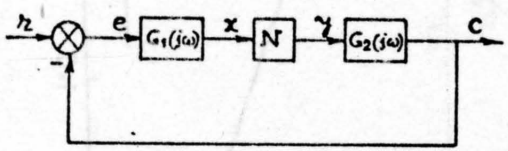

FIG. 22.

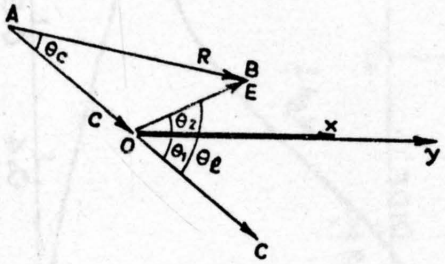

FIG. 23.

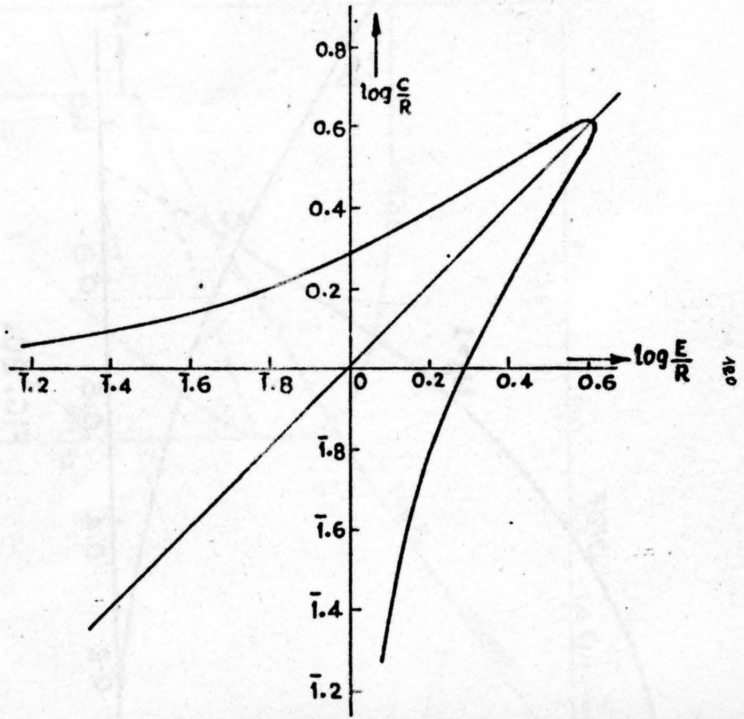

FIG. 24.

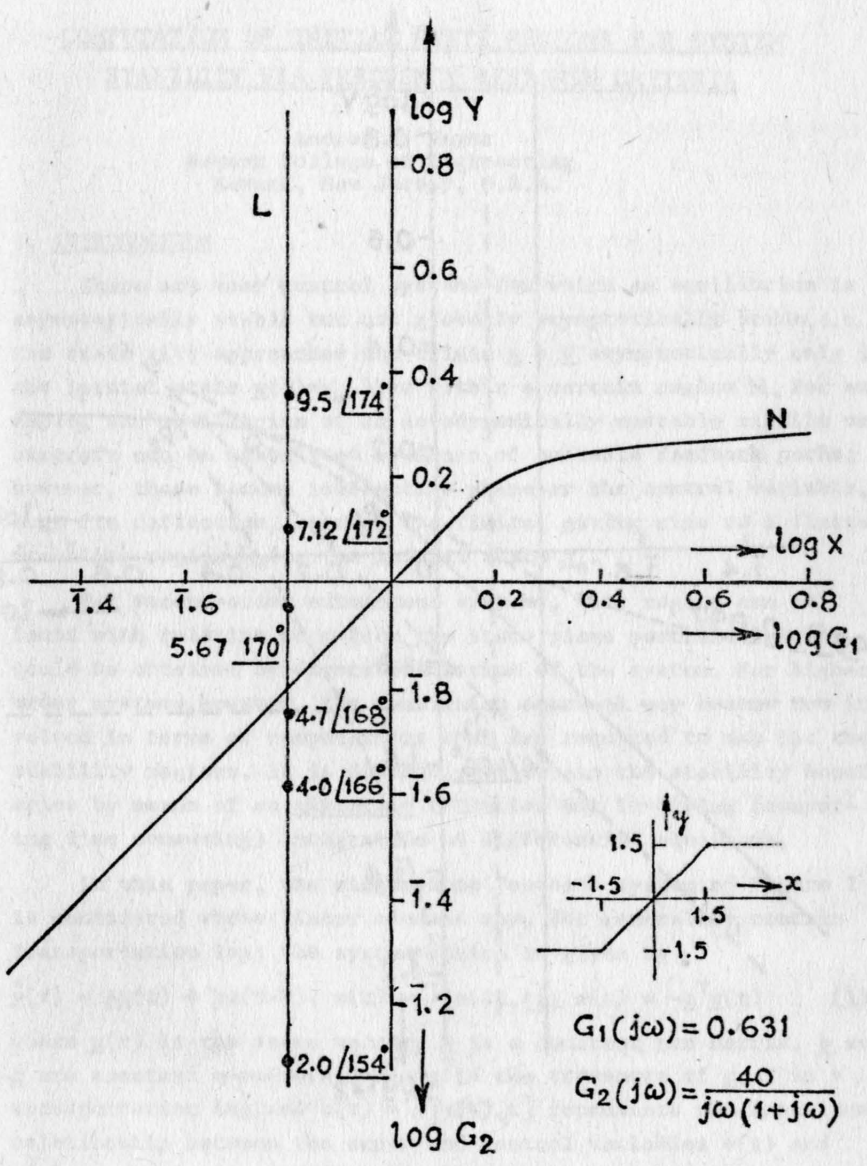
log Y
0.8
L
0.6
0.4
9.5 /174°
N
0.2
7.12 /172°
log X
1̄.4
1̄.6
0.2
0.4
0.6
0.8
5.67 170°
log G1
1̄.8
4.7 /168°
4.0 /166°
1̄.6
1̄.4
1̄.2
2.0 /154°
log G2
y
1.5
-1.5
x
1.5
-1.5
G1(jω) = 0.631
G2(jω) = 40 / jω(1+jω)

FIG. 25.

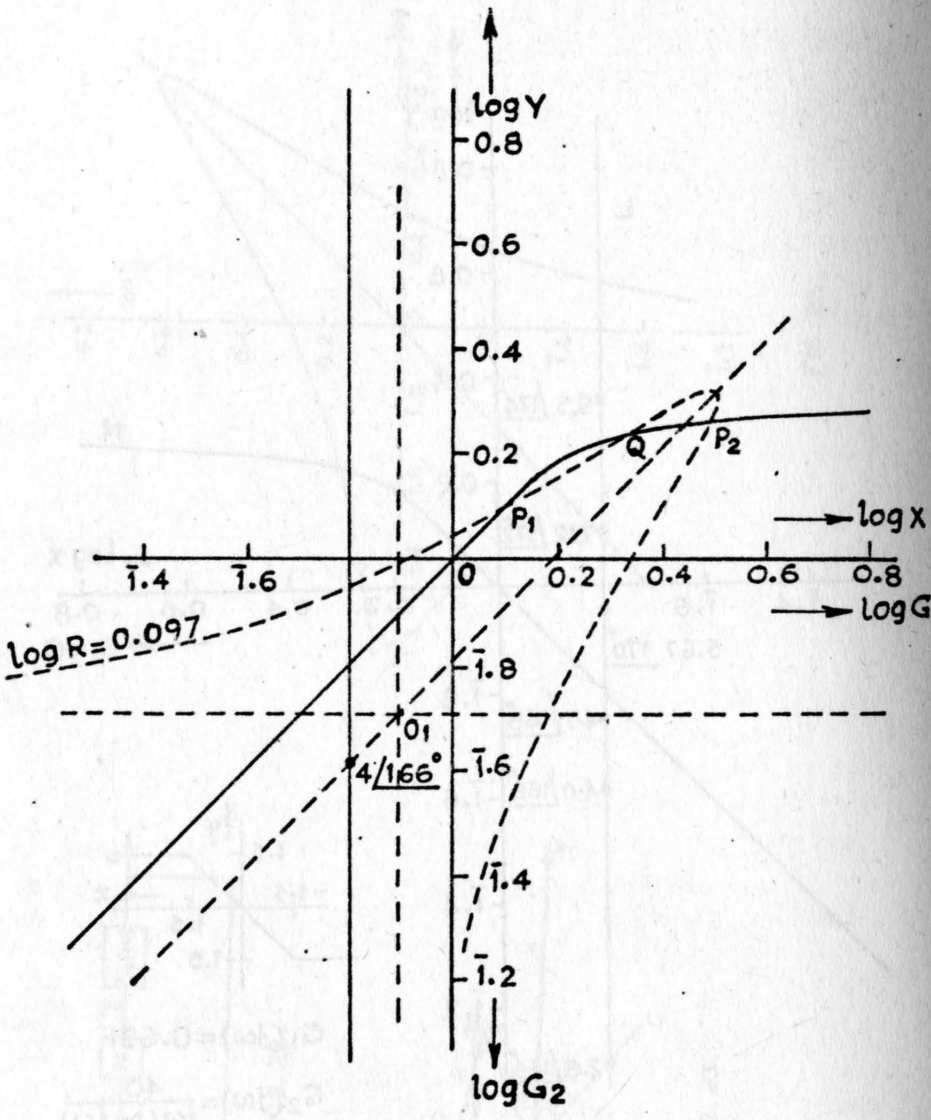
log Y
0.8
0.6
0.4
0.2
Q
P2
P1
log X
1̄.4
1̄.6
0
0.2
0.4
0.6
0.8
log G
log R=0.097
1̄.8
O1
4/166°
1̄.6
1̄.4
1̄.2
log G2

FIG. 26.

COMPUTATION OF INITIAL STATE REGIONS FOR SYSTEM STABILITY VIA FREQUENCY RESPONSE CRITERIA

Andrew U. Meyer
Newark College of Engineering
Newark, New Jersey, U.S.A.

I. INTRODUCTION

There are many control systems for which an equilibrium is asymptotically stable but not globally asymptotically stable, i.e., the state $\underline{x}(t)$ approaches the origin $\underline{x} = \underline{0}$ asymptotically only if the initial state $\underline{x}(0)=\underline{x}_o$ lies within a certain region $\mathfrak{R}$. For example, the equilibrium of an aerodynamically unstable missile or aircraft can be stabilized by means of suitable feedback paths; however, these become ineffective whenever the control variable, e.g. fin deflection, reaches its limits, giving rise to a finite stability region $\mathfrak{R}$ for the initial state $\underline{x}_o$.

For second-order autonomous systems, this region can be found with relative ease from the state plane portrait which could be obtained by direct simulation of the system. For higher order systems, however, the simulation approach may become too involved in terms of computations that are required to map out the stability regions. It is desirable to obtain the stability boundaries by means of an algebraic criterion not involving (computing time consuming) integration of differential equations.

In this paper, the single-loop feedback system of Figure 1 is considered whose linear element may, for generality, contain transportation lag; the system motion is given by

$$\dot{\underline{x}}(t) = \underline{A}\underline{x}(t) + \underline{b}u(t-T);\ u(t) = \mathcal{F}[e(t),t];\ e(t) = -\underline{c}^T\underline{x}(t) \qquad (1)$$

where $\underline{x}(t)$ is the state vector, $\underline{A}$ is a constant nxn matrix, $\underline{b}$ and $\underline{c}$ are constant n-vectors where $\underline{c}^T$ is the transpose of $\underline{c}$, T is a transportation lag and $u(t) = \mathcal{F}[e(t),t]$ represents the functional relationship between the error and control variables e(t) and u(t) respectively; this functional relationship may be time-varying and/or may contain memory. However, it will be assumed that

$$a \le \frac{u(t)}{e(t)} \le b \quad \text{for all } t \ge 0 \text{ and } |e(t)| \le E \qquad (2a)$$

For convenience, this is expressed as

$$\frac{u}{e} \in [a,b] \quad \text{for} \quad |e(t)| \leq E \tag{2b}$$

For E=∞, the (global) asymtotic stability of system (1),(2) has been subject to extensive investigation, of which the most successful results are based on the frequency response method of Popov [1,2,3].

Suppose that, by any method, absolute asymptotic stability for $\frac{u}{e} \in [a,b]$ has been established for E=∞; however, the nonlinear element of the system satisfies $\frac{u}{e} \in [a,b]$ only for some finite E. Then, any set of initial conditions for which $|e(t)| \leq E$ for $t \geq 0$ will be sufficient for asymptotic stability.

In order to establish an algebraic algorithm for computing the stability boundary for the set of initial conditions, one possible approach (not to be considered in this paper, however) involves the use of Lyapunov's second method. Under suitable assumptions, the existence of a Lyapunov function is assured if the frequency domain criterion of Popov is satisfied [2,4,5]. By obtaining the Lyapunov function $V(\underline{x})$ and its derivative $\dot{V}(\underline{x})$ under the assumption that E=∞ and then using the correct (finite) E, the stability region for the set of initial conditions may be obtained [9,10].

Another approach is to obtain an algegraic algorithm for computation of stability regions directly from a frequency respnse criterion, i.e., without the use of a Lyapunov function. This approach will be the subject of the present paper.

A.M. Formalskii[6] has recently shown how a stability region for initial conditions sufficient for asymptotic stability can be computed directly from Popov's theorem*. His method requires that the nonlinear element of sector $\frac{u}{e} \in [0,K]$ is single-valued and that the Popov condition $\mathrm{Re}\,(1+j\omega q)\underline{c}^T(j\omega\underline{I}-\underline{A})^{-1} + \frac{1}{K} \geq \delta > 0$** be

*Formalskii's paper is presented for systems without transportation lag but containing more than one nonlinearity, with an example given for a system with one nonlinearity. The treatment of systems with several nonlinearities is similar to that for single-loop systems with one nonlinearity, except for the use of careful vector-matrix manipulations. Therefore, in the interest of insight, only single-loop systems with one nonlinearity will be considered in this paper.

**For system (1) with T=0 (no transportation lag).

satisfied with $q \neq 0$ ($\underline{I}$ is the identity matrix). Formalskii's method appears to work best when a large magnitude of q can be found that satisfies Popov's condition and yields more conservative (smaller) stability regions as the magnitude of q becomes smaller. It is not applicable for q=0.

In the present paper, an algorithm will be presented that is applicable not only to all finite values of q including q=0 but also to systems with nonlinearities that are time-varying or may contain hysteresis. Moreover, the linear element may contain transportation lag and possibly distributed parameters.

Let $\underline{z}$ be a vector (to be defined later) representing the set of initial conditions. In terms of the system error $e(t) = e(t,\underline{z})$ and the control variable $u(t) = u(t,\underline{z})$, system (1) may be expressed as

$$e(t,\underline{z}) = e_o(t,\underline{z}) - \int_o^t g(t-\lambda)u(\lambda,\underline{z})d\lambda \; ; \; u(t,\underline{z}) = \mathcal{F}[e(t,\underline{z}),t;t\geq 0 \quad (3)$$

where

$$g(t) = \mathcal{L}^{-1}[G(s)] = -\underline{c}^T\underline{\phi}(t)\underline{b} \quad (4)$$

$$\underline{\phi}(t) = \mathcal{L}^{-1}[(s\underline{I}-\underline{A})^{-1}e^{-sT}] \quad (5)$$

and where $\underline{I}$ is the identity matrix. The initial condition response of the (open loop) linear element, $e_o(t,\underline{z})$, depends on the initial state $\underline{x}_o=\underline{x}(0)$ and, if the system contains transportation lag, must include an additional term which can be expressed in terms of the response to a forcing function applied during the time interval $-T\leq t<0$. Thus,

$$e_o(t,\underline{z}) = -\underline{c}^T\underline{\phi}(t)\underline{x}_o - \int_{-T}^t g(t-\lambda)u_o(\lambda)d\lambda \quad (6a)$$

where

$$\underline{x}_o \triangleq \underline{x}(0) \; ; \; u_o(t) \triangleq \begin{cases} u(t), & -T \leq t < 0 \\ 0, & \text{elsewhere} \end{cases} \quad (6b)$$

The terms g(t) and $\underline{\phi}(t)$ defined in (4) and (5) represent the unit-impulse response and the transition matrix respectively of the linear element.

In order to avoid dealing with initial functions $u_o(t)$, it will be convenient to restrict the analysis to classes of functions $|u_o(t)| \leq u_M$. Thus, the following (n+1 -dimensional) vector is defined:

$$\underline{z} \triangleq \begin{bmatrix} \underline{x}_o \\ u_M \end{bmatrix} \tag{7a}$$

where

$$u_M = \sup_{-T\le t<0} |u_o(t)| = \sup_{-T\le t<0} |u(t)| \tag{7b}$$

It is the objective of this work to find regions of $\underline{z}$ that satisfy the given stability requirements.

II. THE CONDITIONS IMPOSED ON THE SYSTEM

For the linear element, the following definition will be used in this work:

DEFINITION 1*: A linear time-invariant element is said to be output stable if the following conditions hold**: $g(t) \in L_1 \cap L_2$; $\sup_{t\ge 0} |e_o(t,\underline{z})| < \infty$, $e_o(t,\underline{z}) \in L_2$, $\dot{e}_o(t,\underline{z}) \in L_2$, each over $(0,\infty)$ for every set of initial conditions $\underline{z}$.

It can be shown that if all eigenvalues of $\underline{A}$ have negative real values, then the element is output stable ***.

For the nonlinear element, cases are considered where it may be time-varying or time-invariant with or without hysteresis. For the latter, two cases are considered [3]:

DEFINITION 2: A time-invariant characteristic $u(t) = \mathcal{F}[e(t)]$ is said to have passive hysteresis (active hysteresis) if

$$\int_{\Gamma}^{e_2} u\,de \le (\ge) \int_{\Gamma_{i2}}^{e_2} u\,de = \int_{0\Gamma_i+\Gamma_{i2}}^{e_2} u\,de - \int_{0\Gamma_i}^{e_1} u\,de \tag{8}$$

holds for every pair e_1, e_2 where Γ represents the path in the u-e characteristic due to any possible history of e(t) and where Γ_i , and Γ_{i2} represent any given path (not a closed path!) on the characteristic between 0 and e_1 and between e_1 and e_2 respectively.

---

*see reference 3, p. 367.

**The classes L_1 and L_2 represent all absolutely and square-integrable functions respectively. $g(t) \in L_1 \cap L_2$ means "g(t) belongs to both L_1 and L_2".

***If all eigenvalues of $\underline{A}$ have negative real parts, then (see reference 3, p.738) there exist real positive numbers α, M, M' such that $\|\underline{\phi}(t)\| = (\sum_{i,j=1}^{n} \phi_{ij}^2(t))^{\frac{1}{2}} \le M \exp(-\alpha t)$, $\|\dot{\underline{\phi}}(t)\| \le M' \exp(-\alpha t)$ for all $t \ge 0$. Output stability follows from this and from (4) to (6).

Examples for these two types are illustrated in Figure 2. The passive type is, of course, the one of practical importance. However, it turns out that the algorithm to be presented later is better expressed in terms of an active hysteresis characteristic. Fortunately, a system containing passive hysteresis can be transformed into another one of the same form containing active hysteresis and vice-versa. This can be done by the transformation u'=Ke-u which is illustrated in Figure 2.

III. THE FUNDAMENTAL RELATIONS

If g(t) and u(t) both are square-integrable functions of t over (0,∞) (to be justified later), then it follows from (3) and from Schwarz's inequality that

$$|e(t,\underline{z})| \leq |e_o(t,\underline{z})| + J_g(t)\, J_u(t,\underline{z}) \tag{9}$$

where

$$J_u(t,\underline{z}) \triangleq \left[\int_o^t u^2(\tau,\underline{z})\, d\tau\right]^{\frac{1}{2}} \tag{10}$$

$$J_g(t) \triangleq \left[\int_o^t g^2(\tau) d\tau\right]^{\frac{1}{2}} \tag{11}$$

It will be shown later that bounds for $J_u(t,\underline{z})$ can be obtained in terms of the initial condition vector $\underline{z}$ that are valid as long as $\frac{u}{e} \in [a,b]$ which, by the statement of the problem (see (2b)) means, as long as $|e(t,\underline{z})| \leq E$. The basic idea then is to compute a region $\mathfrak{R}$ for the initial condition set $\underline{z}$ such that

$$\sup_{t\geq 0}\left(|e_o(t,\underline{z})| + J_g(t)\, J_u(t,\underline{z})\right) \leq E \tag{12}$$

That is, $\mathfrak{R}$ is defined by

$$\mathfrak{R} = \left\{ \underline{z} \;\middle|\; \sup_{t\geq 0}\left(|e_o(t,\underline{z})| + J_g(t)\, J_u(t,\underline{z})\right) \leq E \right\} \tag{13}$$

Note that satisfaction of (12) implies finiteness of $J_u(t,\underline{z})$ which, as it turns out, implies that $e(t)=e(t,\underline{z})\to 0$ as $t\to\infty$. This fact, the obtaining of a bound on $J_u(t,\underline{z})$ as well as another relation used for computation of a stability region by means other than (13) are all based on the following lemma:

LEMMA: For system (3) whose linear element is output stable and whose nonlinear element satisfies

$$\frac{u}{e} \in [0,K] \text{ for all } e(t) = e(t,\underline{z}) \text{ and given } K \text{ in } 0 \leq K \leq \infty \tag{14}$$

Let there be real numbers $\delta > 0$, q and ω such that the (Popov) condition

$$\inf_{\omega \geq 0} \left(\mathrm{Re}(1 + j\omega q)G(j\omega) + \frac{1}{K} \right) \triangleq \delta > 0 \qquad (15)$$

is satisfied. Then, inequalities (16) and (17), given below, each hold:

$$\left[J_u(t,\underline{z}) - \frac{1}{2\delta} J_o(t,\underline{z}) \right]^2 - \frac{q}{\delta} I_\Gamma(t,\underline{z}) \leq \frac{1}{4\delta^2} J_o^2(t,\underline{z}) \; ; \; t \geq 0 \qquad (16)$$

$$-q \, I_\Gamma(t,\underline{z}) \leq J_F(\underline{z}) \quad ; \; t \geq 0 \qquad (17)$$

where $J_u(t,\underline{z})$ was defined in (10) and

$$J_o(t,\underline{z}) \triangleq \left(\int_o^t \left[e_o(\tau,\underline{z}) + q \, \dot{e}_o(\tau,\underline{z}) \right]^2 d\tau \right)^{\frac{1}{2}} < \infty \qquad (18)$$

$$I_\Gamma(t,\underline{z}) \triangleq -\int_o^t u(\tau,\underline{z}) \, e(\tau,\underline{z}) \, d\tau = -\int_{\Gamma}^{e(t,\underline{z})}_{e(0,\underline{z})} u \, de \qquad (19)$$

$$J_F(\underline{z}) \triangleq \frac{1}{4\pi} \int_o^\infty \frac{\left| (1 + j\omega q) E_o(j\omega,\underline{z}) \right|^2}{\mathrm{Re}(1 + j\omega q)G(j\omega) + \frac{1}{K}} \, d\omega \qquad (20)$$

where $E_o(s,\underline{z}) = \mathcal{L}\left[e_o(t,\underline{z}) \right]$ and where $I_\Gamma(t,\underline{z})$ represents the line integral over the (not necessarily unique) path Γ in the functional relation $u(t,\underline{z}) = \mathcal{F}\left[e(t,\underline{z}), t \right]$.

Moreover, if (16) yields $J_u(t,\underline{z}) < \infty$ for $t = \infty$ and for every $\underline{z}$ and if, in addition, all eigenvalues of $\underline{A}$ have negative real parts and (15) is satisfied with $0 \leq q < \infty$, then the origin $\underline{x} = \underline{0}$ is globally asymptotically stable*.

Remarks: (a) Condition (16) represents an important inequality upon which a fundamental stability theorem in reference 3 is proved; that proof involves consideration of various cases of nonlinearities and the finding of conditions for which $J_u(t,\underline{z})$ is finite.

(b) If (16) yields a finite bound of $J_u(t,\underline{z})$ and if for a given initial condition vector $\underline{z}$, (12) is satisfied then, by (9), $|e(t,\underline{z})| \leq E$. Thus, for cases for which $\frac{u}{e} \in [0,K]$ only when $|e| \leq E$ (but not when $|e| > E$), the results of the Lemma are valid as long as (12) is satisfied. Condition (12) then maps out a stability region for $\underline{z}$, defined in (13).

---

*Some linear elements with not completely observable states may be output stable, yet their $\underline{A}$ matrices may have eigenvalues not in the left-half plane (e.g., at the origin). the other hand, in many practical situations, it is only the behavior of the signal $e(t,\underline{z})$ that is of interest.

(c) Condition (17) is related to Formalskii's method[6] and, together with (19) and (20), leads to an integral relation analogous to (12) from which another region of $\underline{z}$ sufficient for stability can be found; this will be discussed in the next section. Condition (17) is also related to a result obtained by Chinnapareddi and Li[11,12] concerning bounds on transient responses.

For a proof of the above lemma with respect to inequality (16) and to the last statement, see reference 3*. The proof of condition (17) can be obtained by derivation analogous to that in Formalskii[6] for the class of systems considered here**.

Condition (17), which also represents the basis for Formalskii's method, is limited to the cases where $q \neq 0$ and decreases its usefulness as the magnitude of q becomes smaller; this represents a shortcoming of Formalskii's method. Condition (16), on the other hand, applies to all values of q.

Before proceeding with the discussion of their application, it is of interest to compare conditions (16) and (17). It follows from (16) and (18) that

$$-\frac{q}{\delta} I_\Gamma(t,\underline{z}) \leq \left[J_u(t,\underline{z}) - \frac{1}{2\delta} J_o(t,\underline{z})\right]^2 - \frac{q}{\delta} I_\Gamma(t,\underline{z}) \leq \frac{1}{4\delta^2} J_o^2(t,\underline{z}) \leq \frac{1}{4\delta^2} J_o^2(\infty,\underline{z})$$

Thus,

$$-q I_\Gamma(t,\underline{z}) \leq \frac{1}{4\delta} J_o^2(\infty,\underline{z}) \qquad (21)$$

The same follows also from (17) upon use of (15), (18), (20) and Parseval's relation which yields

$$J_F(\underline{z}) \leq \frac{1}{4\delta} J_o^2(\infty,\underline{z}) \qquad (22)$$

---

*The conditions of the lemma apply to those of Theorem 10-1 of reference 3 the proof of which contains condition (C-24), Appendix C of reference 3, which (upon the (valid) substitution T by t), is identical to (16).

If (16) yields a finite $J_u(\infty,\underline{z})$ for every $\underline{z}$ then it follows from Lemma 10-1 of reference 3 that $e(t,\underline{z}) \to 0$ as $t \to \infty$ for every $\underline{z}$. Moreover, if all eigenvalues of $\underline{A}$ have negative real parts and $0 \leq q < \infty$ then if follows from the proof of Theorem 10-2 in reference 3 (Appendix C in reference 3) that the origin $\underline{x}=\underline{0}$ is globally asymptotically stable.

**Formalskii considered only systems with single-valued time-invariant functions $u = f(e)$. However, condition (29) of reference 6, for a system with one nonlinearity and appropriate change of notation, is valid for the conditions of this lemma and leads directly to (17).

Though (16) is considerably less conservative than (21), the denominator of the integral in (20) makes (17) also less conservative than (21); however, the integral in (20) represents greater computational complexity.

IV. ALGORITHMS FOR COMPUTATION OF SUFFICIENT STABILITY REGIONS

First of all, it should be recalled that the conditions of the Lemma stated in the previous section do not necessarily refer to asymptotic stability except for the (usual) cases where all eigenvalues of the $\underline{A}$ matrix have negative real parts and $0 \leq q < \infty$. Otherwise, the "stability regions" $\mathcal{R}$ to be obtained from the Lemma refer only to the property that $e(t,\underline{z}) \to 0$ as $t \to \infty$ when $\underline{z} \in \mathcal{R}$; this property, which often suffices for engineering purposes, will be called e-attraction and $\mathcal{R}$ will be called the region of e-attraction.

Further, it should be noted that for given linear and nonlinear elements, the expressions in condition (12) as well as those in conditions (16), (17) and (21) can all be expressed in terms of algebraic functions involving $\underline{z}$ and t. For example, if $T = 0$ (no transportation lag) then it follows from (4), (6), (11) and (18) that

$$J_g(t) = \left(\underline{b}^T \, \underline{\Psi}(t,0) \underline{b} \right)^{\frac{1}{2}} \tag{23a}$$

$$J_o(t,\underline{z}) = \left(\underline{x}_o^T \, \underline{\Psi}(t,q) \underline{x}_o \right)^{\frac{1}{2}} \tag{23b}$$

where $\underline{\Psi}(t,q) \triangleq \int_o^t \left[\underline{\phi}^T(\tau) + q \, \dot{\underline{\phi}}^T(\tau) \right] \underline{c} \underline{c}^T \left[\underline{\phi}(\tau) + q \, \dot{\underline{\phi}}(\tau) \right] d\tau$ (24)

can be determined from the given transition matrix $\underline{\phi}(t)$. An algebraic expression for $e_o(t,\underline{z})$ is given by (6).

The foregoing results will now be applied to several cases of nonlinear elements and ranges of q satisfying (15):

1. $q = 0$; General Functional Relation $u(t) = \mathcal{F}[e(t),t]$; $\frac{u}{e} \in [0,K]$ for $|e| \leq E$, $0 < K \leq \infty$:

For $q = 0$, (15) yields

$$\delta = \inf_{\omega \geq 0} \left(\mathrm{Re}\, G(j\omega) + \frac{1}{K} \right) \geq 0 \tag{25}$$

Also, for q = 0, (16) becomes $J_u(t,\underline{x}_o) \leq (1/\delta)\, J_o(t,\underline{x}_o)$ so that (12) becomes

$$\sup_{t\geq 0}\left(|e_o(t,\underline{z})| + \frac{1}{\delta} J_g(t)\, J_o(t,\underline{z})\right) \leq E \qquad (26a)$$

The objective is to find a region $\mathcal{R}_{10}$ for $\underline{z}$ such that (26a) is satisfied, i.e.,

$$\mathcal{R}_{10} = \left\{ \underline{z} \;\middle|\; \sup_{t\geq 0}\left(|e_o(t,\underline{z})| + \frac{1}{\delta} J_g(t)\, J_o(t,\underline{z})\right) \leq E \right\} \qquad (26b)$$

The computaion of the boundary of $\mathcal{R}$ can be accomplished by means of a suitable search technique.

2. $0\leq q<\infty$; Time-Invariant Functional Relation, Either Single-Valued or with Active Hysteresis, $u(t) = \mathcal{F}[e(t)]$; $\frac{u}{e} \in [0,K]$ for $|e| \leq E$, $0 < K \leq \infty$:

Let the following expressions be defined for convenience:

$$I_o(\underline{z}) = \sup_{\text{all } \Gamma_o}\left(\int_{\Gamma_o}^{e(0,\underline{z})} u\, de\right) \qquad (27a)$$

$$I_m(t,\underline{z}) = \inf_{\text{all } \Gamma_m}\left(\int_{\Gamma_m}^{e(t,\underline{z})} u\, de\right) \qquad (27b)$$

$$I_E = \inf_{\text{all } \Gamma_E}\left(\int_{o}^{E} u\, de\right) \qquad (27c)$$

where Γ_o , Γ_m and Γ_E represent all possible single paths (no closed path allowed) on the u-e characteristic between 0 - e(0,$\underline{z}$), 0 - e(t,$\underline{z}$) and 0 - E respectively. For a single-valued function u = f(e), of course, these paths are all unique.

For active hysteresis (including the special case of a time-invariant function), it follows from (8), (19) and (27) that

$$I_\Gamma(t,\underline{z}) \leq I_o(\underline{z}) - I_m(t,\underline{z}) \qquad (28)$$

Therefore, with $q\geq 0$, it follows from condition (16) that

$$\left[J_u(t,\underline{z}) - \frac{1}{2\delta} J_o(t,\underline{z})\right]^2 \leq \frac{q}{\delta} I_o(\underline{z}) - \frac{q}{\delta} I_m(t,\underline{z}) + \frac{1}{4\delta^2} J_o^2(t,\underline{z})$$

But for $\frac{u}{e} \in [0,K]$ with $0<K\leq\infty$, it follows from (27) that $I_o(\underline{z}) \geq 0$

and $I_m(t,\underline{z})\geq 0$. Therefore, since $q \geq 0$ and $\delta > 0$, the above inequality yields

$$J_u(t,\underline{z}) \leq \frac{1}{2\delta} J_o(t,\underline{z}) + \sqrt{\frac{1}{4\delta^2} J_o^2(t,\underline{z}) + \frac{q}{\delta} I_o(\underline{z})} \tag{29}$$

Thus, (12) and (13) become respectively

$$\sup_{t\geq 0}\left(|e_o(t,\underline{z})| + J_g(t)\left[\frac{1}{2\delta} J_o(t,\underline{z}) + \sqrt{\frac{1}{4\delta^2} J_o^2(t,\underline{z}) + \frac{q}{\delta} I_o(\underline{z})}\right]\right) \leq E \tag{30a}$$

$$\mathcal{R}_{1q} = \left\{ \underline{z} \;\middle|\; \sup_{t\geq 0}\left(|e_o(t,\underline{z})| + J_g(t)\left[\frac{1}{2\delta} J_o(t,\underline{z}) + \sqrt{\frac{1}{4\delta^2} J_o^2(t,\underline{z}) + \frac{q}{\delta} I_o(\underline{z})}\right]\right) \leq E \right\} \tag{30b}$$

Note that (2b) is a special case of (30) for $q = 0$.

For condition (17), another region for $\underline{z}$ can be obtained. From (17) and (28) it follows that

$$I_m(t,\underline{z}) \leq I_o(\underline{z}) + \frac{1}{q} J_F(\underline{z}) \tag{31}$$

Now, for $\frac{u}{e} \in [0,K]$, $0 < K \leq \infty$, it follows from (27b) and (27c) that

$$|e(t,\underline{z})| \leq E \quad \text{if} \quad I_m(t,\underline{z}) \leq I_E \tag{32}$$

Thus another condition and region sufficient for e-attraction will be given by

$$I_o(\underline{z}) + \frac{1}{q} J_F(\underline{z}) \leq I_E \tag{33a}$$

$$\mathcal{R}_{2q} = \left\{ \underline{z} \;\middle|\; I_o(\underline{z}) + \frac{1}{q} J_F(\underline{z}) \leq I_E \right\} \tag{33b}$$

Another region can be defined by condition (21) which, with (28) and (32) yields

$$I_o(\underline{z}) + \frac{1}{4\delta q} J_o^2(\infty,\underline{z}) \leq I_E \tag{34a}$$

$$\mathcal{R}_{3q} = \left\{ \underline{z} \;\middle|\; I_o(\underline{z}) + \frac{1}{4\delta q} J_o^2(\infty,\underline{z}) \leq I_E \right\} \tag{34b}$$

It follows from (22) that region $\mathcal{R}_{3q}$ is more conservative than $\mathcal{R}_{2q}$, i.e., $\mathcal{R}_{3q} \subset \mathcal{R}_{2q}$. On the other hand, it has the advantage that it involves fewer computations.

Since (30), (33) and (34) all define regions that are sufficient for e-attraction, the union of any two or all of these regions will also be sufficient for e-attraction. This means, for example, that the boundaries of the region defined by

$\mathcal{R}_{12} = \mathcal{R}_{1q} \cup \mathcal{R}_{2q}$ will encircle both regions $\mathcal{R}_{1q}$ and $\mathcal{R}_{2q}$.

3. $-\infty < q < 0$; Time-Invariant Function, Either Single-Valued or with Passive Hysteresis, $u(t) = \mathcal{F}[e(t)]$; $\frac{u}{e} \in [0,K]$ for $|e| \leq E$, $0 < K < \infty$:

This case applies when the Popov condition (15) can be satisfied with $-\infty < q \leq 0$ for a system satisfying the conditions of the lemma in the previous section whose nonlinear element is either time-invariant or has passive hysteresis and where $0 < K < \infty$ (i.e., $K \neq \infty$). Then [3] if $E = \infty$, it is guaranteed that for every $\underline{z}$, $J_u(t,\underline{z}) < \infty$ for all $t \geq 0$ and $e(t,\underline{z}) \to 0$ as $t \to \infty$. This was proved in reference 3 by means of the following transformation (see Appendix C of reference 3):

$$u_1(t,\underline{z}) = Ke(t,\underline{z}) - u(t,\underline{z}) \tag{35}$$

Transformation (35) applied to the original system (3) yields the following equivalent system:

$$e(t,\underline{z}) = e_{o1}(t,\underline{z}) - \int_o^t g_1(t-\tau)u_1(\tau,\underline{z})d\tau \quad ; \quad u_1(t,\underline{z}) = \mathcal{F}_1[e(t,\underline{z})] \tag{36}$$

where

$$G_1(s) = \mathcal{L}[g_1(t)] \triangleq \frac{-G(s)}{1 + KG(s)} \quad ; \quad E_{o1}(s,\underline{z}) = \mathcal{L}[e_{o1}(t,\underline{z})] = \frac{E_o(s,\underline{z})}{1 + KG(s)} \tag{37}$$

It follows from (8) and (35) that if the original nonlinear element had passive hysteresis then the transformed element $u_1(t) = \mathcal{F}_1[e(t)]$ has active hysteresis (e.g., see Figure 2). Moreover, if the Popov condition (15) for the original linear element was satisfied with a negative value of q, then it will hold for the transformed element $G_1(s)$ with a value of q of the same magnitude but with positive sign *.

It is indeed possible to obtain a relation for $\mathcal{R}$ in terms of the original system. In that case, the bound on $J_u(t,\underline{z})$, that is needed to compute $\mathcal{R}$ by (13), can be obtained from inequality relations between $u_1(t,\underline{z})$ and $u(t,\underline{z})$ involving (35) and (36). However, in that process, too many terms are lost which will

*This follows from the proof of Theorem 10-1 given in Appendix C of referenc 3.

make the region $\mathcal{R}$ obtained too conservative.

Therefore it is recommended to transform the original system by (35) and (37) when indicated such that the transformed system falls into case 2.

4. Cases where $\frac{u}{e} \in [a,b]$ for $|e| \leq E$, $a < b$:

For such cases, one can easily transform the system by the (pole-shifting) transformation

$$u_a(t,\underline{z}) = u(t,\underline{z}) - a\, e(t,\underline{z}) \tag{38}$$

which transforms the original system (3) into the system

$$e(t,\underline{z}) = e_{oa}(t,\underline{z}) - \int_0^t g_a(t-\tau)\, u_a(\tau,\underline{z})\, d\tau \;;\; u_a(t,\underline{z}) = \mathcal{F}_a[e(t,\underline{z}),t] \;;$$

$$\frac{u_a}{e} \in [0,b-a] \quad \text{for } |e| \leq E \tag{39}$$

where

$$G_a(s) = \mathcal{L}[g_a(t)] \triangleq \frac{G(s)}{1+aG(s)} \;;\; E_{oa}(s,\underline{z}) = \mathcal{L}[e_{oa}(t,\underline{z})] \triangleq \frac{E_o(s,\underline{z})}{1+aG(s)} \tag{40}$$

For stability studies, instead of transforming the system, one can also transform the stability conditions. This approach yielded the generalized circle criterion (valid for $-\infty < q < \infty$)[3]. Because of its flexibility, that criterion is highly useful in stability analysis.

However, when it comes to the establishment of actual bounds of $J_u(t,\underline{z})$ needed in the computation of $\mathcal{R}$ then, as in the previous case, too many terms in the inequalities may be lost in the process of transformation. Therefore, it is recommended also for these cases to use transformation (38), (40) directly on the system when indicated in order to bring it into the form of Case 2 *. For the case of a general time-varying nonlinear element $u(t) = \mathcal{F}[e(t),t]$ and $q = 0$, transformation (38), (40) will yield a system of the form of case 1.

*In order to bring the original system into the form of Case 2, it may sometimes (e.g., in case of passive hysteresis) be necessary to use a combination of transformations (35) and (38).

V. AN EXAMPLE:

Consider the system with transportation lag, given by

$$\left.\begin{aligned} &\dot{x}(t) = -x(t) - 0.8\,u(t-0.5)\ ;\ u(t) = \mathcal{F}[e(t),t] \\ &\frac{u}{e} \in [0,1] \text{ for } |e| \le E = 1 \end{aligned}\right\} \tag{41}$$

Two caes for the nonlinear element will be considered, namely

a) General time-varying nonlinearity $u(t) = \mathcal{F}[e(t),t]$ with $\frac{u}{e} \in [0,1]$ for $|e| \le E = 1$.

b) Single-valued nonlinearity $u = e^3$.

System (41) is of the form of Figure 1, with

$$x(t) = e(t)\ ; \qquad G(s) = \frac{0.8e^{-0.5s}}{s+1} \tag{42}$$

According to (6), the open-loop initial condition response can be expressed as

$$e_o(t,\underline{z}) = x_o e^{-t} - 0.8\int_0^t e^{-(t-\tau)}\, u_o(\tau-0.5)\, d\tau \tag{43}$$

where

$$\underline{z} = \begin{bmatrix} x_o \\ u_M \end{bmatrix} \tag{44}$$

Therefore, with (6b) and (7b),

$$|e_o(t,\underline{z})| \le \begin{cases} |x_o|\, e^{-t} + 0.8\,u_M(1-e^{-t}) \le (|x_o| + 0.519\,u_M)e^{-t}\ , & 0 \le t < 0.5 \\ (|x_o| + 0.519\,u_M)e^{-t}\ , & t \ge 0.5 \end{cases} \tag{45}$$

The time-derivative of $e_o(t,\underline{z})$ can be written as

$$\dot{e}_o(t,\underline{z}) = -e_o(t,\underline{z}) - 0.8\,u_o(t,\underline{z})$$

Therefore, with (6b) and (7b), the following inequality holds:

$$|e_o(t,\underline{z}) + q\,\dot{e}_o(t,\underline{z})| \le \begin{cases} |1-q|(|x_o| + 0.519\,u_M)e^{-t} + 0.8q\,u_M\ , & 0 \le t < 0.5 \\ |1-q|\,(|x_o| + 0.519\,u_M)\,e^{-t}\ , & t \ge 0.5 \end{cases} \tag{46}$$

From (18) and (44),

$$\begin{aligned} J_o^2(t,\underline{z}) \le\ & \tfrac{1}{2}(1-q)^2(|x_o| + 0.19\,u_M)^2(1-e^{-2t}) \\ & + 0.630\,|q|\,|1-q|\,u_M\,(|x_o| + 0.519\,u_M) + 0.320\,q^2u_M^2\ ;\ t \ge 0.5 \end{aligned} \tag{47}$$

From (11) and (42), it becomes

$$J_g^2(t) = \begin{cases} 0 & , \quad 0 \le t < 0.5 \\ 0.320(1-e^{-2(t-0.5)}) & , \quad t \ge 0.5 \end{cases} \tag{48}$$

With K=1, the Popov condition (15) becomes

$$\delta = \inf_{\omega \ge 0} \left(\mathrm{Re}(1 + j\omega q) G(j\omega) + 1 \right) > 0$$

Here, with (42), it is

$$\delta = \inf_{\omega \ge 0} \left(\frac{0.8}{1+\omega^2} \left[(1+\omega^2 q^2)\cos 0.5\omega - \omega(1-q)\sin 0.5\omega \right] + 1 \right) > 0 \tag{49}$$

Case (a): General Time-Varying Nonlinearity:

For this case, it must be q = 0 and the stability region $\mathfrak{R}_{10}$ will be given by (26). For q = 0, (47) yields $\delta = 0.7655$. Using this and relations (46) to (48), condition (26 b) becomes

$$\mathfrak{R}_{1o} = \mathfrak{R}'_{1o} \cap \mathfrak{R}''_{1o}$$

where

$$\mathfrak{R}'_{1o} \triangleq \left\{ \underline{z} \;\middle|\; \sup_{0 \le t < 0.5} \left(|x_o| e^{-t} + 0.8\, u_M (1-e^{-t}) \right) \le 1 \right\}$$

$$\mathfrak{R}''_{1o} \triangleq \left\{ \underline{z} \;\middle|\; \sup_{t \ge 0.5} \left(|x_o| + 0.519\, u_M \right) f(t) \le 1 \right\}$$

where

$$f(t) \triangleq e^{-t} + 0.522 \sqrt{(1-2.718\, e^{-2t})(1-e^{-2t})} \quad ; \quad t \ge 0.5$$

Now, it is $\sup_{t \ge 0.5} f(t) = 0.763$; therefore,

$$\mathfrak{R}'_{1o} = \left\{ \underline{z} \;\middle|\; \max\left[(|x_o|), (0.6065|x_o| + 0.315\, u_M) \right] \le 1 \right\}$$

$$\mathfrak{R}''_{1o} = \left\{ \underline{z} \;\middle|\; 0.763(|x_o| + 0.519\, u_M) \le 1 \right\}$$

Thus,

$$\mathfrak{R}_{1o} = \left\{ \underline{z} \;\middle|\; \max\left[(|x_o|), (0.6065|x_o| + 0.315\, u_M), (0.763|x_o| + 0.395\, u_M) \right] \le 1 \right\} \tag{50}$$

The boundary of this region is shown in Figure 3.

Case (b): Single-Valued Nonlinearity $u = e^3$:

Here, it is permissable to choose any value for $q \ge 0$, which will determine the value of δ according to Popov's condition (49). The value q = 1 is arbitrarily chosen. This, by (49), yields $\delta = 0.2$. Inequality (47) then becomes

$$J_o(t,\underline{z}) \leq 0.565\, u_M \quad , \quad t \geq 0.5 \quad \text{for } q = 1$$

For the given nonlinearity, (27) yields

$$I_o(\underline{z}) = \int_o^{e(0,\underline{z})} e^3 de = \frac{1}{4} e_o^4(0,\underline{z}) = \frac{1}{4} x_o^4$$

$$I_E = \int_o^1 e^3 de = \frac{1}{4}$$

Consider first the region $\mathcal{R}_{1q}$. With the above expressions and also (45) and (48), this region follows from (30b) as

$$\mathcal{R}_{1q} = \mathcal{R}'_{1q} \bigcap \mathcal{R}''_{1q}$$

where

$$\mathcal{R}'_{1q} \triangleq \left\{ \underline{z} \;\middle|\; \sup_{0\leq t<0.5} \left(|x_o| e^{-t} + 0.8\, u_M (1-e^{-t}) \right) \leq 1 \right\}$$

which can be evaluated as

$$\mathcal{R}'_{1q} = \left\{ \underline{z} \;\middle|\; \max \left[(|x_o|), (0.6065|x_o| + 0.351\, u_M) \right] \leq 1 \right\}$$

and

$$\mathcal{R}''_{1q} \triangleq \left\{ \underline{z} \;\middle|\; \sup_{t\geq 0.5} \left((|x_o| + 0.519\, u_M) e^{-t} + 0.8\, u_M \sqrt{1-e^{-2(t-0.5)}} \left[1+\sqrt{1+\frac{5}{8}\left(\frac{x_o^4}{u_M^2}\right)} \right] \right) \leq 1 \right\}$$

The above expression can be manipulated to yield

$$\mathcal{R}''_{1q} = \left\{ \underline{z} \;\middle|\; \begin{array}{ll} \alpha \left[1 + \left(\frac{\beta}{2\alpha}\right)^2 \right] \leq 1 & \text{if } \beta \leq 2\alpha \\ \beta \leq 1 & \text{if } \beta > 2\alpha \end{array} \right\}$$

where

$$\left.\begin{aligned} \alpha &\triangleq 0.6065|x_o| + 0.315\, u_M \\ \beta &\triangleq 0.8\, u_M \left[1+\sqrt{1+\tfrac{5}{8}(x_o^4/u_M^2)} \right] \end{aligned}\right\} \qquad (51a)$$

Thus, $\mathcal{R}_{1q} = \mathcal{R}'_{1q} \bigcap \mathcal{R}''_{1q}$ becomes

$$\mathcal{R}_{1q} = \left\{ \underline{z} \;\middle|\; \max \left[(|x_o|), (\alpha), \begin{pmatrix} \alpha \left[1+\left(\frac{\beta}{2\alpha}\right)^2 \right] & \text{if } \beta \leq 2\alpha \\ \beta & \text{if } \beta > 2\alpha \end{pmatrix} \right] \leq 1 \right\} \qquad (51b)$$

The boundary of this region is also shown in Figure 3.

Next, the region $\mathcal{R}_{3q}$, defined by (34), will be considered. This algorithm is the simplest of the ones discussed in this paper since it does not involve functions of time. For q=1, it yields

$$\mathfrak{R}_{3q} = \left\{ \underline{z} \;\middle|\; x_o^4 + 1.6\, u_M^2 \leq 1 \right\} \qquad (52)$$

All three boundaries, $\mathfrak{R}_{1o}$ (for q=0), $\mathfrak{R}_{1q}$ and $\mathfrak{R}_{3q}$ (for q=1) are shown in Figure 3. The first region is valid for every nonlinear and possibly time-varying element $u = \mathcal{F}[e(t), t]$, as long as $\frac{u}{e} \in [0,1]$ for $|e| \leq 1$, which includes the special case $u = e^3$ for which the latter two regions were obtained. Therefore, since $\mathfrak{R}_{1o}$ includes both $\mathfrak{R}_{1q}$ and $\mathfrak{R}_{3q}$, it clearly represents the least conservative and therefore the most useful of the three (sufficient) stability regions.

The conclusion that in this example the least conservative region is obtained for the most general type of nonlinear element may look encouraging, however, no generalization should be made.

VI. DISTRIBUTED PARAMETER SYSTEMS

The algorithms discussed in this paper can be extended to systems of the same form (Figure 1) where the linear element is governed by a partial differential equation. Suppose that the variable e(t,y) is described by a partial differential equation in time t and distance-location* y. The motion of the linear element can be described by**

$$e(t,y) = e_o(t,y) - \int_o^t g(t-\tau,y)\, u(\tau)\, d\tau \qquad (53a)$$

where g(t,y) represents the unit-impulse response of the linear plant at the space-location y and where $e_o(t,y)$ represents the response at location y due to the initial function e(0,y). It can be shown** that $e_o(t,y)$ is of the form

$$e_o(t,y) = \int_{-\infty}^{\infty} \Psi(t,\lambda,y)\, d\lambda \qquad (53b)$$

Both g(t,y) and $\Psi(t,\lambda,y)$ are given in terms of the partial differential equation and boundary conditions of the distributed parameter plant. The transfer function then is $G(s) = G(s,y) = \mathcal{L}[g(t,y)]$ whereby y is fixed. This plant is connected to a nonlinear element in the manner of Figure 1, i.e.,

---

*This can readily be extended to 3-dimensional space.

**See reference 3, p.83.

$$u(t) = \mathcal{F}[e(t,y),\ t] \tag{53c}$$

Physically, this means that the signal $e(t) = e(t,y)$ is measured at the space location y and fed back to the plant through the nonlinear element.

The objective now is to find a bound on the initial function $e(0,\lambda)$ over $-\infty \leq \lambda \leq \infty$ that assures $e(t,y) \to 0$ for $t \to \infty$. Let $e_M(\lambda)$ be this bound, defined by

$$|e(0,\lambda)| \leq e_M(\lambda) \tag{54}$$

Then, from (53b),

$$|e_o(t,y)| \leq \int_{-\infty}^{\infty} |\Psi(t,\lambda,y)|\ e_M(\lambda)\ d\lambda \tag{55a}$$

$$|e_o(t,y) + q\dot{e}_o(t,y)| \leq \int_{-\infty}^{\infty} |\Psi(t,\lambda,y) + q\frac{d}{dt}\Psi(t,\lambda,y)|\ e_m(\lambda)d\lambda \tag{55b}$$

From $g(t) = g(t,y)$ and from (55b), bounds for $J_g(t)$ and $J_o(t,y)$ can be found by means of (11) and (18) respectively. From here on, the procedure of applying the algorithms (26),(30), (33) or (34) becomes the same as for lumped-parameter systems except that here the object of computaion becomes the search for a suitable bound function $e_M(\lambda)$ over the range $-\infty \leq \lambda \leq \infty$ instead of bounds on the initial state vector in the case of a lumped-parameter plant. The following procedure is recommended:

(a) Check whether for fixed y, g(t,y) is (i) absolutely integrable and (ii) square-integrable, both with respect to t over $t \in (0,\infty)$. Find $J_g(t,y)$ by (11).

(b) Assume a <u>form</u> for the function $e_M(\lambda)$ in terms of a suitable set of parameters (e.g. $e_M(\lambda) = M$ for $-\infty \leq \lambda \leq \infty$, or $e_M(\lambda) = M\, e^{-\theta|\lambda|}$, where M or (M,θ) are the parameters to be evaluated respectively).

(c) With the assumed function $e_M(\lambda)$, obtain bounds for $|e_o(t,y)|$ and $|e_o(t,y) + q\, e_o(t,y)|$, using (55), and check whether these bounds (i) are finite for all $t \geq 0$ and (ii) are square-integrable with respect to t over $0 \leq t \leq \infty$; if so, find $J_o(t,y)$ from (18) and (55). These properties are required in order to satisfy the algorithms.

(d) Find the numerical values for the parameters chosen in (b) such that the particular algorithm (26), (30), (33) or (34) is satisfied.

This procedure is conceptually straightforward. However, the greatest difficulty consists of the finding of a form for the bound-function $e_M(\lambda)$ such that it yields a finite $J_o(t,y)$ for all $t \geq 0$.

VII. BOUNDED INPUT-BOUNDED OUTPUT STABILITY

The algorithms presented in this paper are not applicable to the computation of stability regions for bounded input-bounded output stability. Such stability regions must involve not only the state space but also bounds on the input signal.

Analogous to algorithms (26) and (30) presented here, algorithms for regions of bounded input-bounded output stability can be obtained from expressions for the bounds of $|e(t,\underline{z}_1)|$ where $\underline{z}_1$ represents both the set of initial conditions and the bound r_M of the input $r(t)$ to the feedback system ($|r(t)| \leq r_M$). Such expressions for bounds on $|e(t,\underline{z}_1)|$ are contained in the proofs of theorems for global bounded input-bounded output stability*. The derivation of regions of $\underline{z}_1$ then becomes analogous to that which led to algorithms (26) and (30). An algorithm based on this approach has been obtained by Holtzman[8].

Such an algorithm can, of course, also be used to compute stability regions for the unforced system; however, it is necessarily more restrictive and will therefore produce more conservative (i.e. smaller) stability regions than the algorithms derived in the present paper.

VIII. SUMMARY AND CONCLUSIONS

For the class of single-loop systems of Figure 1, algorithms have been presented to compute regions of the set of initial conditions $\underline{z}$ sufficient for stability, whereby "stability" is defined here in terms of the property that the signal $e(t) = e(t,\underline{z}) \to 0$ as $t \to \infty$ (called "e-attraction"). These algorithms

*See for example reference 7, reference 3 (pp. 433-438 and pp. 740-743) and reference 13.

apply to cases where a frequency-response criterion for global e-attraction ("global" referring to every z) can be satisfied for a certain sector $\frac{u}{e} \in [0,K]$ of the nonlinear element but where the actual nonlinearity lies within this sector only for a limited range of its input-signal e(t). All of the algorithms presented relate to the Popov condition (15). The major results of this paper are the following:

(i) For the general nonlinear (possibly time-varying) element $u(t) = f[e(t),t]$, algorithm (26), yielding region $\mathcal{R}_{1o}$ is valid. It relates to the Popov condition (15) with q=0.

(ii) For single-valued nonlinearities (or the rather uncommon case of active hysteresis), algorithms (30) (region $\mathcal{R}_{1q}$), (33) (region $\mathcal{R}_{2q}$) and (34) (region $\mathcal{R}_{3q}$) are valid. They relate to the Popov condition (15) with $q > 0$. Algorithm (26) (region $\mathcal{R}_{1o}$) is, of course, also applicable to this type of nonlinearity.

For the cases $q < 0$ in the Popov condition (15), which includes the case of a nonlinear element with passive hysteresis, transormation (35) can be performed to bring the system into a form where case (ii) above applies. A similar (pole-shifting) transformation (38) can be used if the nonlinear sector under consideration is $\frac{u}{e} \in [a,b]$ with $a \neq 0$.

Algorithm (34) (region $\mathcal{R}_{3q}$) represents the least amount of computational complexity because it does not involve functions of time. Algorithm (30) (region $\mathcal{R}_{1q}$) appears to represent the greatest amount of computations. It may be noted, however, from the results of the example of Section V, presented in Figure 3, that the most complex algorithm need not always yield the least conservative (largest) region sufficient for stability.

The algorithms were illustrated by an example (Section V) where the linear element contained transportation lag. The application of the method to systems with distributed-parameter elements is indicated (Section VI). The algorithms presented are of an algebraic nature*.

Problems for future work include investigation of optimum choice of q to yield the largest region sufficient for stability;

---

*Note that all integral expressions contained in the algorithms can be expressed algebraically (see, e.g., eqs. (23)).

this applies to the algorithms listed under (ii) above. A comparison should be made between the algorithms presented here and methods based on the use of Lyapunov functions. A major task is the development of computer programs for the implementation of the algorithms, including meaningful search routines.

ACKNOWLEDGEMENTS

The author is indebted to C. D. Han, J. M. Holtzman and J. Rausen for their valuable comments.

REFERENCES

1. M.A. Aizerman, F.R. Gantmacher: "Absolute Stability of Regulator Systems", Holden-Day (1964) (translated from Russian (1963)).
2. S. Lefschetz: "Stability of Nonlinear Control Systems", Academic Press (1965).
3. J.C. Hsu, A.U. Meyer: "Modern Control Principles and Applications", McGraw-Hill (1968).
4. V.A. Yakubovich: "Solution of Certain Matrix Inequalities Occuring in the Theory of Automatic Control", Doklady, Academy of Sciences of the USSR, vol.143, no.1-6 (1962); Engl. translation: Soviet Mathematics, vol.3, no.2 (March 62), pp.620-623.
5. R.E. Kalman: "Lyapunov Functions for the Problem of Lur'e in Automatic Control", National Academy of Sciences (USA) - Proceedings, vol. 49, no. 2 (Febr. 1963), pp. 201-205.
6. A.M. Formalskii: "Construction of Stability Region for Systems not Stable in the Whole", Vestnik, Moscow Univ., 1967, no.1, pp.71-81.
8. J.M. Holtzman: "A Local Bounded-Input Bounded-Output Condition for Nonlinear Feedback Systems", IEEE- Transactions on Automatic Control, vol. AC-13, October 1968.
9. J.A. Walker, N.H. McClamroch: "Finite Regions of Attraction for the Problem of Lur'e", Int. J. Control, vol.6, no.4 (October 1967), pp.331-336.
10. S. Weissenberger: "Application of Results from the Absolute Stability Problem to the Computation of Finite Stability Domains", IEEE- Trans. on Autom. Contr., vol.AC-13, no.1 (February 1968), pp.124-125.
11. K. Chinnapareddy, C.C. Li: "A Time-Varying Bound on Nonlinear System Transient Response", First Annual Princeton Conference on Information Sciences and Systems (March 1967)- Proceedings, pp. 173-177.
12. K. Chinnapareddy, C.C. Li: "Remarks on Time-Varying Upper Bounds of Nonlinear System Transient Response", Second Annual Princeton Conf. on Information Sciences and Systems (March 1968) - Proceedings, pp. 369-373.
13. R. Iwens: "Bounds on the Responses of Nonlinear Control Systems", Journal of the Franklin Institute, vol. 285, no.4 (April 1968), pp. 261-274.

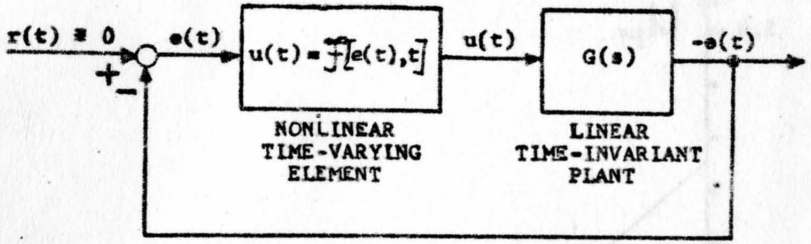

Figure 1. Single-loop control system. The nonlinear element may have hysteresis or be time-varying.

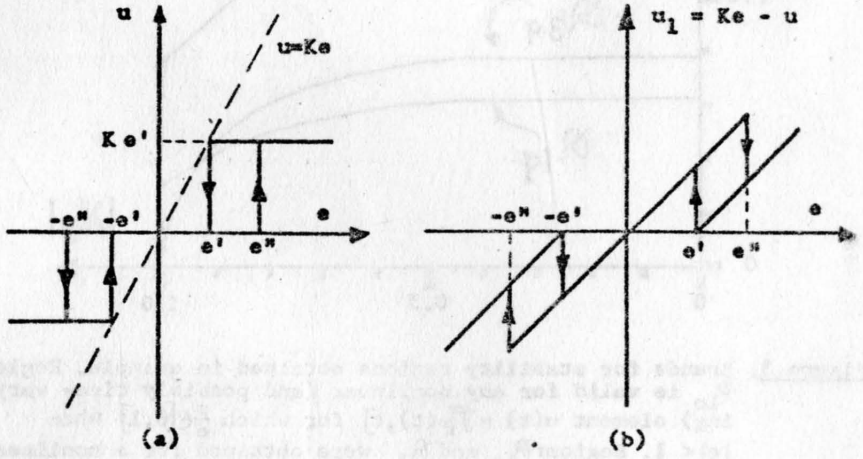

Figure 2. Illustration of a passive hysteresis characteristic (a) and an active hysteresis characteristic (b). Nota that (a) can be transformed into (b) by the relation $u_1 = Ke-u$.

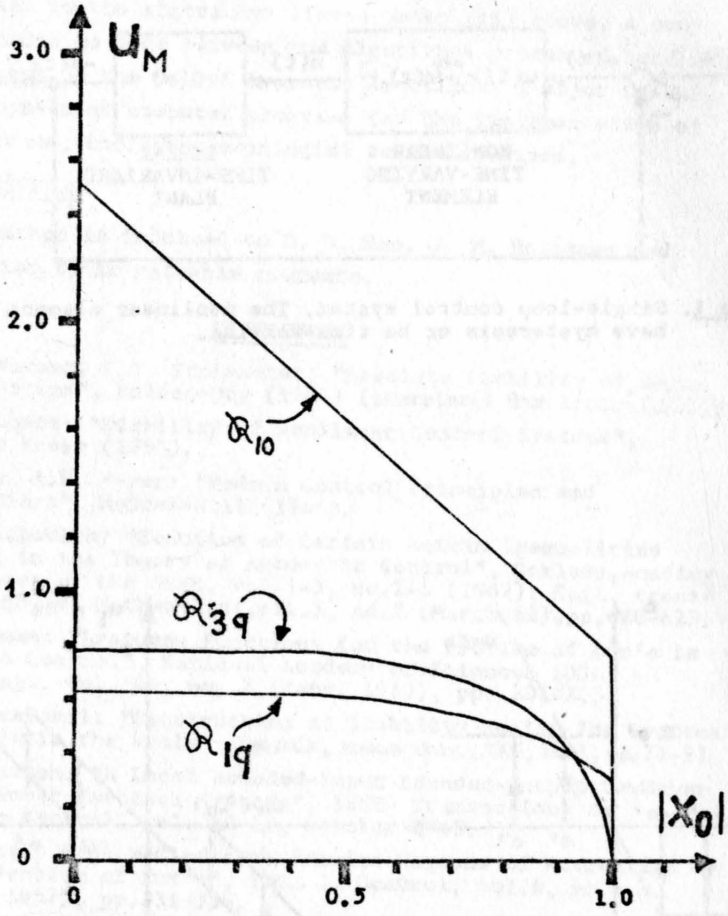

Figure 3. Bounds for stability regions obtained in example. Region $\mathcal{R}_{1o}$ is valid for any nonlinear (and possibly time- varying) element $u(t) = \mathcal{F}[e(t),t]$ for which $\frac{u}{e} \in [0,1]$ when $|e| \leq 1$. Regions $\mathcal{R}_{1q}$ and $\mathcal{R}_{3q}$ were obtained for a nonlinear element $u = e^3$. Note that $\mathcal{R}_{1o}$ is also valid for this element and, since it encloses both regions $\mathcal{R}_{1q}$ and $\mathcal{R}_{3q}$, it represents the mose useful of the three (sufficient) stability regions for this example.